A Reanalysis of Hurricane Hazel (1954)

by
Scott R. Weese

Department of Atmospheric and Oceanic Sciences
McGill University
Montreal, Quebec

A thesis submitted to the Faculty of Graduate Studies and Research in partial fulfilment of the requirements of the degree of Master of Science.

Your file Votre référence
ISBN: 0-612-98759-0
Our file Notre référence
ISBN: 0-612-98759-0

Abstract

Hurricane Hazel struck North America on 15-16 October 1954, leaving a pattern of heavy rainfall and flooding in its wake. A complete analysis of the synoptic-scale conditions associated with the transformation of Hazel from its tropical phase into an extratropical cyclone was first undertaken to discern the dynamic and thermodynamic elements crucial to the intensification of this storm.

An analogue search was then conducted for Hazel using linear correlations of anomaly sea level pressure and 1000-500 hPa thickness. Three cases were found in 1985, 1995 and 1999. A comparison of these analogues to Hazel yielded the conclusion that Hazel is a unique event in recent meteorological history, as none of the analogues produces the extreme precipitation values in Hazel. The lack of significant hurricane circulations in all of the analogues is the important difference, as Hazel provides important moisture and latent heating that are absent in the analogues.

Finally a mesoscale modeling study was carried out to test the sensitivity of Hazel to improved surface vortex structure and increased horizontal resolution. Specification of the vortex led to a dramatic improvement in the simulation results, as precipitation and track closely mimicked the observed values. Enhancing the horizontal resolution to 12 km did not improve upon the 36 km specified vortex simulation. The movement of the storm slowed considerably as the development of an upper tropospheric cutoff circulation was diminished in the 12 km run. The parameterizations governing the interaction between the diabatic outflow from Hazel and dynamics of the midlatitude trough are poorly modeled in this situation, and lead to the severe time lag in the path of Hazel.

Résumé

L'ouragan Hazel a frappé l'Amérique du Nord les 15 et 16 octobre 1954 laissant derrière lui de fortes pluies et inondations. Pour la première fois, une analyse complète des conditions synoptiques associées avec cette tempête tropicale a été faite afin de discerner la dynamique et la thermodynamique des éléments determinants l'intensification de Hazel.

Une analyse analogique a été faite, fournissant des cas répertoriés en 1985, 1995 et 1999. Une comparaison de ces analogies mena à la conclusion que Hazel est un événement unique dans la récente histoire météorologique car aucun des autres cas n'a produit autant de précipitations que cet ouragan. Dans tous les analogues, le peu de caractéristique typique d'un ouragan est la plus grande différence. Hazel a apporté beaucoup d'humidité et de chaleur latentes que ce que nous avons trouvé dans les autres cas.

Finalement, une étude du modèle meso-echelle a été faite pour tester la sensibilité de Hazel à une structure de vortex plus fine et augmentation la résolution horizontale. Les spécifications du vortex ont apporté un énorme progrès dans les résultats des simulations : les précipitations et la trajectoire simulées ont presque reproduits les observations. La resolution de 12km n'a cependant pas amélioré les resultats obtenus pour celle de 36km. La vitesse de déplacement de la depression a considérablement diminué à cause du développement d'une circulation fermée dans la partie supperieur de la troposphere. Dans ce cas, les paramêtres qui gouvernent l'intéraction entre le débit diabatique de Hazel et la dynamique de moyenne latitude, ne sont pas très bien représentés, ce qui explique le décalage de la trajectoire.

Acknowledgements

Many people deserve recognition for their input and support over the course of my research. Foremost is my thesis advisor, Dr. John Gyakum, whose encouragement and insight have inspired me to thoroughly explore Hurricane Hazel. Ron McTaggart-Cowan provided countless hours of programming assistance and technical guidance, and the patience with which this was dispensed is greatly appreciated. Thanks go to Dorothy Durnford for her willingness to decipher my many computer-related problems in the early going. Discussions with Jason Milbrandt, Werner Wintels and Rick Danielson yielded suggestions that motivated me to expand my investigation of Hurricane Hazel. Peter Bowyer of the Canadian Hurricane Center contributed obscure technical documents that exposed detail surrounding this storm that was not readily available. The translation of the abstract was furnished by Hélene Mitko and Thomas Duhaut. Grants from CFCAS (Canadian Foundation for Climate and Atmospheric Sciences) and NSERC (Natural Sciences and Engineering Research Council) must be acknowledged as they enabled me to conduct this research. Sincere gratitude must be expressed to Dr. Terry Gillespie of the University of Guelph. His captivating and humorous teaching approach made meteorology fascinating, sparking my unappeasable interest in the weather. An immeasurable amount of support came from my wife Megan, who became a Hurricane Hazel expert in her own right through our many brainstorming sessions.

Table of Contents

1. Introduction

1.1 Motivation

Hurricane Hazel is still one of the most talked about storms to ever strike the province of Ontario. Long-time residents recall the rapidity with which the storm developed, and the ensuing heavy rains and flooding that quickly drove them to seek higher ground. To this day, many precipitation recording stations in southern Ontario experienced their most extreme rainfall amounts as a result of the storm Hazel (EC 2003). Over 78 deaths and $2.3 billion damage (in 2003 equivalent dollars) were left in the wake of Hazel (Davis 1954). Studying the underlying thermodynamic and dynamic properties of such a deadly and costly disaster is indeed necessary.

A common misconception by the casual observer of this event is that Hazel was categorically a hurricane upon hitting Ontario. In actual fact, Hazel had undergone an extratropical transformation (ET) whereby the tropical characteristics of the hurricane were replaced by a system more resembling an extratropical cyclone. These tropical characteristics are recognizable as a uniform temperature distribution and symmetric height contours, whereas an extratropical cyclone exhibits pronounced baroclinicity and strong vertical wind shear (Gyakum 2002a). When the interaction between these structures results in near surface frontogenesis and temperature advection, along with the dissolution of the tropical cyclone warm core, one can conclude that the ET is well underway (Klein et al. 2002).

As the identification of these transforming mechanisms is often subjective, so too is the definition of what truly constitutes an ET (Malmquist 1999). A definition provided by the National Hurricane Center (NHC) allows for the assessment of two factors, sea surface temperature beneath the storm track and visual inspection of the storm structure and assymmetry via satellite imagery (Hart and Evans 2001). This definition still is quite subjective in nature.

Reintensification of the ET can subsequently follow the transformation, ending when the minimum central pressure is reached and then succeeded by a steady rise in the sea level pressure (Klein et al. 2002). Transformed storms can often intensify explosively, and present problems when forecasting the associated precipitation and track of the cyclone (Gyakum 2002a). The transition and the following reintensification of the extratropical storm Hazel constitute the focus of the research problem. Knox (1955) discusses the difficulty of forecasting this storm, a process made especially difficult by the rapidity of Hazel's reintensification. One could argue that the resources available to forecasters at this time (e.g. numerical weather prediction models, satellite data) were the limiting constraint, but even today the ET presents a formidable forecasting challenge.

Palmén (1958) conducted a thorough study of hurricane Hazel, assessing the conversion taking place between potential and kinetic energy. Anthes (1990) followed up on this work by verifying Palmén's views on the physical processes responsible for Hazel's ferocity, utilizing a limited area numerical model. Yet this work failed to accurately capture the track and phase speed of the cyclone. Studies on other cases have strived to address the forecasting dilemma associated with the ET, as shown for example by Henderson et al. (1999) in the instance of Hurricane Opal. Opal's poorly forecasted northward motion led to an underestimation of the expected time of landfall, thereby reducing the warning time for individuals in the path of the intense storm. The availability of sophisticated models and abundant atmospheric data does not ensure a successful prediction of the cyclone.

The necessity of these studies is compounded by an investigation of the frequency with which the ET occurs. Hart and Evans (2001) created a climatology of the ET in the North Atlantic Ocean, from a record of tropical cyclones that occurred in the last half of the 20th century. The authors deduced that since 1950, 46% of these tropical cyclones have undergone an ET, or roughly one to two storms per year that affect the northeastern coast of North America. Furthermore, a closer examination of 61 extratropical transformations from 1979 to 1993 reveals that 51% of these storms intensify after the transition. These findings support the contention that an analysis of the dynamic and thermodynamic properties of a storm such as Hurricane Hazel is essential to improving the treatment of the ET by numerical weather prediction models. An accurate representation of the precipitation intensity and track of the ET reduces the threat posed to people directly in the line of the storm by providing ample warning and a true sense of the seriousness of the event.

1.2 Objectives

The focus of this research is to discern the crucial dynamics associated with Hurricane Hazel. Elucidating these properties will aid in the improvement of numerical predictions of similar weather events, which is essential to mitigating the vast destruction and fatalities that often befall these situations. A specific format to accomplish this goal will be adhered to, and is presented in the following discourse.

A discussion of the atmospheric conditions during the occurrence of Hazel is first conducted, to potentially flag crucial features contributing to this powerful storm. To further isolate the important components of Hurricane Hazel, an analogue search is executed. This analogue search will result in a comparison of the atmospheric fields relevant to Hazel and the best analogues found. Differences between the atmospheric states of Hazel and the analogues will be examined to determine if the dissimilarities can account for the intensity and severity of Hazel. Searches of this sort can often uncover subtle information not easily recognized by an analysis of standard meteorological variables (Gyakum and Roebber 2001).

The third aspect of this research involves the application of the MC2 (Mesoscale Compressible Community Model). Utilization of the MC2 will help resolve the mesoscale dynamic and thermodynamic features of Hazel. Successfully reproducing the ET with the accompanying frontogenesis and heavy precipitation over Ontario will allow for sensitivity testing. Sensitivity to an increased spatial resolution and to model initializations with an improved structure of the offshore vortex of Hazel to replace the initially poorly resolved vortex will be scrutinized. By conducting these simulations, one hopes to definitively identify the factors driving the intensity and location of the precipitation associated with Hurricane Hazel.

1.3 Event description

Hurricane Hazel developed in an easterly wave early on the 5th of October 1954 in the Eastern Caribbean Sea as a tropical storm (Davis 1954). From October 5th to 10th Hurricane Hazel steadily grew in strength as the storm tracked through the West Indies, peaking as a category four hurricane on the Saffir-Simpson scale (Simpson 1976). Sustained winds approached 60 m s^{-1} in this mature storm. At this point Hazel began to weaken, and by the 11th had stalled south-southeast of Jamaica after the westward motion was significantly reduced (NHC 2003). A pronounced northward component to Hazel's motion was becoming evident on the 12th and 13th, with Hazel passing over Haiti and inflicting a deadly blow on the country as the loss of life was estimated at nearly 1000 individuals (Davis 1954). Early of the 14th Hurricane Hazel was tracking towards the United States from a position north of Cuba (Mason et al. 1955). Reintensification was underway during this movement towards the United States, accompanied by stronger winds and heavy precipitation. The eye of the hurricane made landfall near Myrtle Beach, South Carolina at approximately noon on the 15th (Knox, 1955).

Meanwhile, Knox (1955) describes the synoptic situation in central and eastern Canada on the 14th. A cold front was tracking progressively across southern Ontario, associated with a cyclone in northwestern Ontario that was advecting a large mass of cold air into the U.S. Midwest. The motion of this front steadily diminished as the day went on and by the morning of the 15th the front had stalled in a north-south orientation east of the city of Toronto, Ontario and remained in this position for the remainder of the day (Fig. 1.3.1a). This deceleration was primarily due to an enhancement in the strength of the Bermuda high pressure system over the Atlantic Ocean, creating a block over eastern Canada. Massive amounts of ridging occurred rapidly over northern Quebec to promote this blocking.

Shifting the focus back to Hurricane Hazel, Mason et al. (1955) notes that the storm was moving through Virginia and into Pennsylvania by the evening of the 15th. At this stage it is pointed out that a clearly observable eye was no longer present in the hurricane, apparently lost in the Appalachian mountain range. Later on the 15th of

October a center was identifiable again, but further north in Pennsylvania. Data from the National Hurricane Center during this time period indicates that Hazel was no longer a tropical system, as at 1800 UTC on the 15th they issued an extratropical storm status to the transformed storm. This pinpoints the approximate time of the extratropical transformation of Hurricane Hazel. An assessment by Knox (1955) at this time mentions the rapid deepening occurring to the north of the hurricane vortex center, in the direction of the extratropical cyclone located over northwestern Ontario. By 0300 UTC on the 16th, the extratropical low pressure system and the hurricane remnants are no longer separately distinguishable entities, having merged into the new low center over northern Pennsylvania.

Around 0030 UTC, the new storm center was situated south of Buffalo, New York (Mason et al., 1955). Transformed storm Hazel still retained the strong northward motion, moving towards Toronto while reintensifying significantly. The previously stalled cold front now regressed to a position west of Toronto by 0100 UTC on the 15th (Fig. 1.3.1b). The following three hours produced the most significant and damaging precipitation, along with sustained winds of over 25 m s^{-1} and wind gusts of nearly 33 m s^{-1} (Knox, 1955). The near stationary cold front resulted in sizeable amounts of convective rainfall over the city (Palmén, 1958). Figure 1.3.2, adapted from Mason et al. (1955), shows the track and timing of Hazel's progress over North America.

Major flooding due to the rains from Hazel was the primary cause of the deaths in southern Ontario (Mason et al. 1955). Mason et al. (1955) looked at the circumstances in the few weeks prior to the occurrence of Hazel. Rainfall in Toronto and surrounding areas was well above normal for late September and early October in 1954, possibly as

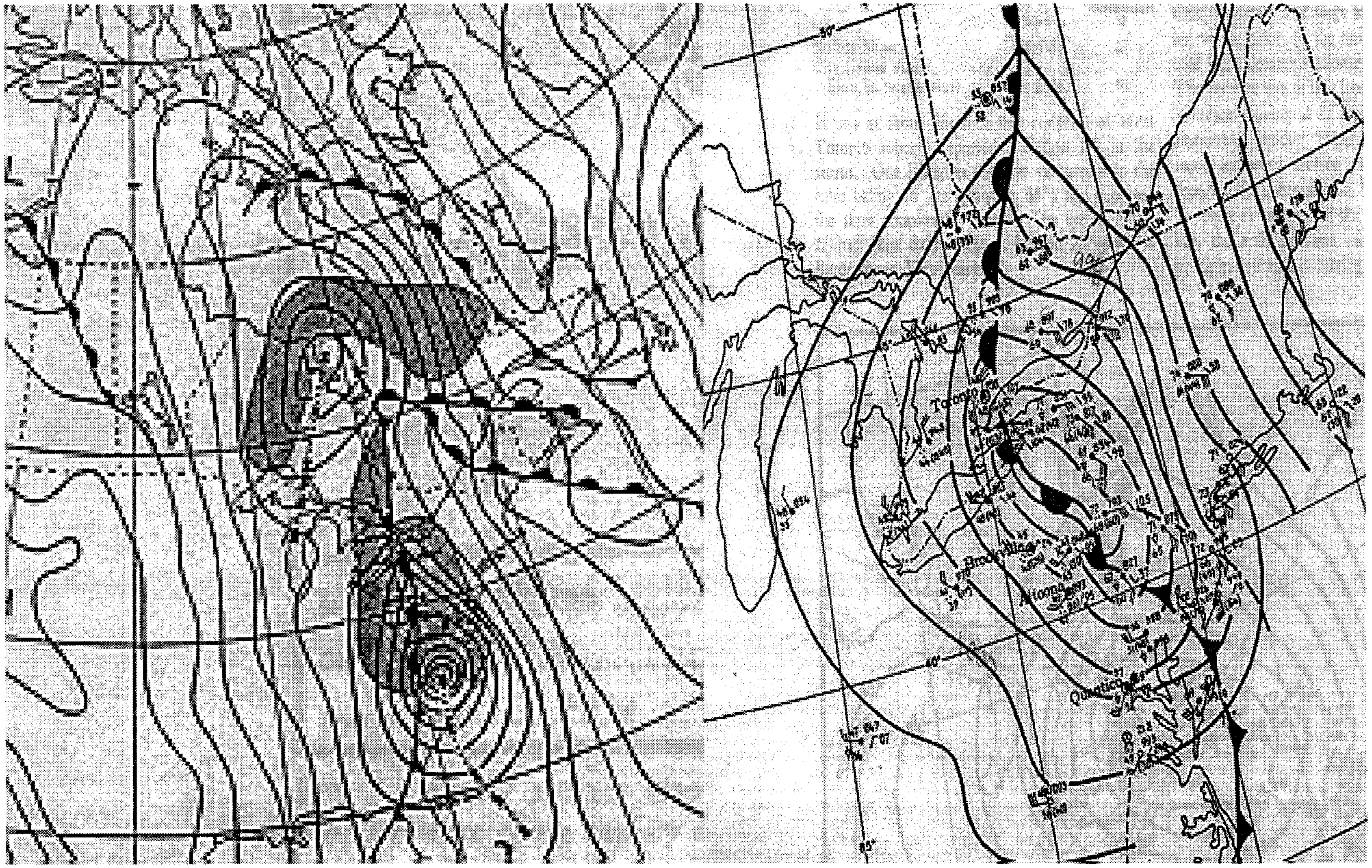

Fig. 1.3.1. (a) surface map at 1830 UTC 15 October from Knox (1955); (b) surface map at 0030 UTC 16 October from Knox (1955).

much as 149% above mean values. This excess precipitation would suggest that soil moisture would be in surplus, bringing about the saturation of the ground before the storm. The coming rains from Hazel would largely become surface runoff and overland flow. Consider the situation at Brampton, Ontario for an example of the magnitude of this water runoff. Hazel dumped 178 mm of rain on this city during October 14^{th} to 15^{th}, which translates to an enormous volume of water inundating low-lying areas.

This was indeed the case as the Humber, Don and Credit River valleys, along with the Holland Marsh all experienced tragic flooding as a result of the rains from Hazel.

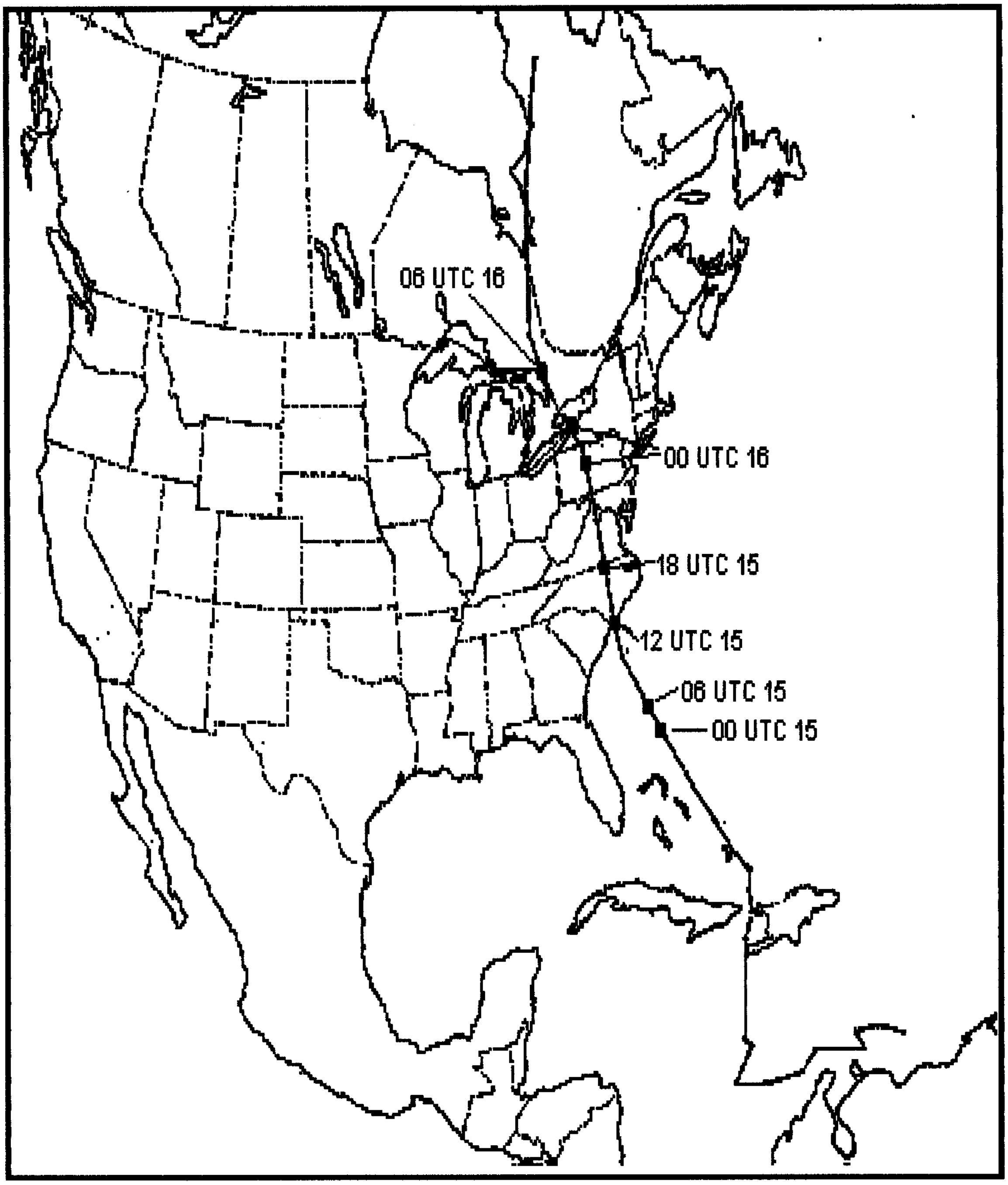

Fig. 1.3.2. Path of the storm Hazel, 6 October – 17 October 1954, adapted from Mason et al. (1955) .

2. Theoretical Concerns for Synoptic Analysis

2.1 Sea level pressure

In order to calculate the sea level pressure (hPa), UCAR (2003a) provides equation (2.1.1):

$$slp = 1000 \exp\left(\frac{z_{1000}}{1.5422885\,(z_{500} - z_{1000})}\right) \tag{2.1.1}$$

where z_{1000} is the 1000 hPa height (m) and z_{500} is the 500 hPa height (m). This formula is based on the hypsometric equation, where the thickness between the 500 hPa and 1000 hPa levels supplies the mean temperature field (Bluestein 1992).

2.2 Equivalent potential temperature

The equivalent potential temperature (θ_e) is determined as the resultant temperature achieved by a parcel of air that first undergoes a dry adiabatic lift to the lifting condensation level. This is followed by a pseudo-wet adiabatic (with respect to water saturation) lift to an elevation such that all condensate precipitates out of the parcel, and is then returned to the 1000 hPa level by means of a dry adiabatic process (Bolton 1980). Bolton (1980) provides an empirically derived formula to calculate this quantity, shown in equation (2.2.1):

$$\theta_e = T_K\left(\frac{1000}{p}\right)^{0.2854\left(1-0.28x10^{-3}r\right)} \exp\left[\left(\frac{3.376}{T_L} - 0.00254\right) r\left(1 + 0.81x10^{-3}r\right)\right] \tag{2.2.1}$$

where p is the pressure (hPa), r is the mixing ratio (g/kg) and T_K is the temperature (K). All of the aforementioned variables are measured at the start of the dry adiabatic lifting process. T_L is the temperature at the lifting condensation level, and is found by means of equation (2.2.2):

$$T_L = \frac{1}{\frac{1}{T_D - 56} + \frac{\ln(T_K/T_D)}{800}} + 56 \qquad (2.2.2)$$

which requires information about T_D, the dewpoint temperature (K), from the lift initiation point. Values of mixing ratio necessary to determine the equivalent potential temperature can be obtained through a series of equations. First, the saturation vapour pressure (hPa) must be calculated from equation (2.2.3) (Bolton 1980):

$$e_s(T) = 6.112 \exp\left(\frac{17.67\,T}{T + 243.5}\right) \qquad (2.2.3)$$

with T representing the temperature (°C). Employing the saturation vapour pressure in conjunction with equation (2.2.4) (Rogers and Yau 1996) yields the value of the mixing ratio (kg/kg):

$$w_s = \frac{\varepsilon\, e_s(T)}{p - e_s(T)} \qquad (2.2.4)$$

where ε is a constant valued at 0.622. The mixing ratio is the mass of water vapour (kg) contained in one kilogram of dry air.

2.3 Coupling index

Coupling index (CI) is a measure of bulk atmospheric stability, calculated with equation (2.3.1):

$$CI = \left(\theta_{DT} - \theta_{e,850\,hPa}\right) \qquad (2.3.1)$$

where θ_{DT} is the potential temperature at the dynamic tropopause and θ_e is the equivalent potential temperature at the 850 hPa level. A negative or small positive value of coupling index defines an area that is susceptible to convective (potential) instability (Bosart and Lackmann 1995). Strictly speaking, convective instability is defined by (2.3.2) (Rogers and Yau 1996):

$$\frac{\partial \theta_e}{\partial z} < 0 \tag{2.3.2}$$

where z represents height (m). The use of potential temperature in place of equivalent potential temperature at the dynamic tropopause in equation (2.3.1) is acceptable as the miniscule amount of moisture at this level will render the two quantities approximately equal (Bluestein 1993).

2.4 Dynamic tropopause mapping

An assessment of the atmospheric conditions is conducted using PV (potential vorticity) analysis, a technique first championed by Hoskins et al. (1985). The distinct advantage of this procedure lies in the conservative nature of PV. Advective processes in a frictionless and adiabatic flow only alter distributions of PV on isentropic surfaces (McTaggart-Cowan et al. 2001). A disadvantage of this method is that it requires the plotting of multiple isentropic levels to comprehend the three dimensional structure and evolution of the PV (Morgan and Nielsen-Gammon 1997). This problem can be readily circumvented by constructing dynamic tropopause maps.

The dynamic tropopause is defined for the purposes of this study as the 1.5 PVU (potential vorticity unit) surface. A PVU is $10^{-6}\ m^2 \cdot s^{-1} \cdot K \cdot kg^{-1}$. Near the 1.5 PVU level in the atmosphere the gradient of potential vorticity on an isentropic surface is largest, delineating the zone separating large PV values in the stratosphere from smaller tropospheric PV values (Bosart and Lackmann 1995). To obtain values of PV, equation (2.4.1) (Bosart and Lackmann 1995, Henderson et al. 1999, Durnford 2001) calculates Ertel's (1942) PV:

$$EPV = -g\frac{\partial\theta}{\partial p}\left(f + \frac{\partial v}{\partial x} - \frac{\partial u}{\partial y}\right) + g\left(\frac{\partial v}{\partial p}\frac{\partial\theta}{\partial x} - \frac{\partial u}{\partial p}\frac{\partial\theta}{\partial y}\right) \qquad (2.5.1)$$

where f is the Coriolis parameter, v is the meridional wind, and u is the zonal wind.

A vertical interpolation of potential temperature onto the dynamic tropopause allows for an examination of the advection of potential temperature (or similarly pressure) at this level to identify regions of ascent or descent. Ascent coincides with advection of low potential temperatures (or high pressures) on the dynamic tropopause, with the opposite holding true for descent (Bosart and Lackmann 1995). A region of lower (higher) potential temperatures on the dynamic tropopause has structure analogous to a positive (negative) PV anomaly, with a counterclockwise (clockwise) flow induced around the anomaly in the Northern hemisphere (Morgan and Nielsen-Gammon 1997). Strong gradients of dynamic tropopause potential temperature (or pressure) imply a steeply sloping tropopause, revealing the location of important baroclinic zones and significant upper level features such as jets and troughs (Nielsen-Gammon 2001, Bosart and Lackmann 1995). The interpolation of other useful variables such as wind onto the dynamic tropopause can also be accomplished with this technique, to produce a complete two dimensional picture of the meteorological state of the atmosphere at the dynamic tropopause (Morgan and Nielsen-Gammon 1997).

Arising from this method is a significant complication, encountered when the tropopause becomes folded. A fold is created by an extreme undulation in the PV distribution, such that multiple instances of equally valued PV occur at different isentropic surfaces in a given vertical profile. The level of the dynamic tropopause in this situation is then determined by the choice of search direction for the 1.5 PVU surface, that is either upward or downward (Morgan and Nielsen-Gammon 1997). Searching from the top of the atmosphere will yield a higher dynamic tropopause than a search initiated from the surface. In this study, a search from the top of the atmosphere towards the surface is chosen.

A succinct assessment of the dynamics of the whole troposphere can be achieved by applying the Eady model perspective (Eady 1949). Utilizing maps of potential temperature at the dynamic tropopause and near the boundary layer yields a qualitative assessment of the characteristics of the troposphere flow. For this study, the 850 hPa level potential temperature is subjectively chosen to be representative of the boundary layer potential temperature. Diabatic processes must be accounted for when using the Eady model view, as diabatically created PV in the lower troposphere can trigger the development of significant dynamic structures. Potential temperature at the surface behaves in a similar fashion to potential temperature on the dynamic tropopause, except for a change in sign. Warm (cold) surface potential temperature pools are dynamically equivalent to cold (warm) dynamic tropopause potential temperature zones, in that they both are associated with ascending motion. Regions of non-conservative PV distributions on the dynamic tropopause can be isolated as regions where redistribution of potential temperature occurs in the presence of non-advective (i.e. diabatic) processes (Morgan and Nielsen-Gammon 1997).

2.5 Data sources

The NCEP/NCAR reanalysis data were utilized to obtain the necessary atmospheric fields for analysis in this study (Kalnay et al. 1996, Kistler et al. 2001). Globally gridded data is provided at 144 x 73 grid points and on 17 pressure levels, yielding a horizontal resolution of 2.5° latitude and longitude. Over the reanalysis period the data assimilation system is kept constant, removing climatic changes solely attributed to modifications in the assimilation scheme (Kalnay et al. 1996). System dependent discontinuities may still arise depending on the availability and quality of standard meteorological data and remotely sensed data (Nielsen-Gammon 2001). For the period of 1948-1957, upper air data was conducted three hours earlier than current synoptic times and at fewer locations, rendering the reanalysis less reliable for this time frame (Kistler 2001 et al.). The majority of these sparse observations were conducted in the Northern Hemisphere (Kistler et al. 2001).

Variables from the reanalysis data fall into four different categorizations, based on the level of relative influence imposed on the variable by the observational data and the model output. In this project only A and B type variables are used. Class A quantities are highly verifiable as they are mainly influenced by observations, whereas class B quantities rely slightly more on the model characteristics (Kalnay et al. 1996).

A multitude of data sources were used to compile a comprehensive set of surface precipitation observations. The National Climatic Data Center (NCDC) provided measurements from the Global Climate Observing System (GCOS) Surface Network (NCDC 2003). Columbia University furnished precipitation records from the Global Historical Climate Network (Columbia 2003). The University Corporation for

Atmospheric Research (UCAR) rendered information from the U.S. First Order Summary of the Day, U.S. Control Cooperative Hourly Precipitation, Air Weather Service (AWS) Global Surface Observations, and the Canada Summary of the Day (UCAR 2003b). A final contribution from the Meteorological Service of Canada's National Climate Data Archive afforded a detailed set of daily precipitation amounts (EC 2003). Radiosonde data produced jointly by the Forecast System Laboratory (FSL) and NCDC proffered measurements of upper air variables for North and Central America (FSL-NCDC 1993).

Processing and display of all the aforementioned data was done with use of GEMPAK (General Meteorological Package) (Koch et al. 1983). A Barnes objective analysis (Koch et al. 1983) was performed on the surface and upper air data with GEMPAK to interpolate the non-uniform station data points to uniform grid points. Contouring of the gridded data was subjectively conducted to yield sufficient detail in the atmospheric field.

3. Synoptic Overview

3.1 Mapping parameters

Hurricane Hazel tracks over a broad portion of the Northern Hemisphere during the first half of October 1954. The time of most interest to this study is centered on the extratropical transition of Hazel, namely the 15^{th} and 16^{th} of October 1954. Data were used in 12-hourly increments, comprising a 36-hour period from 00 UTC 15 October to 12 UTC 16 October. A domain spanning 20°N to 60°N and 50°W to 110°W sufficiently captures all of the dynamics and thermodynamics relevant to this event. The diagrams and discussion accompanying the analyses will be limited by the range of these parameters.

3.2 Surface synoptic overview

At 00 UTC 15 October 1954, the sea level pressure field over eastern North America is dominated by the vortex attributed to Hurricane Hazel (abbreviated as HH) centered over the Bahamas, an extratropical low pressure system over the Great Lakes (GLL), and a large high pressure system located near Bermuda (BH) (Fig. 3.2.1a). A pronounced thermal ridge exists in the thickness field east of the GLL, along with a discernable thermal trough to the west. A slight warm core structure can be made out in Hazel from the circular thickness contour running nearly parallel to the sea level pressure isobars. The BH exhibits some ridging into the lower St. Lawrence River valley, reinforcing the highly meridional flow pattern at this time. Ridging from BH also can be seen into Virginia. Strong flow occurs to the east and west of the GLL, and symmetrically around HH. No signs of interaction are obvious between the GLL and HH at this point in time.

In the following 12 hours up to 12 UTC 15, the interaction between HH and the GLL begins (Fig. 3.2.1b). As HH moves to a position southeast of South Carolina and the GLL moves towards James Bay, a closing of the distance separating the two features occurs. The flow is decidedly more meridional as the ridging into Virginia has weakened noticeably, and significantly strengthened over Northern Quebec. Meanwhile, a ridge has protruded from the high over the Rocky Mountains towards the Great Lakes, raising the sea level pressures considerably. The disappearance of the zonal current leads to the development of a block, as noted by Knox (1955). Specifically, this block is a stationary, high-amplitude ridge (Bluestein 1993). A southeasterly flow over North Carolina advects warm, moist oceanic air over the continent in advance of HH. Deformation of the thickness field continues, leading to a near meridional orientation over the Great Lakes. Thicknesses have risen by roughly 8 dam over Quebec, and fallen nearly 16 dam over the U.S. Midwest.

A distinct transformation of the sea level pressure field results at 00 UTC 16. A strengthened entity over Pennsylvania is composed of the remnants of HH, the now extratropical, transformed storm Hazel (ETH) (Fig 3.2.1c). The GLL has lost its circular appearance and filled slightly, translating to a position over Hudson Bay in the process. ETH has deepened markedly as a consequence of the thickness decreases taking place to the northwest of HH at 12 UTC 15. A strengthened meridional geostrophic wind is present around ETH, further promoting the deformation of the thickness field by displacing higher thickness values over the southeast and lower thickness values over northern Quebec. ETH no longer retains a visible warm core structure, and a cutoff cold pool of air is visible in the thickness field over Illinois. A compaction of the thickness contours occurs over these first 24 hours, along with the meridional elongation of this field. The orientation of the enhanced atmospheric flow to the east of ETH drives more moisture-laden air into southern Ontario, providing a rich source for the devastating precipitation.

The extratropical storm rapidly moves into northern Ontario by 12 UTC 16. Zonal flow becomes re-established in southern Ontario, as the meridionally directed region of flow progresses into northern Quebec (Fig. 3.2.1d). Removal of the blocking ridge follows, as the BH moves to a position over Newfoundland. A large body of isolated low thickness is situated over the eastern United States, and the extent of the thermal ridging over northern Quebec has increased.

Objectively analyzed surface data from radiosonde stations at the synoptic times of 1954 (i.e. 03 UTC and 15 UTC) are also shown in Fig. 3.2.2. At 03 UTC 15 the sea level pressure field displays similarities to the 12 UTC 15 field from the NCEP/NCAR reanalysis, as a col has formed near Virginia (Fig. 3.2.2a). The thickness plot exhibits the familiar elongated and meridional pattern. Sea level pressures are also very comparable to the NCEP/NCAR reanalysis values. By 15 UTC 15 the observed sea level pressure structure (Fig. 3.2.2b) resembles the 00 UTC 16 NCEP/NCAR reanalysis field, whereas the thickness is more closely related to the reanalysis at 12 UTC 15. Comparing the locations of ETH and HH in the observations at 15 UTC 15 to the 00 UTC 16 reanalysis information shows a slightly farther west ETH and south HH, consistent with the known patterns of motion.

A final set of measurements for 03 UTC 16 confirms the severity of the situation

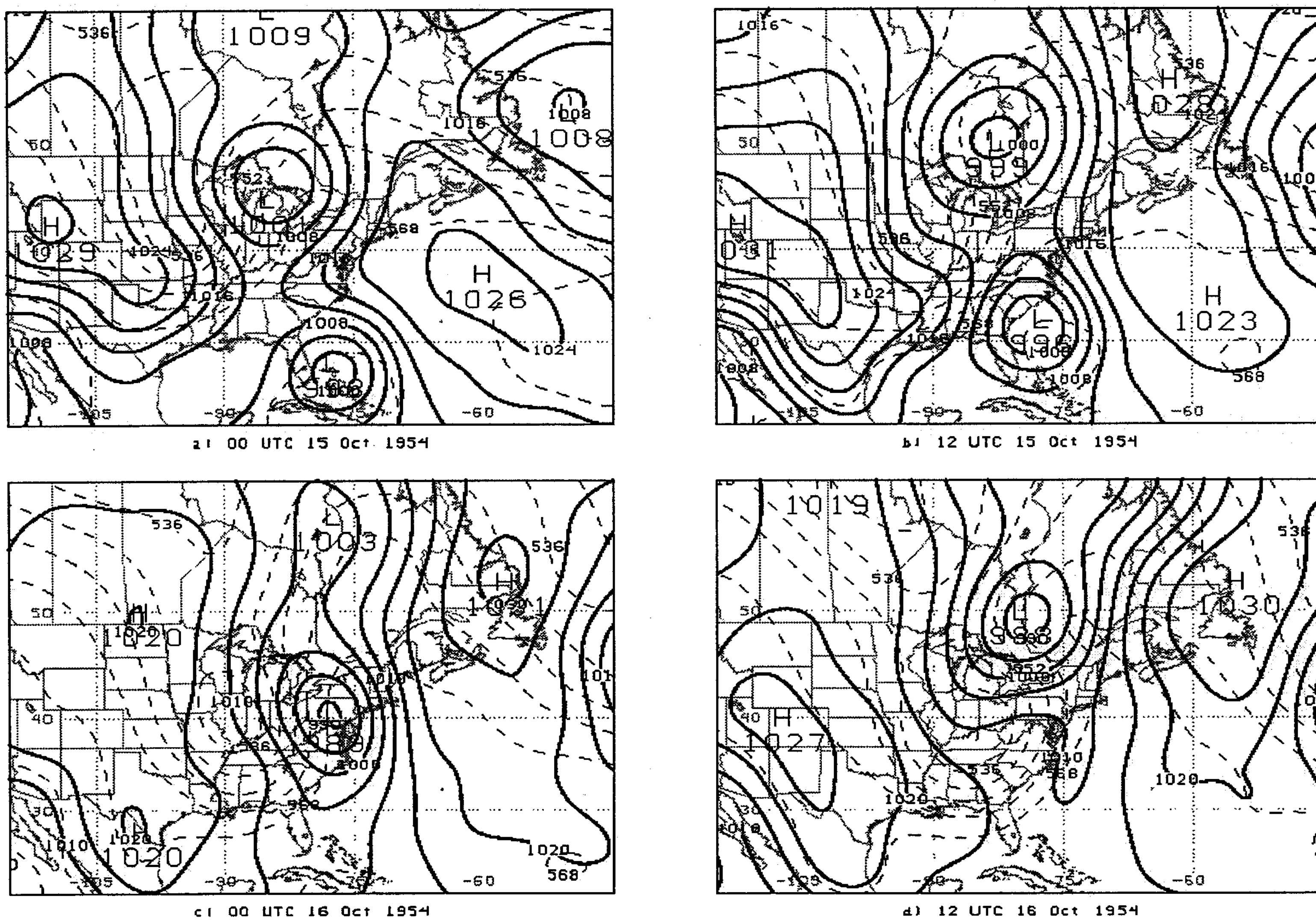

Fig. 3.2.1. Sea level pressure (solid, contour interval of 4 hPa) and 1000-500 hPa thickness (dashed, contour interval of 8 dam).

in southern Ontario (Fig. 3.2.2c). ETH is located west of Toronto, with increasing pressure to the east over Quebec. Comparing the orientation of the trough at this time with the reanalysis at 00 UTC 16 and 12 UTC 16, one can see a difference as the trough in the objective analysis is reaching towards the southeast. NCEP/NCAR plots display a southwest pointing trough at 00 UTC 16, and a weakened trough at 12 UTC 16. Thickness fields for the observations at 03 UTC 16 and reanalysis at 00 UTC 16 shows convincing agreement in the form of a cutoff pool of low thickness established over Illinois.

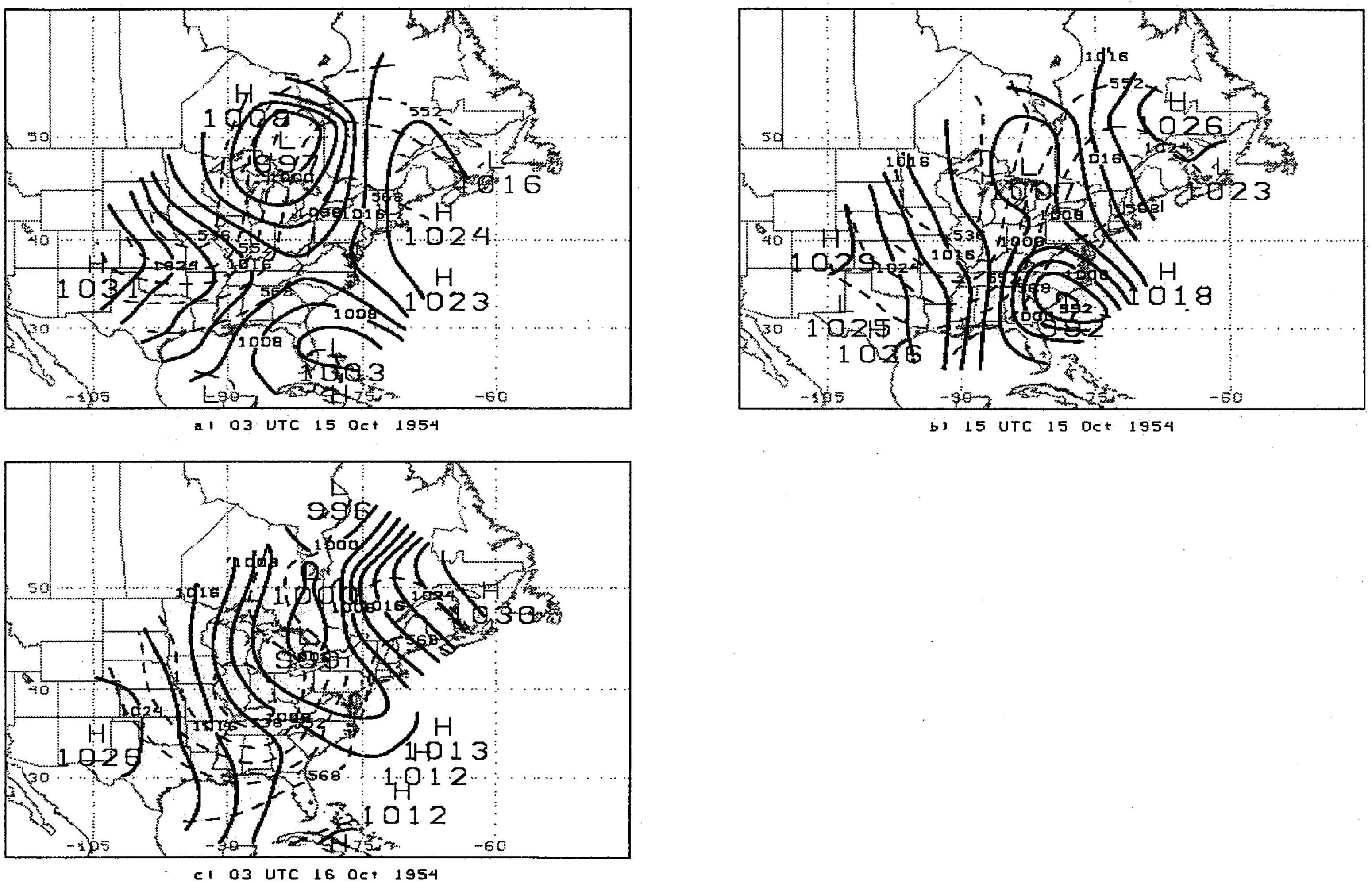

Fig. 3.2.2. Objectively analyzed sea level pressure (solid, contour interval of 4 dam) and 1000-500 hPa thickness fields (dashed, contour interval of 8 dam).

3.3 Upper level synoptic overview

Hurricane Hazel is distinguishable near the east coast of Florida at 00 UTC 15 (Fig. 3.3.1a) and begins to interact with the midlatitude trough by 12 UTC 15, shown by the bulge in the contours over the southeastern U.S. (Fig. 3.3.1b). One can see that Hazel's associated structure is not yet in the baroclinic zone in Fig. 3.2.1b, yet by 00 UTC 16 Hurricane Hazel is no longer identifiable, and a large cutoff forms in the deepening trough center south of Lake Michigan (Fig. 3.3.1c). A four dam drop in height is visible in the center of the high amplitude trough. Little change is evident at 12 UTC 16 (Fig. 3.3.1d), with the exception of continued southeastward movement of the atmospheric pattern visible at 00 UTC 16.

Objectively analyzed observations of the geopotential and thermal fields for 03 UTC 15 at 500 hPa confirm the veracity of the reanalysis fields, exhibiting an inland movement of the warm air mass near the Carolinas (Fig. 3.3.2a). Hurricane Hazel is evident at 15 UTC 15 as a sharp trough over the Carolinas and the Atlantic Ocean, and also as a pool of higher temperatures coming inland at South Carolina (Fig. 3.3.2b). Cold air continues to move over the Midwest from the northwest. A final analysis at 03 UTC 16 places a large cutoff of low pressure near the southern extent of Lake Michigan, with an isolated cold region to the southwest of the cutoff low pressure (Fig. 3.3.2c). Hazel is no longer distinguishable as a hurricane at this time, with the previously observed warm core characteristics and sharp trough over the Carolinas at 15 UTC 15 no longer present at 03 UTC 16. A highly baroclinic system is in place over the continent. At the highest levels of the atmosphere we see a picture that still contains a perceptible Hazel. Noticeable at the 250 hPa level is a closed contour of 235 K over the Bahamas at 00 UTC

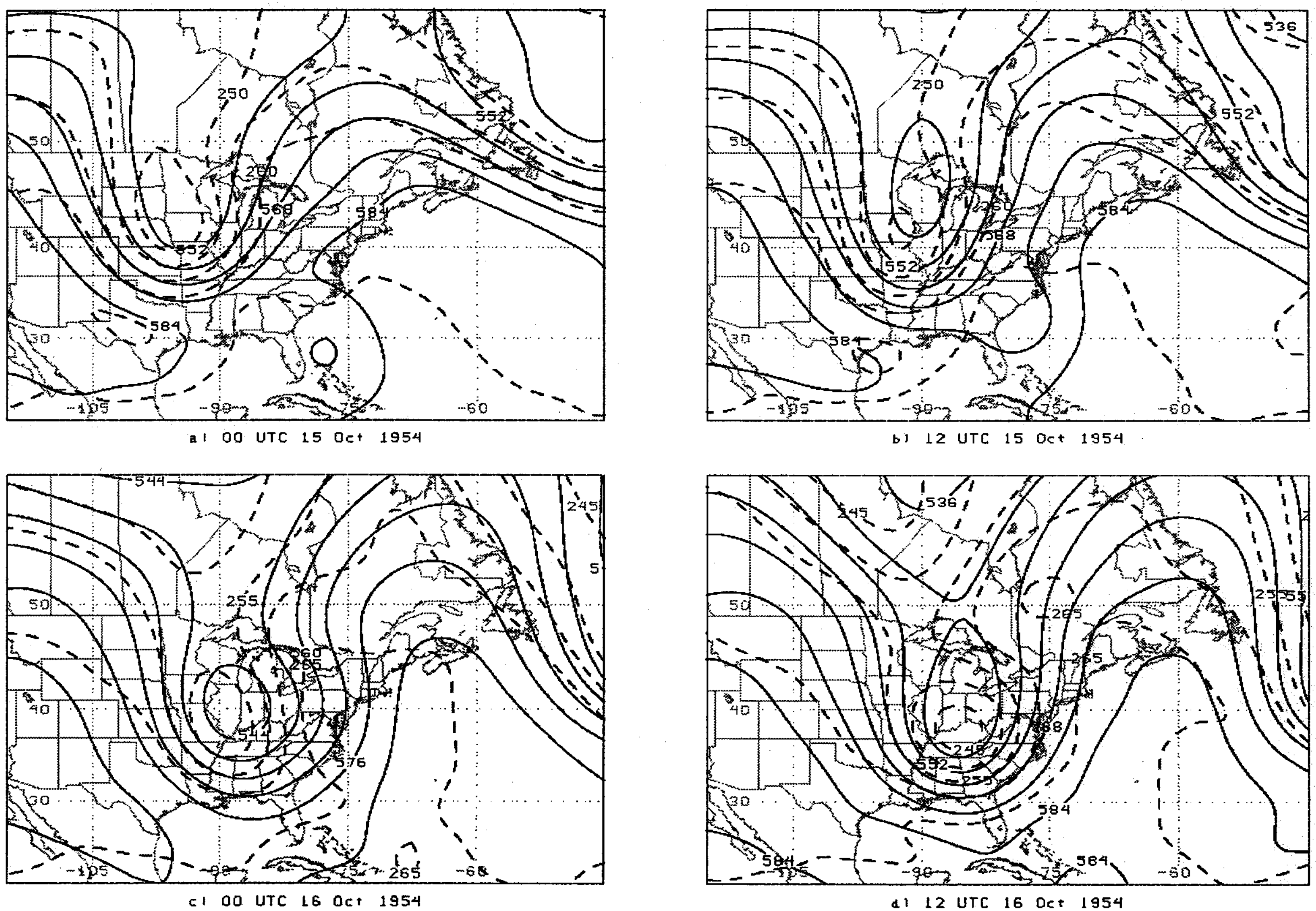

Fig. 3.3.1. 500 hPa heights (solid, contour interval of 8 dam) and temperatures (dashed, contour interval of 5 K).

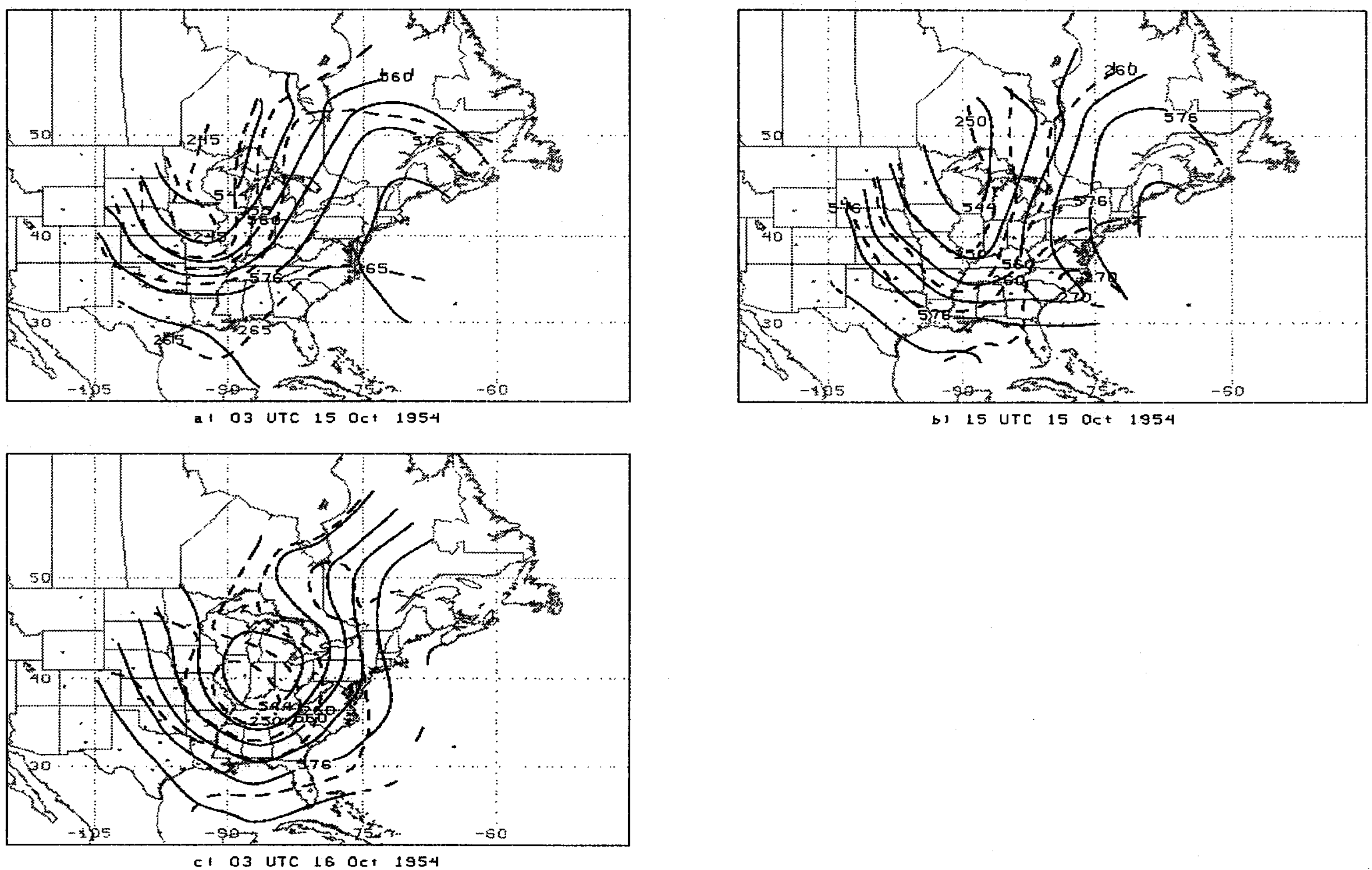

Fig. 3.3.2. Objectively analyzed 500 hPa heights (solid, contour interval of 8 dam) and temperatures (dashed, contour interval of 5 K).

15, moving progressively towards the continent (Fig. 3.3.3a). The same contour is then located south of Lake Michigan at 00 UTC 16, coinciding with the baroclinic zone beneath the midlatitude trough (Fig. 3.3.3c). This baroclinicity is responsible for the steady dissipation of the warm core structure of the hurricane (Bosart and Lackmann 1995). Identification of the position of the jet streaks and Hurricane Hazel at this level finds the hurricane vortex located in the right entrance region at 12 UTC 15 (Fig. 3.3.3b) and 00 UTC 16, leading to strong quasigeostrophic forcing for ascending motion (Bluestein 1993).

Comparison of the reanalysis at 250 hPa with the objectively analyzed data from observations at the same level again confirms the reliability of the analysis. The synoptic situation at 03 UTC 15 (Fig. 3.3.4a) has few differences from the reanalysis at 00 UTC 15. Hazel's dynamic and thermodynamic signature is visible as a weak trough and warm pocket of air near the Carolina coast by 15 UTC 15 (Fig. 3.3.4b). A negative trough tilt in the 03 UTC 16 pressure field and the distinct warm zone south of the Great Lakes (Fig. 3.3.4c) agrees with the development in the reanalysis between 00 UTC 16 and 12 UTC 16. The temperature gradient west of the midlatitude trough has tightened considerably, and the positioning and extent of the low pressure center matches well with the reanalysis fields.

Throughout the 36 hour sequence the surface sea level pressure trough over the continent strongly advects cold air over the U.S. Midwest and warm air over the eastern seaboard, digging equatorward all the while. Initially stronger upstream jet-level winds create a cyclonic vorticity maxima that is advected southeast of the trough. This advection of cyclonic vorticity promotes height falls in the zone of advection, giving the

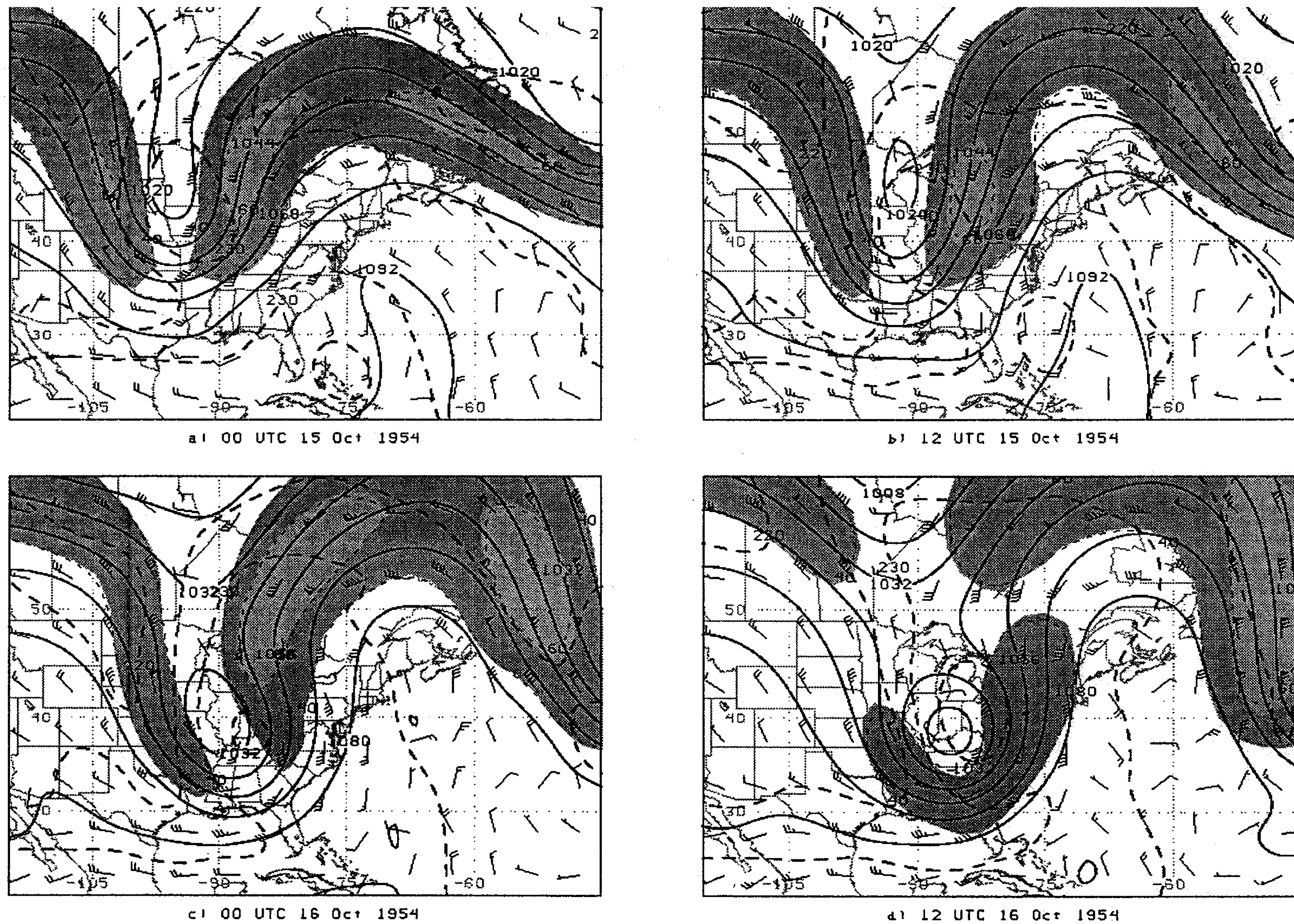

Fig. 3.3.3. 250 hPa heights (solid, contour interval of 12 dam), temperature (dashed, contour interval of 10 K), winds (m s^{-1}), and wind modulus (light shading, winds in excess of 30 m s^{-1}; dark shading, wind in excess of 50 m s^{-1}).

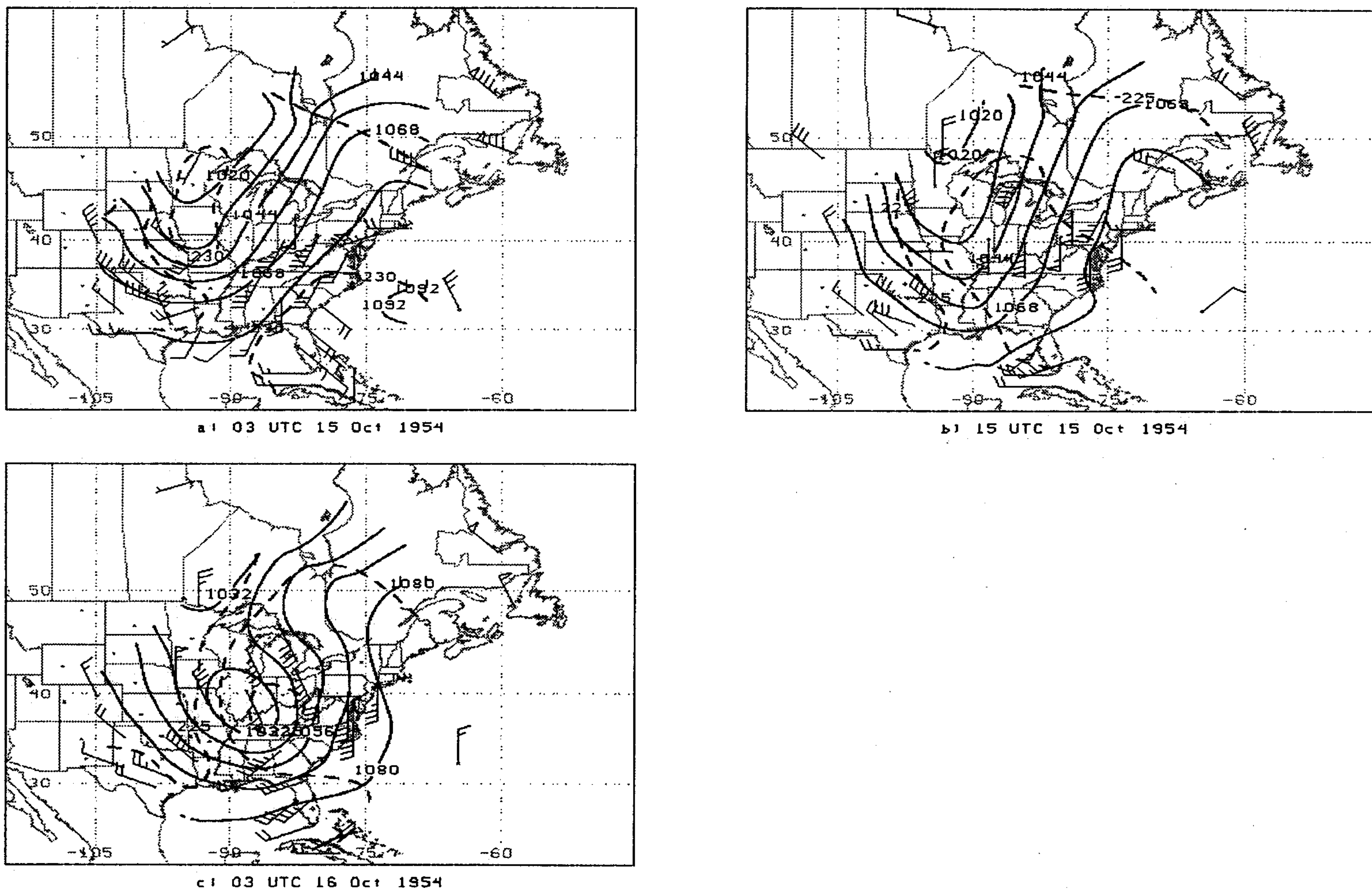

Fig. 3.3.4. Objectively analyzed 250 hPa heights (solid, contour interval of 12 dam), temperature (dashed, contour interval of 10 K), observed wind (m s^{-1}).

trough a prominent northwesterly component of motion (Bluestein 1993). Further, by 00 UTC 16 the trough gains a negative tilt, an orientation conducive to the equatorward flux of angular momentum. It is probable that this flux of momentum from the westerly midlatitude jet towards the equator could feed into a developing system via barotropic instability (Bluestein 1993). Negatively tilted troughs have been shown to be statistically linked to higher rates of convective activity than positively tilted troughs (Glickmann 1977).

Looking at a radiosonde profile for Washington/National, Virginia (DCA) at 15 UTC 15 discloses the structure of a nearby Hurricane Hazel, prior to extratropical transition (Fig. 3.3.5a). The sounding is that of a Miller Type II, with tropical characteristics such as a deep layer of high relative humidity, warm temperatures and a near moist adiabatic lapse rate (Bluestein 1993). Winds veer slightly in the lowest and highest atmospheric levels, suggesting that warm temperature advection is transpiring. These winds retain a strong southerly component to their motion throughout the profile, from the warm, moist sector of the hurricane circulation. Simultaneously surveying the atmospheric profile at Pittsburgh International, Pennsylvania (PIT) for 15 UTC 15 yields a very similar picture with one recognizable difference (Fig. 3.3.5b). Temperatures throughout the sounding are approximately 5°C to 10°C lower than at DCA, implying that the profile at PIT is more closely related to the Miller Type III sounding (Bluestein 1993). A Miller Type III sounding is often associated with cold core upper level cyclones and troughs, bearing more similarity to the GLL. A deep layer of saturation is present between 925 hPa and 700 hPa, and winds again tend to veer while maintaining a prominent southerly component of motion.

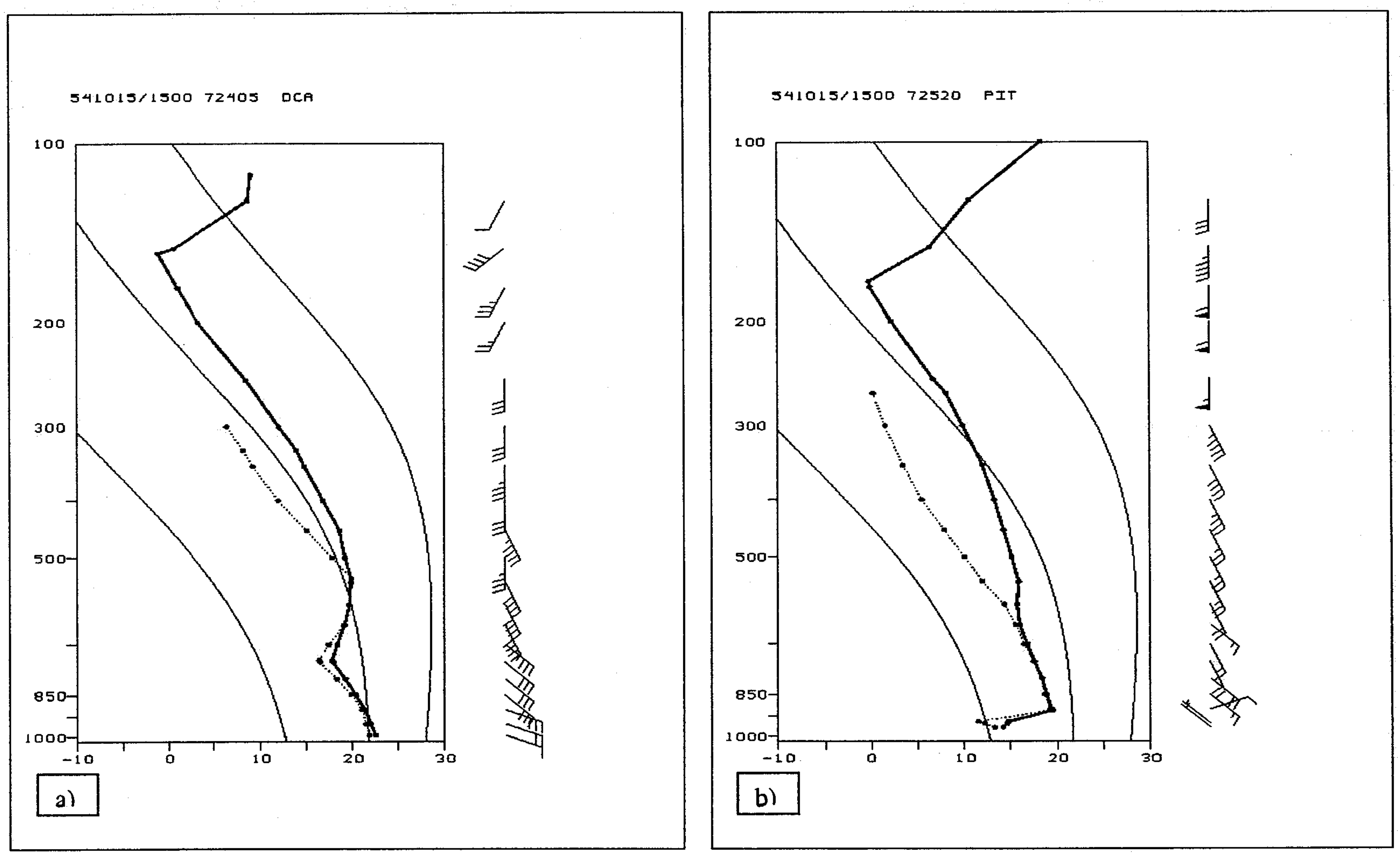

Fig. 3.3.5. Soundings of temperature (solid), dewpoint temperature (dotted) (units of K), and winds (flag is 25 m s^{-1}, large barb is 10 m s^{-1}, small barb is 5 m s^{-1}).

3.4 Moisture overview

Viewing the coupling index (CI) and precipitable water fields succinctly captures the condition of the atmosphere with respect to moisture. The CI at 00 UTC 15 reveals a very prominent region of low CI over the Midwest, indicative of a region susceptible to deep convection (Fig. 3.4.1a). The low CI values steadily track southeastward in the cold sector of the GLL and eventually the ETH (Fig. 3.2.1a). Possible mechanisms for the creation of the broad zone of weak layer stability includes subsidence in the presence of upper level convergence in the cold sector, which can lead to the development of acute potential instabilities (Huo et al. 1995). A strong gradient of CI is well established by 00 UTC 16 and persists for the duration of the event, again following a northwesterly path with time (Figs. 3.4.1c). The previously entrenched zone of convective instability works to establish this gradient as the strengthening area of higher CI values develops to the east.

Plots of precipitable water at the onset of the event demonstrate a distinct pattern, with values in excess of 50 mm near southern Florida attributed to Hurricane Hazel at 00 UTC 15 (Fig. 3.4.1a). Near the Quebec-Ontario border a tongue of precipitable water exceeds 30 mm, with an orientation suggesting a separation of the moisture sources for this region and Hurricane Hazel. A transition over the next 12 hours occurs as a steady channeling of the tropical precipitable water segment from Hazel takes place over the continent, visible in the streaming of values over 60 mm in North Carolina (Fig. 3.4.1b). The shifting alignment of the tongue into Ontario and Quebec positions the source region as the Atlantic Ocean at 12 UTC 15, and not the drier continent as at 00 UTC 15.

Following the extratropical transition, the precipitable water field is arranged such that the moisture is supplied from the Atlantic Ocean into Pennsylvania at 00 UTC 16 (Fig. 3.4.1c). For this event, the highest values around southern Ontario, New York State and Pennsylvania are observed at this time. Pennsylvania experiences precipitable water values approaching 50 mm, while Ontario and New York State see values of approximately 40 mm. The approaching cold front results in a rapid reduction in the quantity of precipitable water at 12 UTC 16, dropping by 30 mm in southern Ontario alone (Fig. 3.4.1d).

Having a substantial region of potential instability in close proximity to abundant atmospheric moisture can generate a set of ideal conditions for the occurrence of significant precipitation. This is true provided ample lifting coincides with this situation. To quantify the amount of lifting present, one can look at the work of Palmén (1958), who determined vertical velocities and horizontal convergence for 5° latitude by 5° longitude blocks in the path of the storm. In concluding the study, the author notes that there indeed was "slight mean convergence in the lowest atmospheric layers and divergence above 700 mb" (Palmén 1958). An overall pattern of this sort leads to a net upward vertical circulation, thereby unleashing the convective instability in the presence of large precipitable water values.

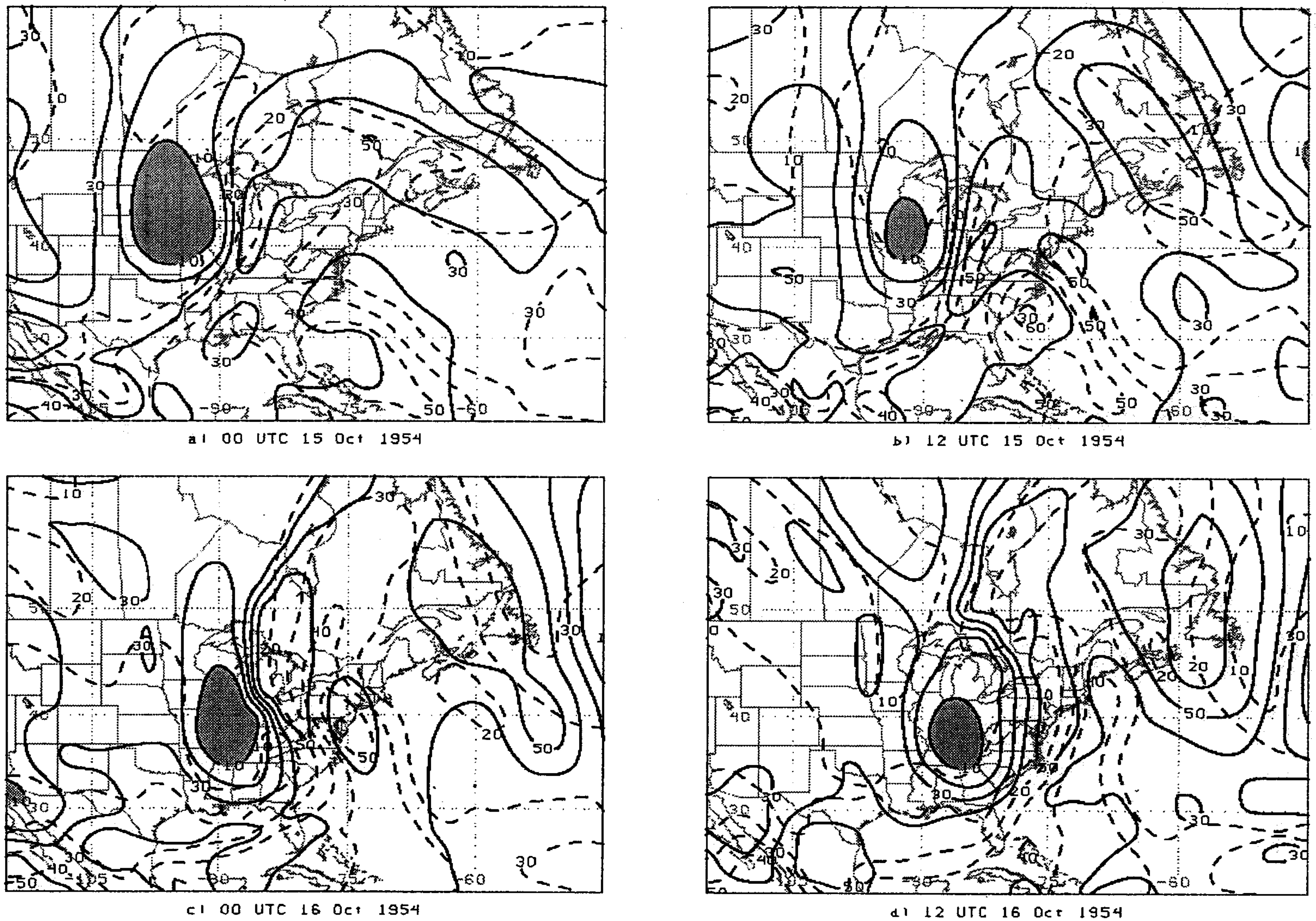

Fig. 3.4.1. Coupling index (solid, values below ten shaded) and precipitable water (dashed, contour interval of 10 mm).

3.5 Dynamic tropopause overview

A detailed understanding of the thermodynamic and dynamic characteristics of the atmosphere is readily available by examining the dynamic tropopause maps of this event. Starting at 00 UTC 15 the meridional potential temperature contours are highly compacted over Wisconsin and Illinois, implying a steeply sloping tropopause and revealing the location of the principal baroclinic zone in the atmosphere (Fig. 3.5.1a). The dynamic tropopause potential temperature field exhibits a high amplitude pattern with strong jet-like winds in excess of 65 m s^{-1} over Lake Superior. A cutoff pool of low dynamic tropopause potential temperature forms over Minnesota and is advected southeastward, forcing for ascending motion. Warm dynamic tropopause potential temperatures advected over Quebec drive descending motion in this region. Advection of warm near surface potential temperatures surrounding Florida concurrently create upward motion, with downward motion being generated over Manitoba by cool 850 hPa potential temperatures.

As time progresses to 12 UTC 15, the advection of low potential temperature on the dynamic tropopause continues towards the southeast U.S., along with a non-advective increase in potential temperature over northern Quebec (Fig. 3.5.1b). 850 hPa potential temperatures are further deformed, fashioning a lower level field that mimics the potential temperature distribution on the dynamic tropopause. Winds on the dynamic tropopause remain strong, blowing at roughly 60 m s^{-1} over Lake Erie. The amplitude of the potential temperature fields has increased while continuing to be aligned along a north-south direction.

Searching the plots at 00 UTC 16 provides a few new developments (Fig. 3.5.1c).

Over the Great Lakes the now intensely compacted dynamic tropopause potential temperature gradient has acquired a negative tilt, favouring cyclogenesis due to an increase in differential cyclonic vorticity advection (Atallah and Bosart 2003). Northwesterly movement of cool dynamic tropopause and 850 hPa potential temperatures has continued, and over northern Quebec large dynamic tropopause potential temperatures have pushed farther to the north. This northward progression is not caused by advection as briefly stated at 12 UTC 15. Dynamic tropopause winds in the vicinity of this growth run parallel to the contours of potential temperature, thereby not inducing an advective increase in potential temperature. A diabatic mechanism is responsible for the rise in potential temperature over Quebec, specifically latent heating in the outflow of Hurricane Hazel. Consequentially, an environment is created that is susceptible to the ongoing advection of low potential temperatures on the dynamic tropopause from the U.S. Midwest (Bosart and Lackmann 1995). Atallah and Bosart (2003) noted similar development in Hurricane Floyd (1999), as latent heating in the outflow eroded the northeast flank of the upstream midlatitude potential temperature trough and anticyclonic flow became prominent in the outflow region. Dynamic tropopause wind patterns around the trough in Hazel and Floyd are also alike, with along contour winds north of the low potential temperature pool and cross contour flow to the south. These mechanisms working in conjunction aid in the evolution of the tilt of the trough, making for a sharpening negative slope. In the proximity of James Bay winds on the dynamic tropopause have strengthened back to 65 m s^{-1} as a result of the deformation the potential temperature gradient.

At the last time interval 12 UTC 16, the gradient of dynamic tropopause potential temperature decreases slightly and becomes more uniform along the eastern edge of the midlatitude trough (Fig. 3.5.1d). This uniformity is a repercussion of reduced outflow from Hazel, as the extratropical transition has taken place well before this time. Reduced outflow from the system in turn abates the latent heating required for the powerful increase in potential temperatures seen earlier. Potential temperatures on the dynamic tropopause now only increase in the far north of Quebec and Labrador. Trough slope is still negative, and advection of the isolated low potential temperatures continues from the northwest into the Carolinas. Jet winds have dropped over the eastern seaboard to values near 50 m s^{-1} as the storm episode comes to an end.

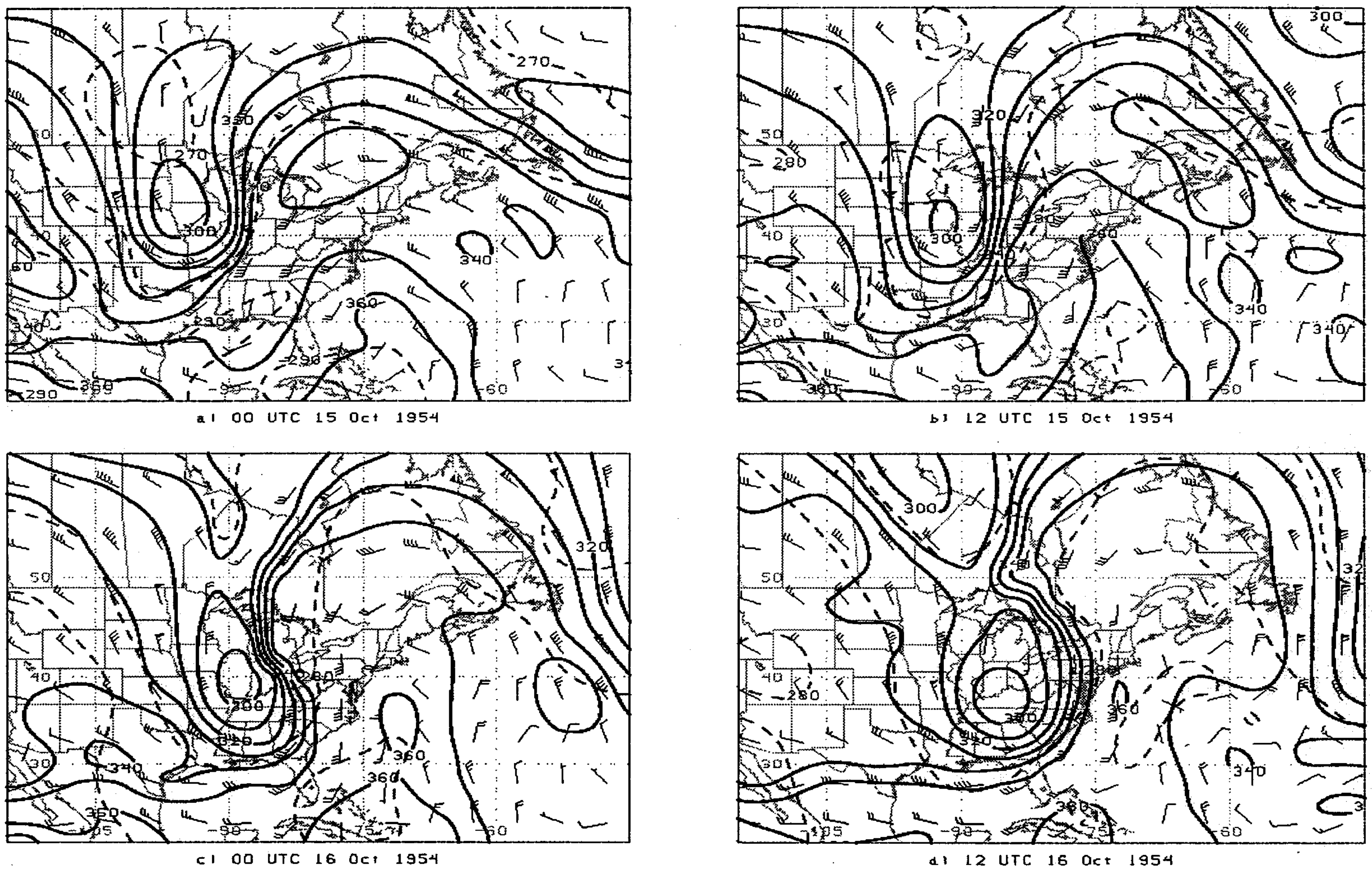

Fig. 3.5.1. Dynamic tropopause potential temperature (solid, contour interval of 10 K), winds on the dynamic tropopause ($m\ s^{-1}$), and 850 hPa potential temperature (dashed, contour interval of 10 K).

3.6 Precipitation

As mentioned in the introduction (Section 1.1), Hazel produced significant rainfall amounts along the landfall track and record accumulations in the Toronto region. Only results for the period from 00 UTC 15 to 00 UTC 16 are provided (Fig. 3.6.1a). Justification for this limited time frame is that the 24 hour period covering the 15th of October constitutes the maximum accumulation for stations from South Carolina to Ontario for this event, whereas by the 16th the storm has moved out of this range and precipitation amounts drop accordingly. An objective analysis of raw daily precipitation accumulation was conducted, exposing a highly meridional organization that correlates well with the path taken by Hazel (Fig. 1.3.1). A contour of 180 mm is defined near Myrtle Beach, South Carolina, Hurricane Hazel's point of landfall, and values in excess of 135 mm can be spotted near the North Carolina and Virginia border. Infrequent extreme values and an increased density of observations in Canada compared to the U.S. leads to an analyzed contour of 90 mm in southern Ontario, not reflecting the large magnitude of precipitation falling in selected locales near Toronto.

A surface frontal analysis by Knox (1955) for 2230 UTC 15 reveals a collocation of the precipitation and the cold front of the ETH (Fig. 3.6.1b). Maximum intensities were observed to be concentrated to the west of this front (Palmén 1958), and can be qualitatively confirmed by comparing Figs. 3.6.1a and 3.6.1b. This front induced these intense rains to fall west of Toronto as the front became stationary and facilitated the lifting of moist air flowing from the south (Knox 1955). By referring to Fig (3.3.5) one can see that at 1500 UTC 15 October southerly flow from the tropical air delivered by Hurricane Hazel persisted up to nearly 100 hPa in the atmosphere. The frontal motion quickly slowed from approximately 40 km/h to a standstill in only six hours, a rapid development (Knox 1955). Upon this stalling the shape of the cold front became, in the words of Knox (1955) " flattened", causing a shift in the rain pattern to west of the front from the previously observed prefrontal rains. A deep contrast in the thermal properties of the air masses separated by the cold front existed, with an overall variation of 15°C present between the cold trough and tropical air from Hazel at the 500 hPa level (Palmén 1958). Palmén (1958) computed mean divergence profiles over 5° latitude by 5° longitude blocks of North America in the path of Hazel. Calculations of expected precipitation from the derived divergence profiles and specific humidity measurements are in good agreement with the observed values. This conclusion can be utilized to ensure the trustworthiness of the large observed values at the stations. Combining the moisture conditioning provided by Hurricane Hazel with the strong thermal gradient associated with the extratropical low accounts for the severe precipitation event observed on 15 October 1954.

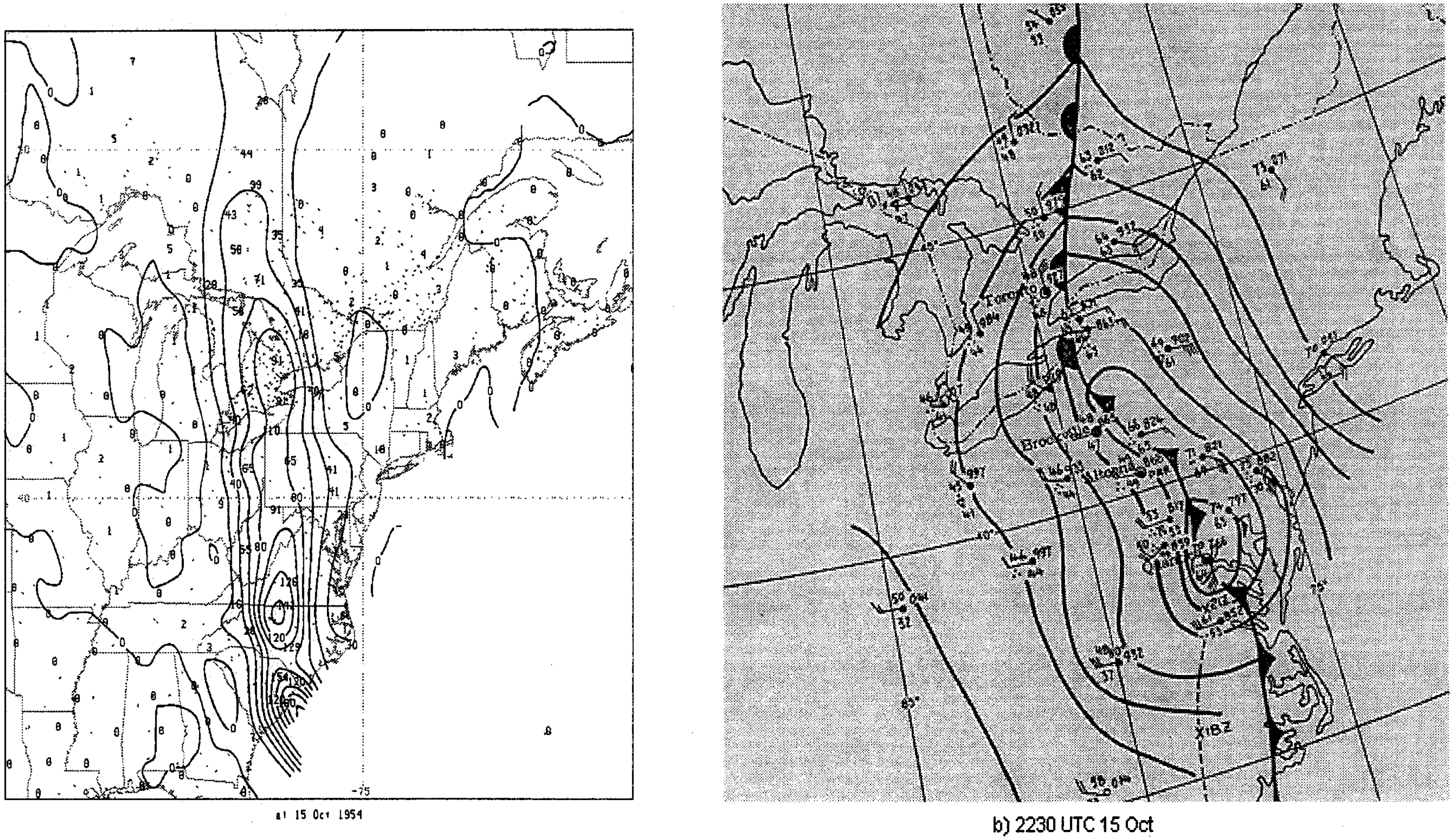

Fig. 3.6.1. (a) Storm total precipitation (solid, contour interval of 20 mm). Values plotted at select stations, dots indicate reporting stations; (b) Sea level pressure (solid, contour interval of 4 hPa) from Knox (1955).

4. Analogue Search

4.1 Search philosophy and design

Analogue searches have a history rooted in their potential as a weather forecasting tool. To understand the rationale behind such thought, a definition is in order. An analogue is defined by Lorenz (1969) as the occurrence of two atmospheric states that bear a high degree of similarity. Given that these two atmospheres have close initial conditions, then the ensuing weather should undergo parallel development (Radinovic 1975). The value of this type of pattern recognition as a predictive tool is advocated for on the basis that anticipating the general characteristics of the atmospheric circulation allows for one to focus on potential major hazards, while downplaying less likely threats (van den Dool 1989). Since analogues are based on actual historic events, all orographic, diabatic and local influences are contained in the analogue-derived forecast (Ruosteenoja 1988). This practical prognostic method is objective and fast to implement (Radinovic 1975), and requires no simplifying assumptions about the physics of the atmosphere (van den Dool 1989).

A few drawbacks to this concept do exist that severely limit the predictive ability of analogues. A lack of high quality three dimensional atmospheric analogues limits the possibility of finding homogeneous initial conditions for the case in question and the potential analogue (Lorenz 1969). Short-range forecasts by numerical weather predictions routinely outperform the analogue forecast method, owing to the poor representation of the initial conditions (Ruosteenoja 1988). Abandoning the forecasting motivation leads to another more useful application of the analogue search, as conducted in this study. The weather from Hazel and the analogues is a known quantity, and differences in this weather are implied to be a result of the slightly differing initial conditions. Subtle changes in the initial circulation can allow for a qualitative assessment of the relative impacts of synoptic and mesoscale phenomena (Roebber and Bosart 1998). Identification of the significant atmospheric details can permit a determination of the mechanisms that distinguish the harmless storm from a deadly case like Hazel (Gyakum and Roebber 2001).

Obtaining better initial conditions is possible with an adjustment of the search parameters, thereby improving the quality of the analogues. Selecting an appropriate objective method to detect the best analogue is important for minimizing the differences in initial atmospheric states (Lund 1963). Past researchers have utilized linear correlation, root mean square difference and covariance to name a few statistical techniques (Gutzler and Shukla 1984). Of these three techniques, linear correlation tends to consistently outperform the other statistics with respect to phase matching of the analogue and test case (Gutzler and Shukla 1984). Differences visible in the synoptic fields are better emphasized with this method.

The choice of fields to correlate varies widely in the literature, with examples of mean sea level pressure (Lund 1963) and 500 hPa height (Ruosteenoja 1988, Gutzler and Shukla 1984). Multiple fields may be correlated simultaneously to further screen the analogues, with three concurrent correlations being conducted by Gyakum and Roebber (2001) for example. For the purposes of this study, the correlation of anomaly fields, specifically anomaly sea level pressure and 1000-500 hPa thickness, is the chosen method. Calculation of the linear correlation coefficients is completed using equation(4.1.1) (Gyakum and Roebber 2001):

$$r = \frac{\sum_i \sum_j a\{1\}_{i,j} a\{2\}_{i,j}}{\left[\sum_i \sum_j \left(a\{1\}_{i,j}\right)^2 \sum_i \sum_j \left(a\{2\}_{i,j}\right)^2\right]^{1/2}} \tag{4.1.1}$$

where $a\{1\}_{i,j}$ is the anomaly of the first full field at point (i,j) and $a\{2\}_{i,j}$ is the anomaly at the same point for the second full field. To derive the anomaly values at each point, equation (4.1.2) is employed (Durnford 1999):

$$a\{1\}_{i,j} = \overline{A}_{i,j} - A\{1\}_{i,j} \tag{4.1.2}$$

with the first term on the right hand side representing the mean of the full field value at point (i,j) and the second term denoting the full field value at the same point. A 30 year monthly climatology from 1971 to 2000 was utilized as the mean fields for this research.

Determination of an acceptable tolerance in the correlation values has been discussed by many studies. A higher coefficient limit reduces the number of analogues, favouring the best matches as a correlation of one implies a perfect synchronization of phase. Hollingsworth et al. (1980) determined that a threshold between 0.5 and 0.6 for the linear correlation coefficient provides useful analogues. Setting the threshold at 0.7 sufficiently removes the poorer quality analogues while leaving only the best cases for this examination of Hazel.

Lorenz (1969) was highly skeptical that good analogues existed over the global domain, and provides a strong motivation to reduce the geographical scale of the search. A limited area from 110°W to 50°W and 60°N to 20°N sufficiently captures all the dynamics and thermodynamics essential to Hazel, including the accompanying Great Lakes trough and Bermuda high pressure system (see section 3.2). This domain will be the view region in the plots for this chapter. A 36-hour period commencing on 00 UTC

15 October 1954 is the temporal domain of the analogue search. A four to five day correlation period is cited as the maximum extent that one can expect to obtain viable analogues over, so the use of a 1.5 day period is well within the confines of acceptability (Gutzler and Shukla 1984). A requirement that the average of the sea level pressure anomaly and the 1000-500 hPa thickness anomaly correlation coefficients remain above 0.7 for the three 12-hour intervals in this 36-hour time frame is a further restriction on the search. The analogues are permitted to evolve at rates different from the base case of Hazel, as long as the linear correlation coefficient threshold is still exceeded. Continuous NCEP/NCAR Reanalysis data were available from 1963 to 2000 for comparison of the anomalies between each test case and Hazel. Hurricane season is set by the National Hurricane Center as June 1st to November 30th, and this study uses this limit to search only these months for analogues to Hazel. This data set provides a long period of time favoured by Lorenz (1969) in the pursuit of the best atmospheric analogues.

4.2 Analogue search statistics and anomalies

As a result of the analogue search, three mass analogues were found to the sea level pressure and 1000-500 hPa thickness anomaly fields of Hazel from 00 UTC 15 October to 12 UTC 16 October 1954. Analogues were found on 00 UTC 5 - 12 UTC 5 October 1985, 12 UTC 14 - 00 UTC 15 October 1995, and on 00 UTC 9 - 12 UTC 10 September 1999. Ruosteenoja (1988) found that the best analogues were exposed when the seasonal difference between the analogue and the event was less than three weeks, a finding supported by the discovery of the 1995 and 1985 cases in this study. The occurrence of only three useful analogues is not surprising as autumn and summer season events generally produce the least viable analogues, whereas winter events generate the better correlated and longer-lived analogues (Lorenz 1969, Ruosteenoja 1988). As well, Hazel presumably possesses a relatively unprecendented track and development in a historical context, making the event somewhat of an outlier. This works to further diminish the potential for high quality analogues. A summary of the average values of the linear correlation coefficients over the whole synoptic time period is shown in Table (4.2.1). Comparing the four synoptic time average of the correlation coefficients shows the 1985 event with the highest correlation value of 0.7782, followed by the 1999 event at 0.7636 and the 1995 event at 0.7558. Evolution rates for the separate analogues vary widely, with only the 1999 event evolving at the same rate as Hazel. After matching Hazel's evolution for the first 12 hours, the 1985 event progresses no further in time, and only covers two synoptic times. In the 1995 event only two synoptic times are covered as well, but with a different evolution pattern. No progress is made in the first 12 hours, followed by a step forward in the next 12-hour period, and yet another stalling for the last 12-hour frame. Owing to the highly variable evolution of the individual analogues with respect to Hazel, the base correlation time of 00 UTC 15 October 1954 will be referred to as T-00 and each 12-hour time step forward will be labeled T+12, T+24 and T+36 when referring to each analogue time phase.

Table 4.2.1. Anomaly statistics

Event	Average Anomaly Correlation Value
15-16 October 1954	1.0000
5 October 1985	0.7782
14-15 October 1995	0.7636
9-10 September 1999	0.7558

The reduced number of synoptic times covered by the 1985 and 1995 analogue (i.e. two times) versus Hazel (i.e. four times) implies the presence of a persistent atmospheric pattern in the anomaly sea level pressure and 1000-500 hPa thickness plots. Common to Hazel and all the analogues correlated to Hazel at T-00 is an anomalous low pressure near the Great Lakes (Figs. 4.2.1a-d). Locations do vary slightly for these anomalies, as does the extent of these features. This anomalous low is very similar for Hazel and the 1985 event in terms of coverage and location, while the 1995 and 1999 events cover a much broader area. A poor phase match exists in the 1999 event, as its low anomaly sea level pressure is shifted to the west of James Bay. Important to note is the prominent low sea level pressure anomaly associated with Hurricane Hazel near the Bahamas, which is not reflected in the anomaly fields of any of the analogue cases. Thickness anomalies at this time display a low thickness anomaly west of the Great Lakes and a high thickness anomaly situated over Quebec in all of the events (Fig. 4.2.2a-d). Hazel has generated a lower anomaly thickness with a greater extent than any of the analogues. An enormous thickness anomaly covering most of the eastern part of North America in the 1954 Hazel case dwarfs the analogue thickness anomalies.

At T+12, the picture of Hazel and the analogues is still marked by noticeable differences (Fig. 4.2.1e-h). The sea level pressure anomaly for Hazel consists of two separate low anomaly centers that none of the analogues replicate. An anomalously high sea level pressure in Hazel over the Rocky Mountains is poorly represented or completely absent in the analogues. The large, high anomaly thickness in Hazel over Quebec is better emulated in the 1995 analogue than either of the 1999 or 1985 cases

(Fig. 4.2.2e-h). None of the analogues compare well to the anomalous low thickness in 1954 in terms of extent, magnitude or location.

Anomaly fields at the correlation time of T+24 exhibit a slight reduction in the sea level pressure field differences (Fig. 4.2.1i-l), but a continuing disparity in the 1000-500 hPa thickness anomaly plots (Fig. 4.2.2i-l). The low sea level pressure anomaly for Hazel is now a single entity, as is the case with the analogues. Now the low sea level pressure anomaly is much deeper in the case of Hazel than the analogues, with a combined orientation and coverage unique to Hazel. Hazel's deep anomaly low thickness progresses farther southeastward, and the positive anomaly thickness is unparalleled.

Final correlations at T+36 tell the same story as the previous three synoptic correlation times. The negative and positive anomaly thickness regions over the U.S. southeast and northern Quebec respectively are distinct from the analogues anomaly fields (Fig. 4.2.2m-p). Analogue sea level pressure anomaly plots fail to mimic those of Hazel as well in terms of magnitude or extent (Fig. 4.2.1m-p).

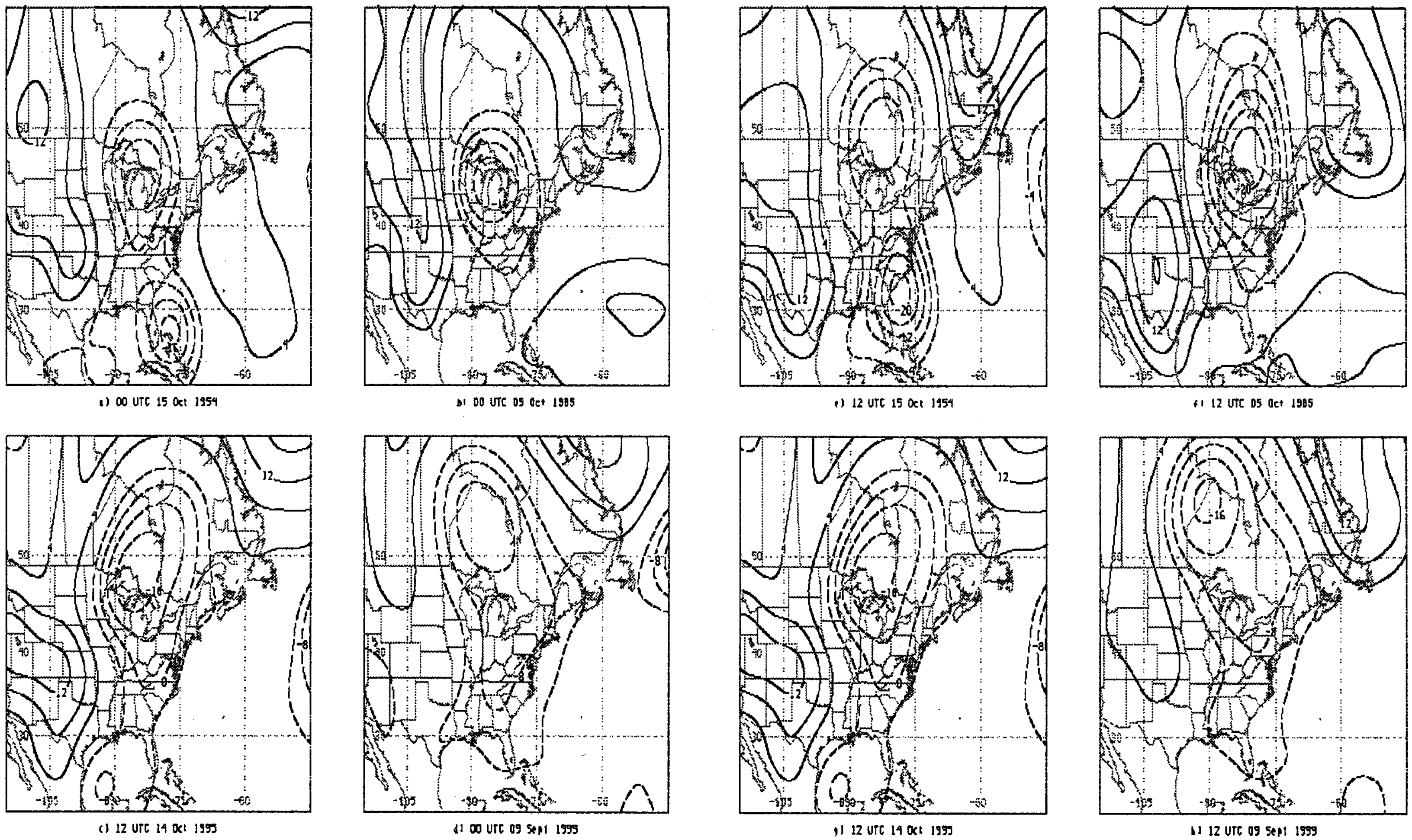

Fig. 4.2.1. Sea level pressure anomalies (positive anomalies in solid, negative anomalies in dashed, contour interval of 4 hPa). Zero contour is omitted. For: (a) and (e) Hazel; (b) and (f) 1985 analogue; (c) and (g) 1995 analogue; (d) and (h) 1999 analogue.

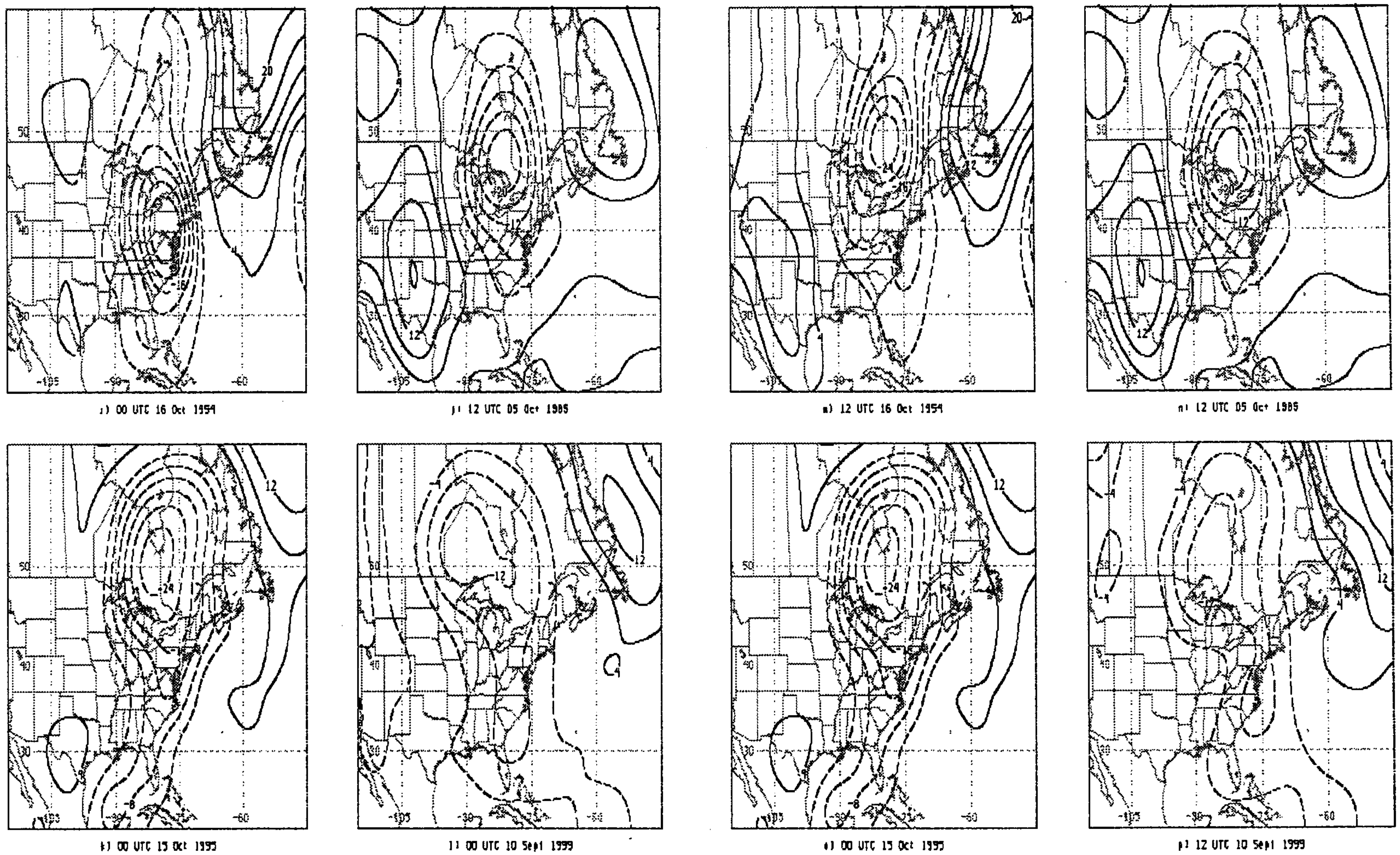

Fig. 4.2.1. (Continued) For: (i) and (m) Hazel; (j) and (n) 1985 analogue; (k) and (o) 1995 analogue; (l) and (p) 1999 analogue.

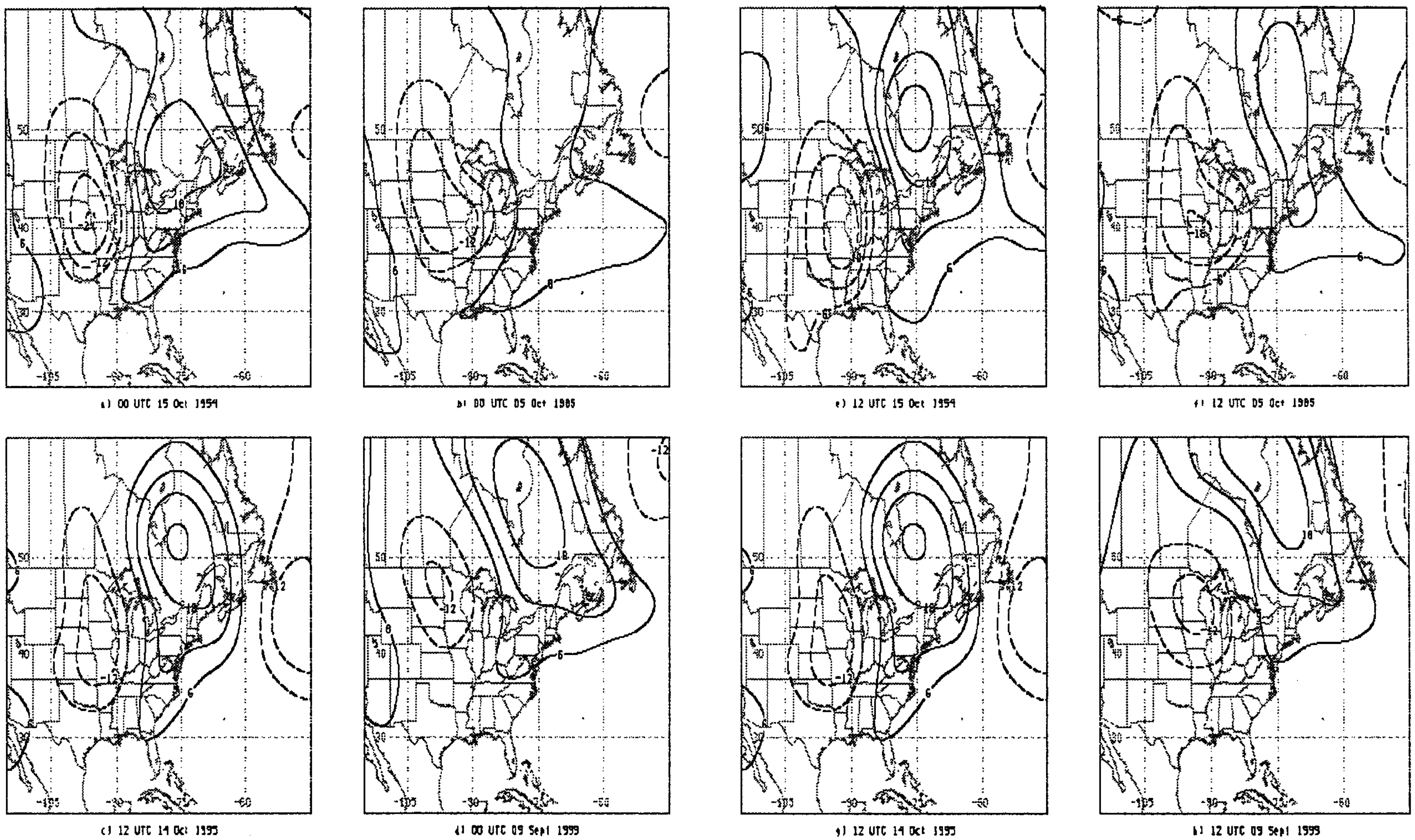

Fig. 4.2.2. 1000-500 hPa thickness anomalies (positive anomalies in solid, negative anomalies in dashed, contour interval of 6 dam). Zero contour is omitted. For: (a) and (e) Hazel; (b) and (f) 1985 analogue; (c) and (g) 1995 analogue; (d) and (h) 1999 analogue.

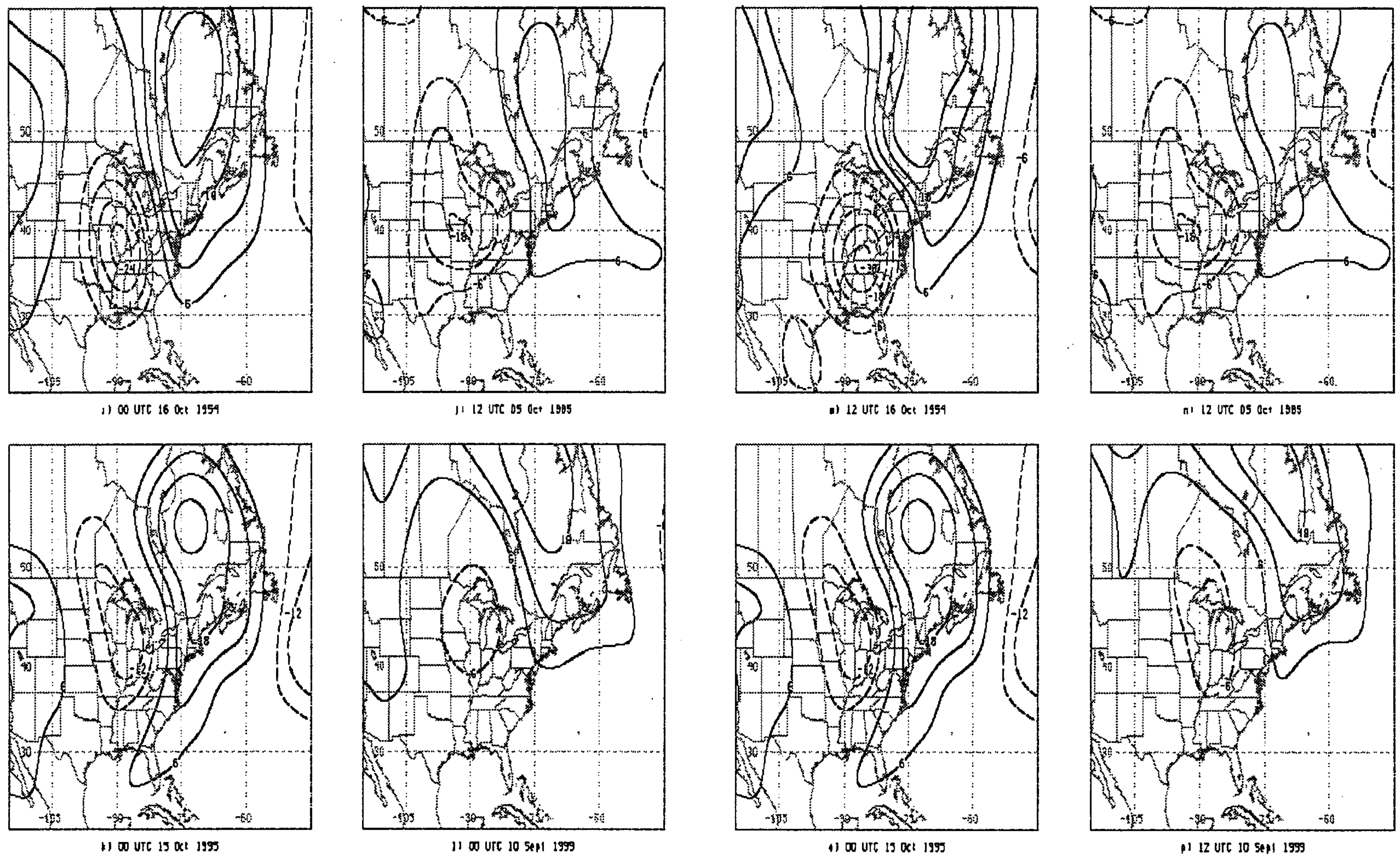

Fig. 4.2.2. (Continued) For: (i) and (m) Hazel; (j) and (n) 1985 analogue; (k) and (o) 1995 analogue; (l) and (p) 1999 analogue.

4.3 Synoptic field comparison

Comparison of the full atmospheric fields and not the correlated anomaly fields provides information that helps distinguish Hazel from the analogue cases. Thoroughly examining the sea level pressure and 1000-500 thickness fields at T-00 shows four noticeably different cases (Fig. 4.3.1a-d). Similarities do exist in the form of broad high pressure systems over Bermuda and near the Rocky Mountain range, and an extratropical low pressure in the vicinity of the Great Lakes with a trough extending southward. The differences arise from many sources, including the presence of Hazel in 1954. No hurricanes or tropical disturbances are in or near the domain for the 1985 and 1999 cases, while the 1995 situation has a weakening Hurricane Roxanne in the Gulf of Mexico. Flow strengths and orientations around the extratropical lows are highly dissimilar, with stronger meridional flow surrounding the low in 1954 than in any of the analogues. The extratropical low in the 1985 case has an appearance not completely unlike the 1954 system, but with weaker southerly geostrophic winds over eastern Ontario that lead to a lessened northward progression of the warm thickness values. In 1995 the orientation and shape of the sea level pressure fields forming the extratropical low are much different than in 1954. Atmospheric flows are directed between the northeast and southwest predominately, lacking a strong meridional component and presumably supplying air from a drier continental region. Weak winds over New England again promote a decreased northward extension of the large thickness values. A negatively tilted extratropical low in 1999 leads to geostrophic flows that deform the thickness plots in a manner unlike the 1954 storm. These winds in all the analogue cases produce baroclinic zones with less compact and more zonal thickness values than those in Hazel.

Moving to T+12, one can see a situation highly similar to the one 12 hours earlier (Fig. 4.3.1 e-h). Hazel has a much more meridional and compacted baroclinic zone than any of the analogues. The 1985 case does experience strengthened geostrophic winds over Quebec but does not exhibit the large thermal ridge over this region as in the case of Hazel. These stronger winds blow from a source region over New England and not the Atlantic Ocean as in 1954. A regression to the northwest by the extratropical low has occurred in the 1999 case, distancing the low center much too far from the Great Lakes to be comparable to the location of the 1954 center. This shift places the circulation pattern in a position that does little to reinforce the strength of the baroclinic zone or induce a meridional orientation. Again the absence of a tropical storm embedded in the domain is the major difference between 1954 and all of the analogues.

At the next timestep, T+24, the extratropically transformed low of Hazel is the dominant feature over the east coast (Fig. 4.3.1 i-l) None of the analogue events have a circulation as compact as the one present in 1954, and all the analogue lows tend to be situated farther to the north. Flow strengths are much weaker for the analogues at this stage, with sea level pressure orientations that suggest drier air masses are being drawn over Quebec. The 1999 event continues deteriorate in quality and does not resemble the 1954 sea level pressure and 1000-500 hPa thickness fields. Regarding the situation in 1995, the thickness plot has the most correspondence to the 1954 event of any of the analogues. The low thickness contours do not push as far southeast as the Hazel case, and the large thickness values over Quebec are lower in magnitude than those in 1954. This mismatch is connected to the large spatial coverage and center location of the low pressure, situated near James Bay and covering the northeast portion of the continent. Flow around the

1995 low is not as strong due to the weaker pressure gradient and does not penetrate as deep to the south, thereby reducing the deformation of the thermal field.

At T+36, only the 1999 case continues to evolve (Fig. 4.3.1m-p). The 1985 and 1995 events have a slower rate of development than that of Hazel and the 1999 case. Similarities existing between Hazel and the analogues at this point are weak at best. As Hazel continues to evolve the differences between the 1954 storm, and the stalled 1995 and 1985 analogues are minimizing. Movement northward by Hazel is responsible for this process, along with a broadening of the circulation of the system. The severely deformed and zonally compressed baroclinic zone acquires a negative tilt for the 1954 event that is not replicated by either of the 1985 or 1995 analogue. Hazel still experiences a strong onshore flow from the Atlantic Ocean that is unique from all the analogues. A deep cutoff low of thickness develops below the Great Lakes at this stage in the 1954 case that distinguish it further from the comparative cases. The location and magnitude of the surrounding high pressure systems is
relatively well matched in the 1985 analogue fields, while the other cases have little in common with the 1954 event in this aspect. Over Newfoundland the high pressure from 1985 does not extend as far southward when compared to 1954, as a weak trough protrudes from the east coast of the U.S. out over the Atlantic Ocean.

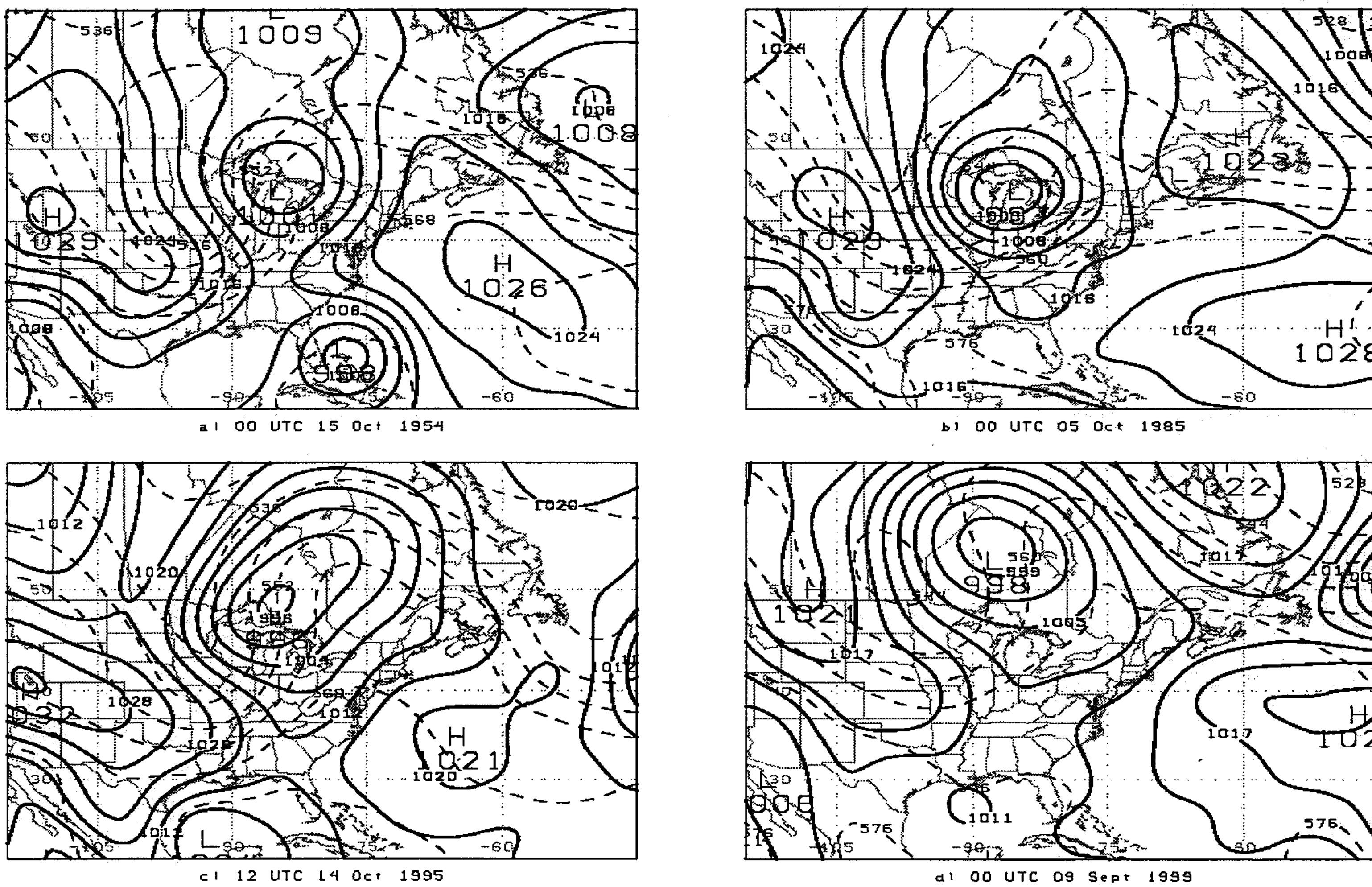

Fig. 4.3.1. Sea level pressure (solid, contour interval of 4 hPa) and 1000-500 hPa thickness (dashed, contour interval of 8 dam). For (a) Hazel; (b) 1985 analogue; (c) 1995 analogue; (d) 1999 analogue.

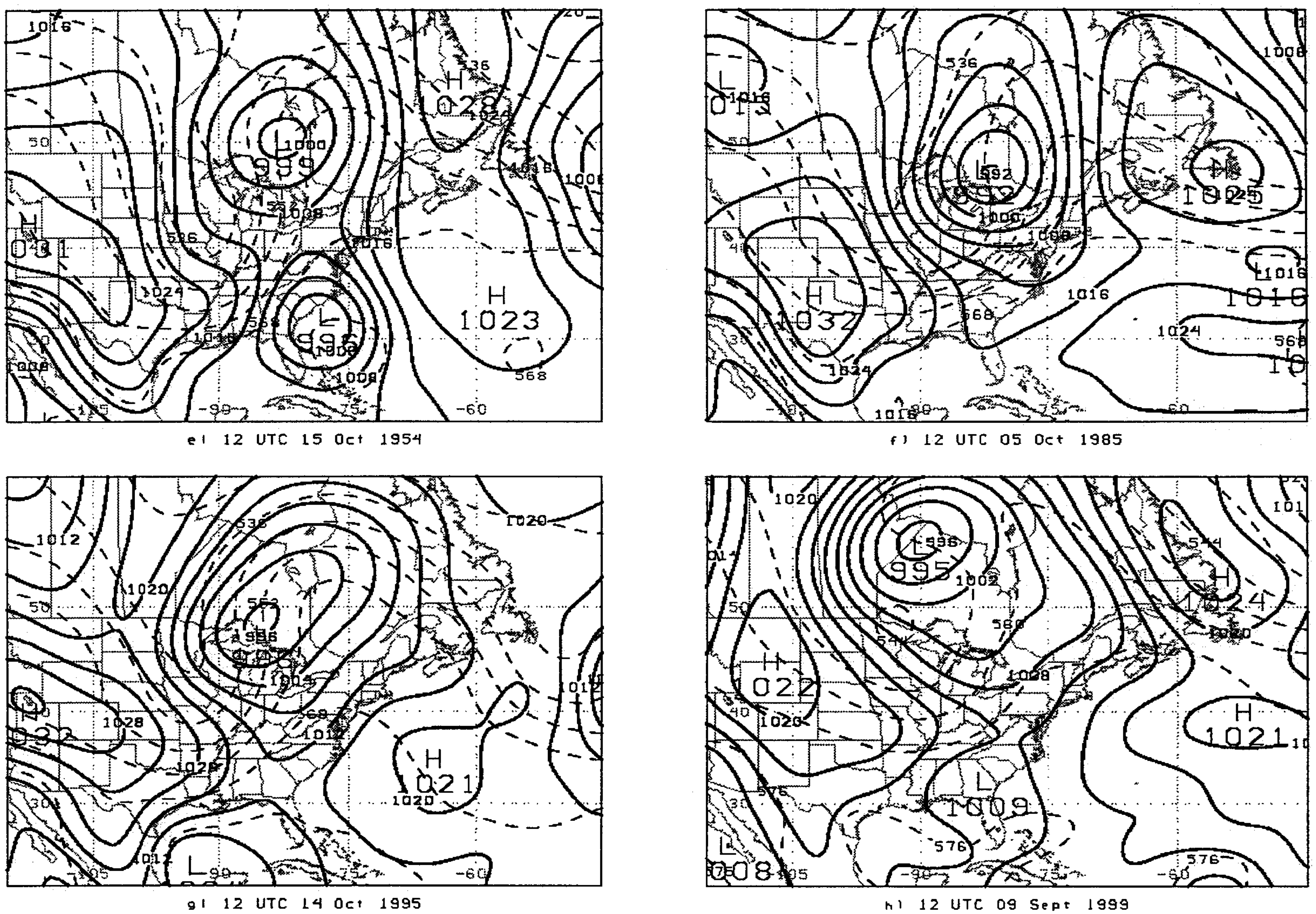

Fig. 4.3.1 (Continued) For: (e) Hazel; (f) 1985 analogue; (g) 1995 analogue; (h) 1999 analogue.

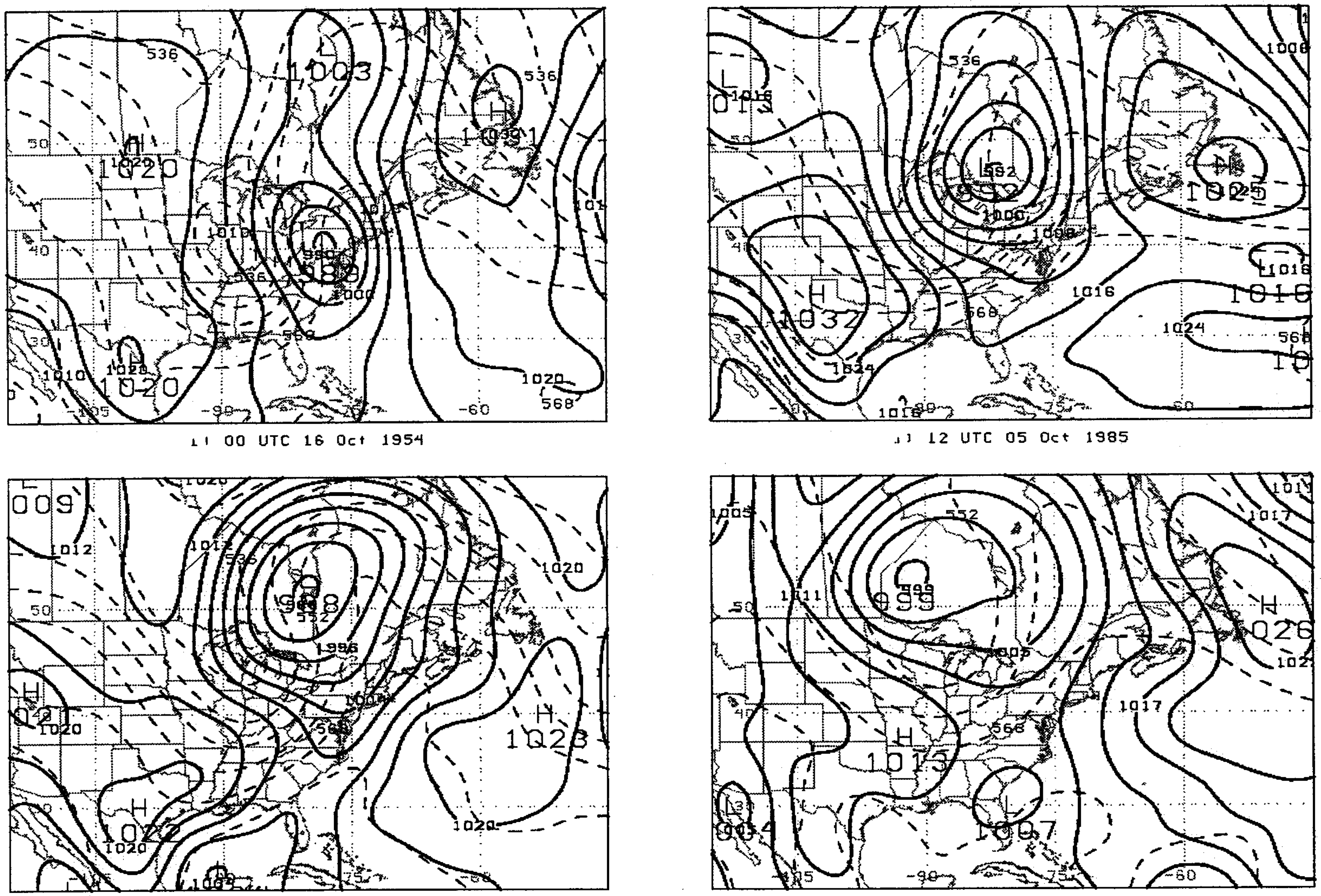

i) 00 UTC 16 Oct 1954 j) 12 UTC 05 Oct 1985

k) 00 UTC 15 Oct 1995 l) 00 UTC 10 Sept 1999

Fig. 4.3.1. (Continued) For: (i) Hazel; (j) 1985 analogue; (k) 1995 analogue; (l) 1999 analogue.

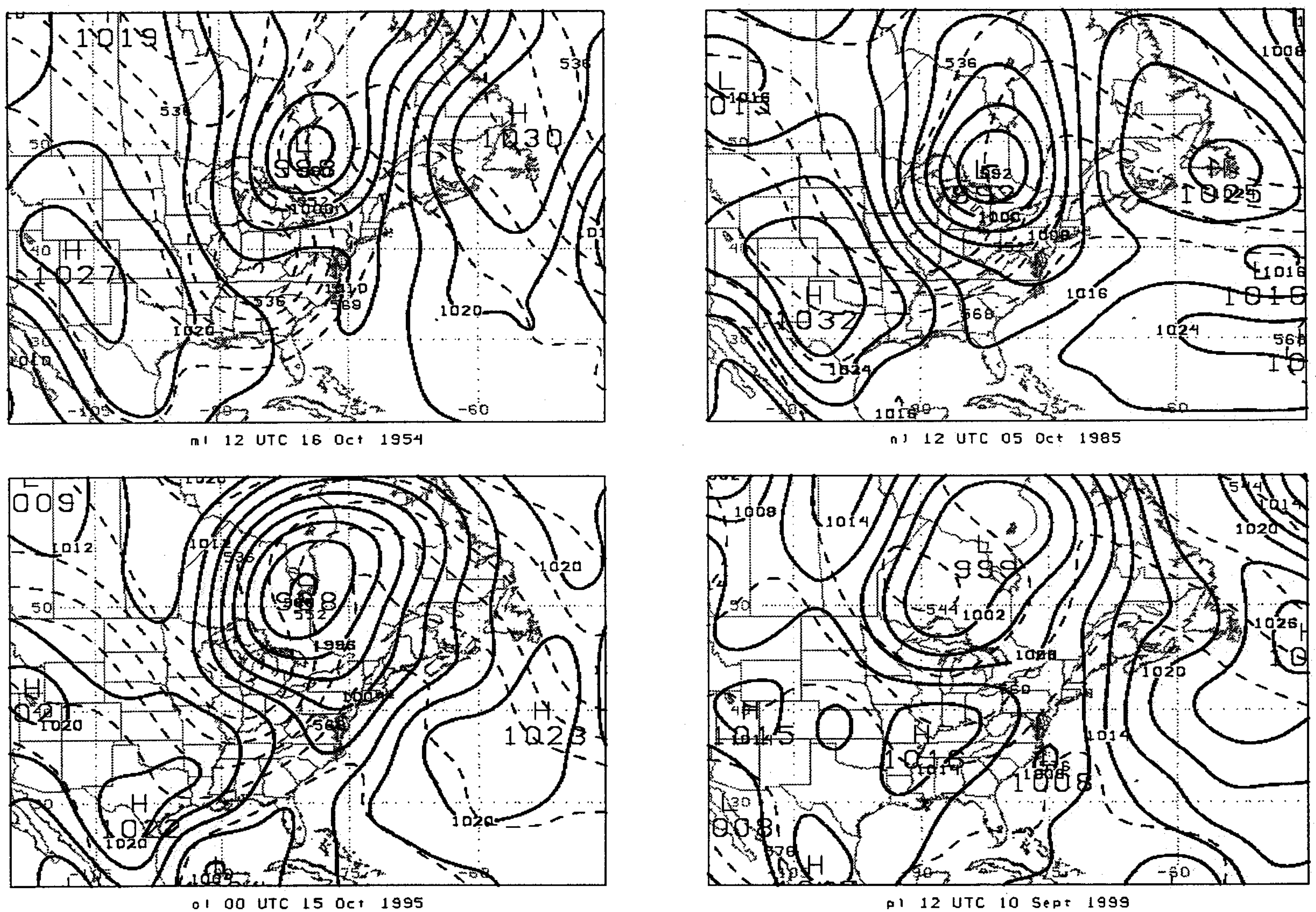

Fig. 4.3.1. (Continued) For: (m) Hazel; (n) 1985 analogue; (o) 1995 analogue; (p) 1999 analogue.

4.4 Dynamic tropopause comparison

Using the maps of dynamic tropopause potential temperature and winds with 850 hPa potential temperature for Hazel and each analogue reveals a high degree of dissimilarity between the events. At T-00 Hazel has an intense potential temperature gradient near Lake Michigan that is roughly paralleled by the 1995 event only (Fig. 4.4.1a-d). The tilt of this feature is positive in 1995 though, unlike the meridional oriented gradient in 1954. Gulf of Mexico conditioned air is supplied from Hurricane Roxanne in 1995, unlike the Atlantic Ocean source for Hurricane Hazel. A complete absence of a dynamic tropopause potential temperature gradient is the case in both 1999 and 1985, implying weak baroclinicity in the atmosphere. A predominately zonal pattern of potential temperature is prevalent in 1985 and 1999, with weak dynamic tropopause depressions over the Manitoba-Ontario border. Lower dynamic tropopause potential temperature is evident in this region during the 1995 event, but not in the magnitude exhibited by the 1954 case. Elevated dynamic tropopause is situated over the U.S. northeast in 1995 similar to the pattern displayed by Hazel, but again at a significantly reduced extent. Lower troposphere potential temperature is similar in the 1995 case to Hazel, while the 1999 and 1985 analogues have little in common to the 1954 test case. The pattern and magnitude of the 850 hPa potential temperature in 1995 and 1954 are very similar, with a bulge of high potential temperatures near Florida and lower values over Manitoba. A high amplitude wave of isentropes is also present in these cases, visible when following the 280 K contour through the southern U.S., over the Great Lakes and into central Quebec. Winds on the dynamic tropopause are most alike 1954 in the 1995 analogue, with comparable magnitudes near Lake Michigan (approximately 60 m s^{-1} in 1995 and 65 m s^{-1} in 1954), southern Quebec (approximately 30 m s^{-1} in 1995 and 35 m s^{-1} in 1954) and North Dakota (55 m s^{-1} in 1995 and 50 m s^{-1} in 1954). Weak winds plague the 1999 event owing to the shallow slope of the dynamic tropopause. In 1985 dynamic tropopause winds exceed 55 m s^{-1} but are located in positions poorly matched with similarly strong winds in 1954, a result of the low amplitude of the dynamic tropopause in the analogue. Advection in all the analogues does not resemble the configuration associated with Hazel, with considerable advection occurring only in 1995. This advection in 1995 takes place along the tightest dynamic tropopause potential temperature gradient from Arkansas to Ohio, driving ascent as lower dynamic tropopause potential temperatures are imported. Of interest to note is the presence of former Hurricane Dennis in southeastern Ontario at this time in 1999. Dennis works to condition the environment much like Hazel, prior to this correlation period. The status of Dennis, an extratropical depression by NHC (2003) definition, generates a weak baroclinic zone unlike Hurricane Hazel.

The situation at T+12 evolves for the 1985 and 1999 analogues, but does not produce a significant improvement in the relationship of the dynamic tropopause features (Fig. 4.4.1 e-h). Closed pools of low potential temperature on the dynamic tropopause move farther south in each of these analogues, in the same manner as the 1954 test case. This change does little to help correct the lack of a strong dynamic tropopause potential temperature gradient and high amplitude wave pattern. Winds at this upper level still are too weak or located in positions much too unlike those in 1954 to confer much confidence in the analogues. Near surface potential temperature is still disorganized compared to the case of Hazel. The development of Hazel changes the likeness to the

1995 analogue little, with all features relatively well complemented.

Allowing for an evolution in the 1995 and 1999 plots at T+24 produces some useful information (Fig. 4.4.1 i-l). Dynamic tropopause potential temperature increases in 1995 over Maine in the absence of advective winds, likely due to diabatic heating in the outflow of Hurricane Roxanne. This increase is much less than that experienced in 1954, due to the weakened state of Roxanne and the large distance from the tropical storm in the Gulf of Mexico. Tilt is now a major difference between the 1995 and 1954 cases, as Hazel acquires a negatively sloped dynamic tropopause gradient and the 1995 analogue retains the positive slope. Differential cyclonic vorticity advection indicates that this negative orientation is favourable to enhanced cyclogenetic forcing when compared to a positively sloped gradient (Atallah and Bosart 2003). A zone of intensely compressed dynamic tropopause potential temperatures stretches over a longer area in 1954 than in 1995 as well. Moisture sources derived for each event from the wind field suggests that the 1995 event requires air parcels to pass from the Gulf of Mexico over the continent for a longer duration than the air originating from the Atlantic Ocean in 1954, drying the air substantially in 1995. Isolation of the low dynamic tropopause potential temperature in 1954 over Illinois is not replicated in 1995, due in part to the lack of significant diabatic outflow downstream of the dynamic tropopause trough. Fields of 850 hPa potential temperature contain a degree of likeness over the North American continent east of the Great Lakes. Near the Gulf of Mexico in 1954 cooler low level potential temperatures exist than in 1995. The 1999 analogue continues to be a poor comparative case on the dynamic tropopause, with light winds and no definable potential temperature gradient, and much the same can be said about the 1985 analogue.

The final stage at T+36 shows Hazel to be an entirely distinct entity (Fig. 4.4.1 m-p). A pronounced dynamic tropopause gradient with a large isolated low dynamic tropopause to the west and an enormous bulge of elevated dynamic tropopause to the east is not represented in any of the analogues. The sheer size of the baroclinic zone separates Hazel from the rest. Low isentropic temperatures at 850 hPa penetrate deep towards the Gulf of Mexico in 1954, and soars to high values over northern Quebec unlike any of the other events. A unique wind pattern is established in the 1954 test case that modifies the advection configuration of the dynamic tropopause potential temperature field and moisture transports to structures unlike those in the analogues.

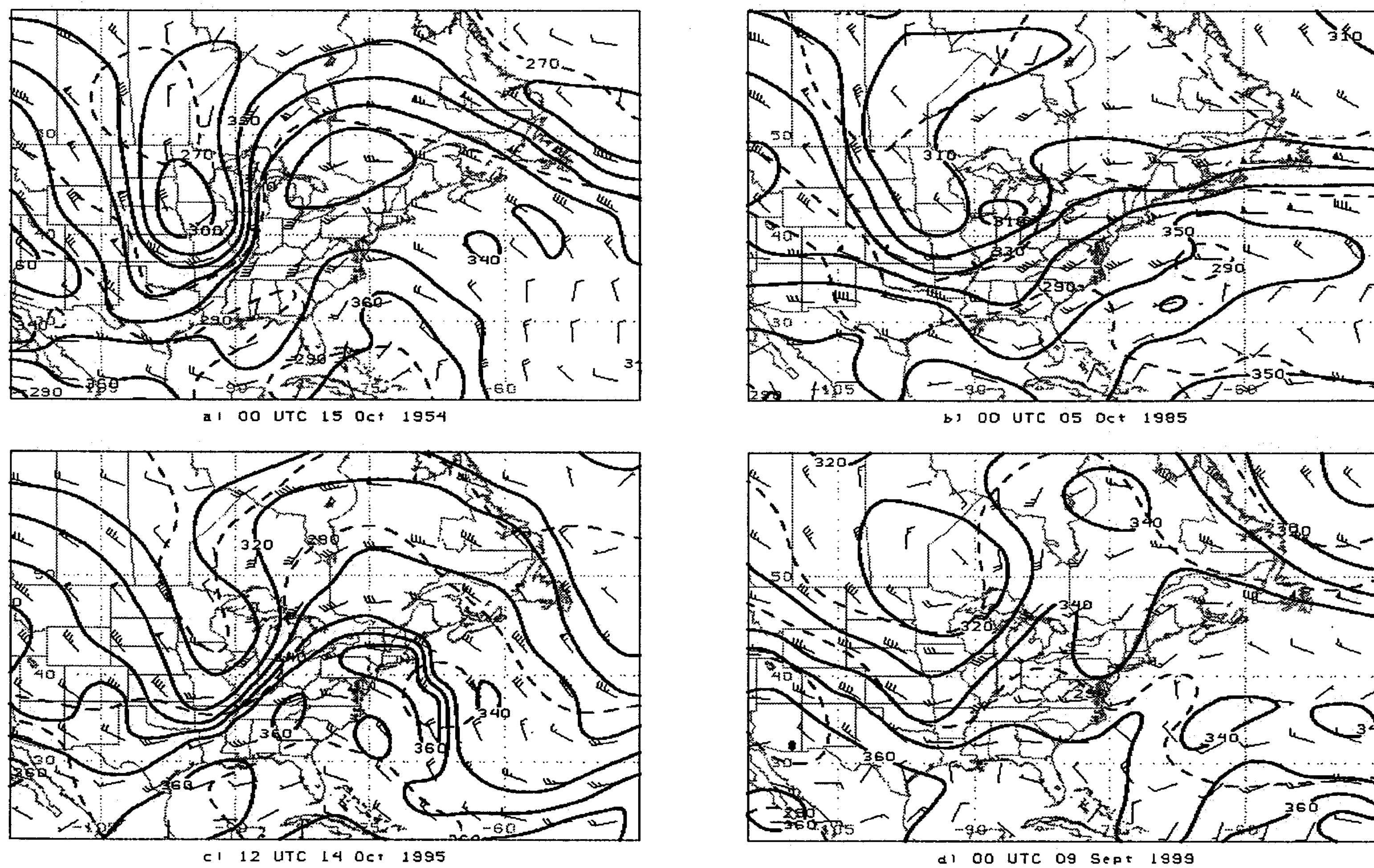

Fig. 4.4.1. Dynamic tropopause potential temperature (solid, contour interval of 10 K), winds on the dynamic tropopause (m s^{-1}), and 850 hPa potential temperature (dashed, contour interval of 10 K). For (a) Hazel; (b) 1985 analogue; (c) 1995 analogue; (d) 1999 analogue.

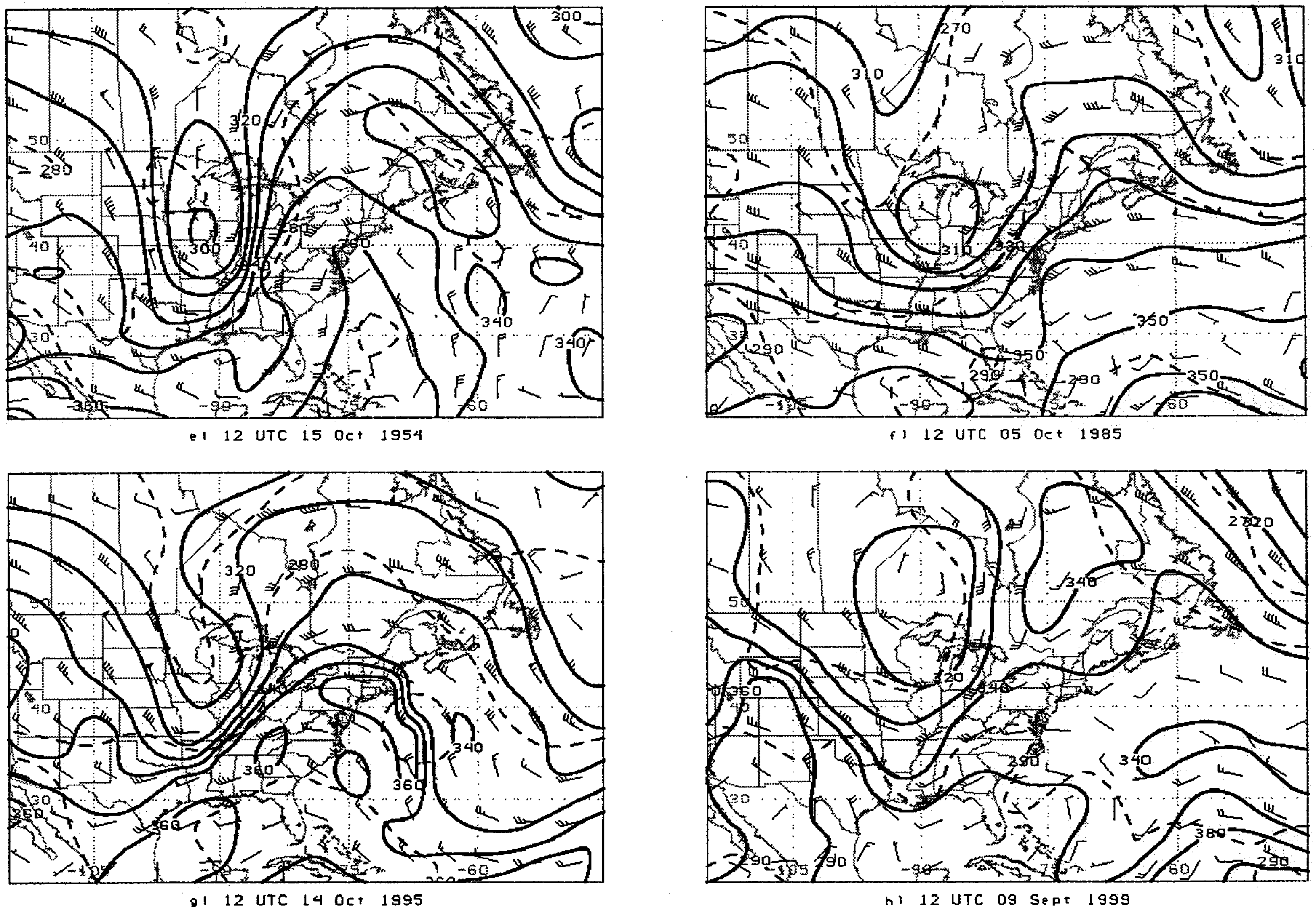

Fig. 4.4.1. (Continued) For: (e) Hazel; (f) 1985 analogue; (g) 1995 analogue; (h) 1999 analogue.

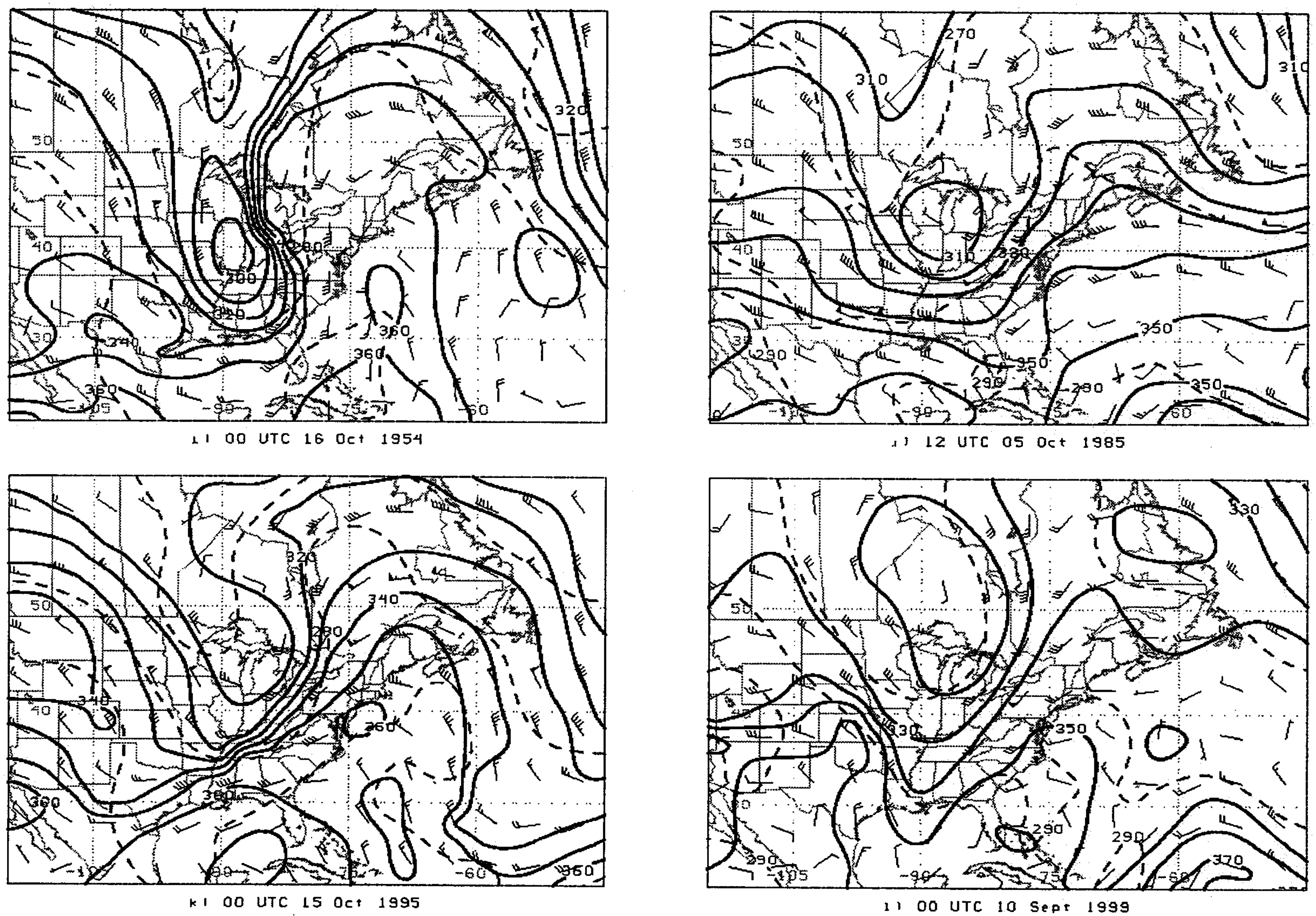

Fig. 4.4.1. (Continued) For: (i) Hazel; (j) 1985 analogue; (k) 1995 analogue; (l) 1999 analogue.

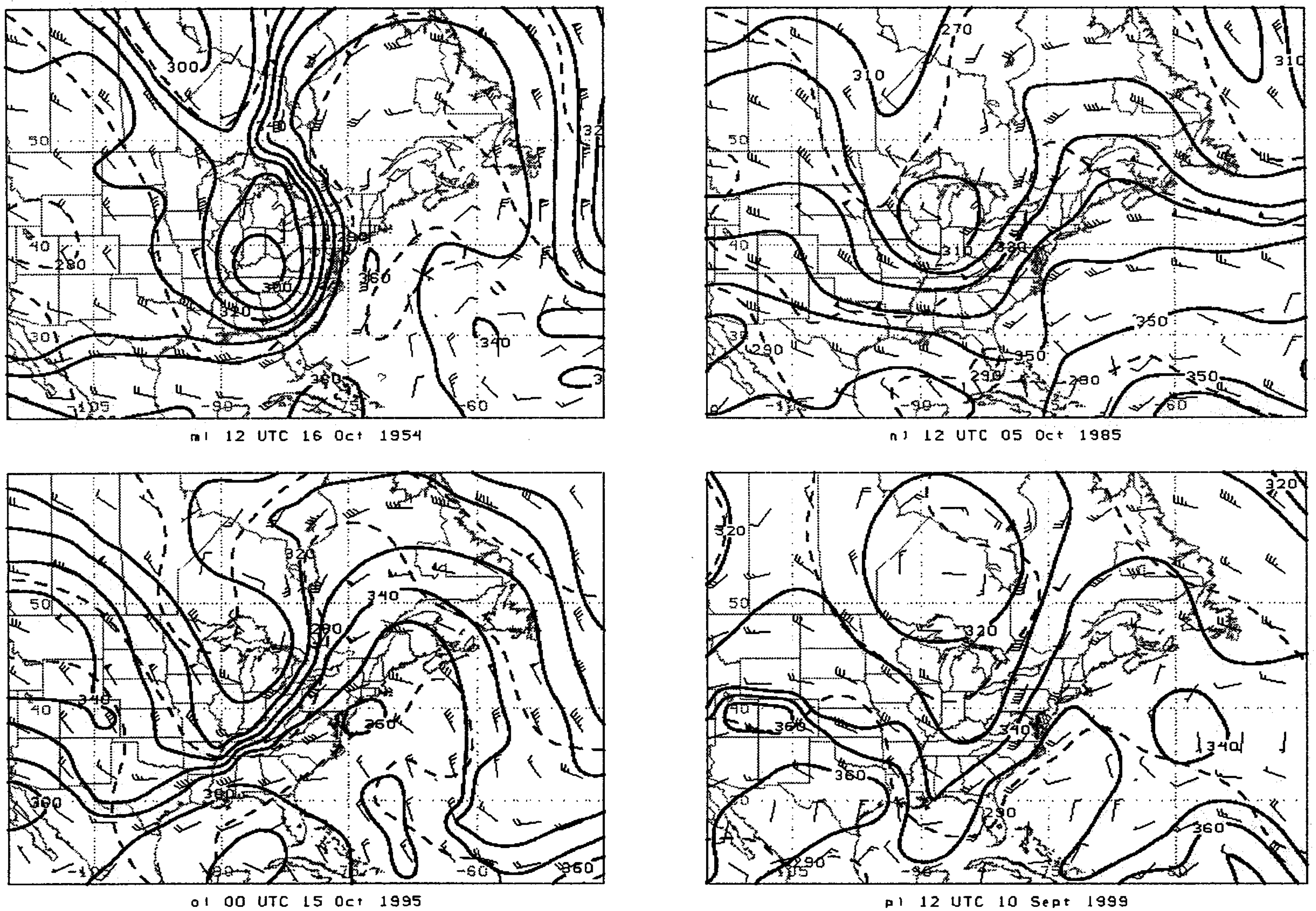

Fig. 4.4.1. (Continued) For: (m) Hazel; (n) 1985 analogue; (o) 1995 analogue; (p) 1999 analogue.

4.5 Moisture comparison

An assessment of the coupling index and precipitable water plots at T-00 shows four differing cases with minimal resemblance to each other (Fig. 4.5.1 a-d). Hazel exhibits a large zone of low coupling index west of the Great Lakes. These low values show the strong susceptibility to convection owing to the potential instability present. This large potential instability dwarfs the instabilities in all of the analogues. Two isolated instabilities 1985 exist in the U.S. Midwest, while small areas of low coupling index above and below Lake Superior are in evidence during the 1999 and 1995 events respectively. A gradient of coupling index values similar to that in 1954 is set up in the 1995 analogue, but with a distinct orientation. The slope of the coupling index gradient is positive in 1995 whereas the 1954 test case is nearly meridional. Precipitable water fields also tell widely varying stories. Hazel has values prior to landfall over 30 mm well into Ontario, a figure only matched by the 1999 analogue. Remnants of Hurricane Dennis in the 1999 analogue have supplied a reservoir of higher precipitable water values over central Quebec. This conditioning in 1999 is not sustainable as extratropical depression Dennis is rapidly dissipating and losing a definable moisture transport. The driest analogue atmosphere is clearly 1985 as 20 mm precipitable water values protrude into southern Ontario. Hurricane circulations are traceable in the atmospheric moisture field at this time, as Hurricane Hazel has accompanying high quantities, over 50 mm near Florida, and Hurricane Roxanne in 1995 carries a 60 mm contour in the Gulf of Mexico. A tongue of precipitable water over 30 mm has advanced to southern Ontario in 1995 from the Gulf of Mexico, likely associated with Roxanne. Source regions of moisture are the biggest cause of variance between 1954 and 1995, as Hazel derives moisture from the

Atlantic via the circulation of Hurricane Hazel.

Comparison of the moisture characteristics of Hazel and the analogues at T+12 finds a great deal of disparity between all of the events (Fig. 4.5.1e-h). Coupling index values are still lowest over the Midwest in 1954, also the case in 1995. During the 1999 and 1985 events there is little cause to believe that convection is imminent, as the coupling index remains high enough to indicate that no potential instabilities exist. The 1995 potential instability is significantly smaller the instability in 1954 even after a large reduction in coverage. Precipitable water values of 30mm are found for Hazel in Quebec, far exceeding the amounts in the analogues. A steady drying of the atmosphere occurs in 1999, as values drop to 20mm near Vermont from 30mm at the previous correlation time. Fields of atmospheric moisture in 1985 are lowest over the continent with a tight gradient concentrated along the coasts.

A broadening region of potential instability is shown at T+24 centered over Illinois in the case of Hazel (Fig. 4.5.1 i-l). This growth is also displayed in 1995, but the zone of low coupling index is still smaller than for Hazel. The enhancement in the coupling index gradient surrounding the low potential stability in 1954 is captured somewhat by the 1995 event. This gradient is not at any point as intensely compact, nor does it cover as large an area or reduce its positive slope to a more meridional slope as in the case of Hazel. A low coupling index region on the western edge of the domain in 1999 has an insignificant impact on the quality of the analogue. Precipitable water values rise over Pennsylvania in 1954, as a 50 mm contour pushes onshore from the Atlantic. Compaction and extension of the moisture gradient in 1995 occurs from Mexico to New York State, along with an increase in quantities to 40mm over southern Quebec. Slight augmentation of precipitable water over the U.S. southeast happens in 1999, but the atmosphere over northern Ontario and the U.S. Midwest continues to be dried.

The moisture characteristics of Hazel are distinguished from the analogues by T+36 (Fig. 4.5.1 m-p). A southward movement of the low coupling index values reduces the quality of the match with the 1995 analogue. The complete absence of any areas of potential instability in 1985 and 1999 cast serious doubt on the utility of these analogues. Moisture transport is conducted along the east coast of the continent in 1999, resulting in a structure similar in orientation and location to 1985 and 1995. A shift eastward in the precipitable water plot of Hazel does improve the correlation of this field to all of the analogues, but the extent of the high precipitable water values in northern Quebec impairs this assessment.

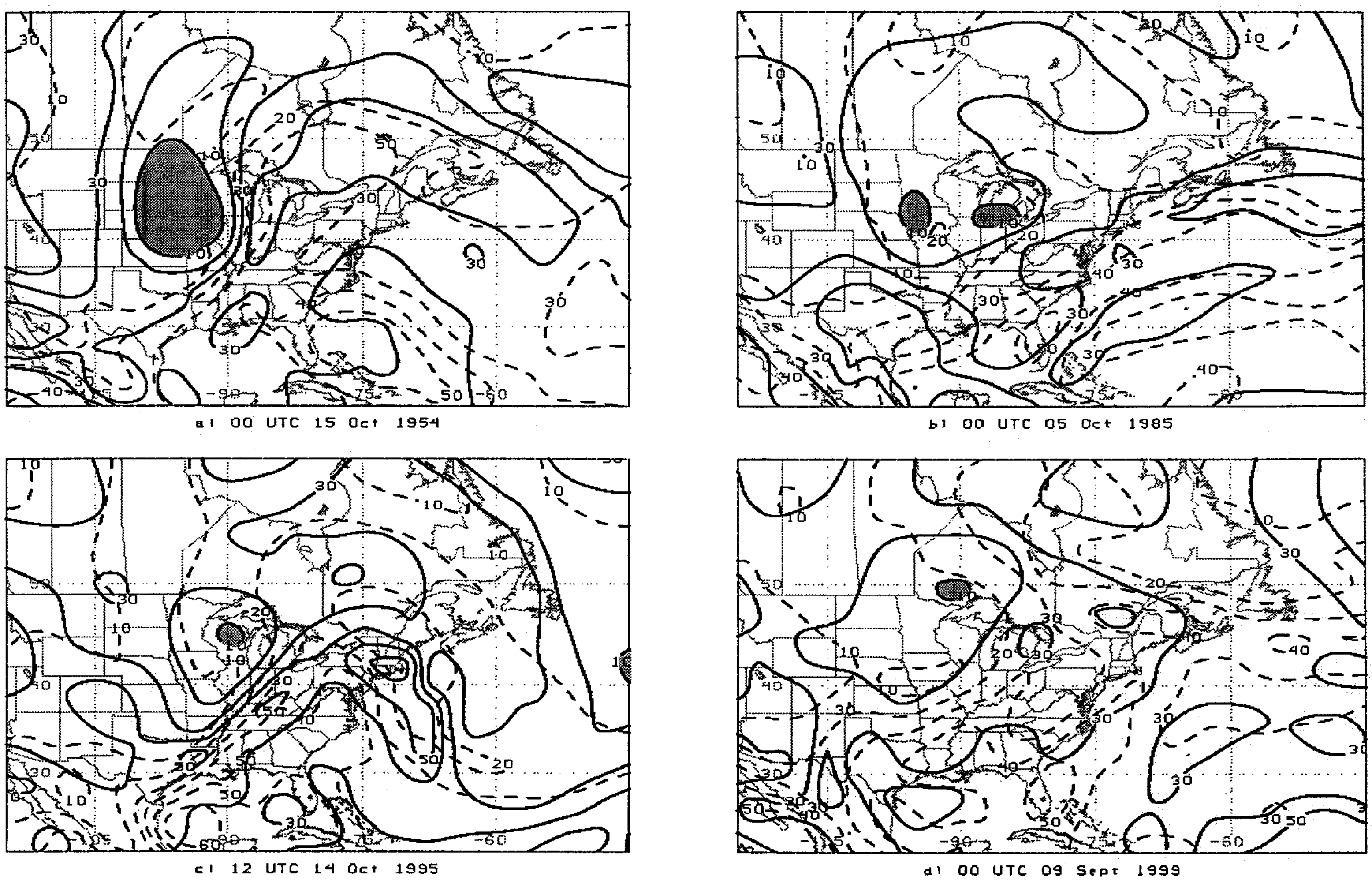

Fig. 4.5.1. Coupling index (solid, values below ten shaded) and precipitable water (dashed, contour interval of 10 mm). For: (a) Hazel; (b) 1985 analogue; (c) 1995 analogue; (d) 1999 analogue.

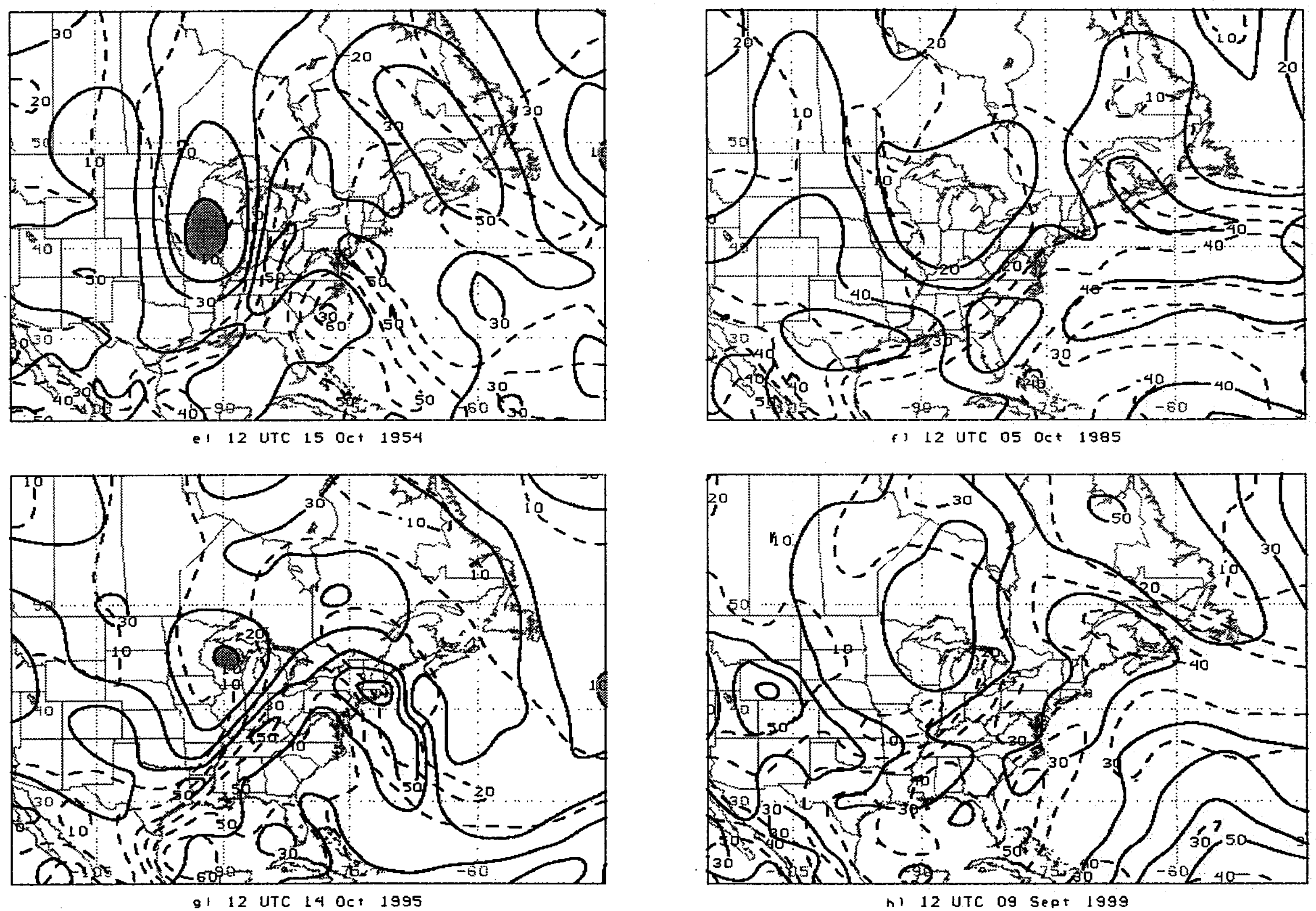

Fig. 4.5.1. (Continued) For: (e) Hazel; (f) 1985 analogue; (g) 1995 analogue; (h) 1999 analogue.

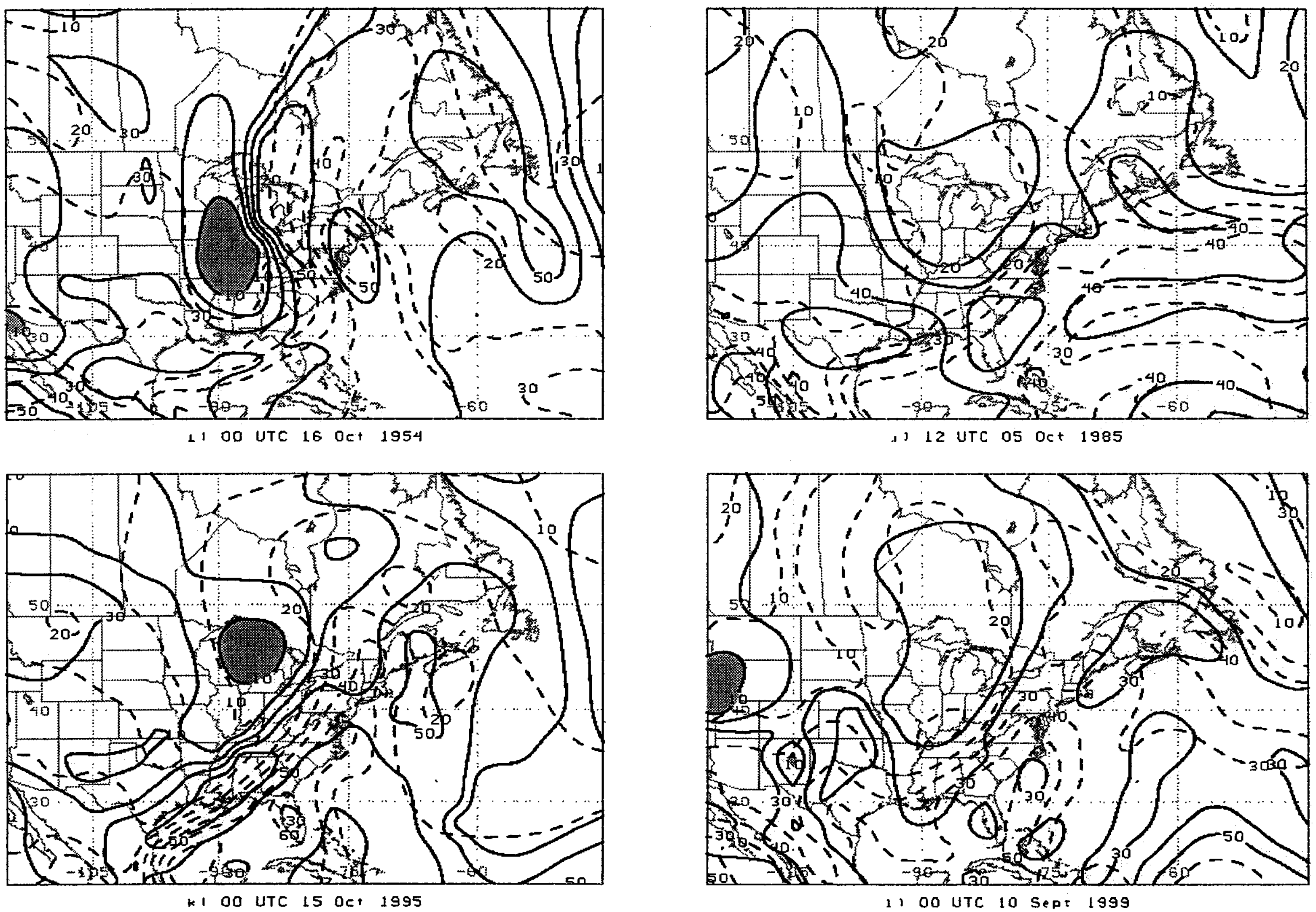

Fig. 4.5.1. (Continued) For: (i) Hazel; (j) 1985 analogue; (k) 1995 analogue; (l) 1999 analogue.

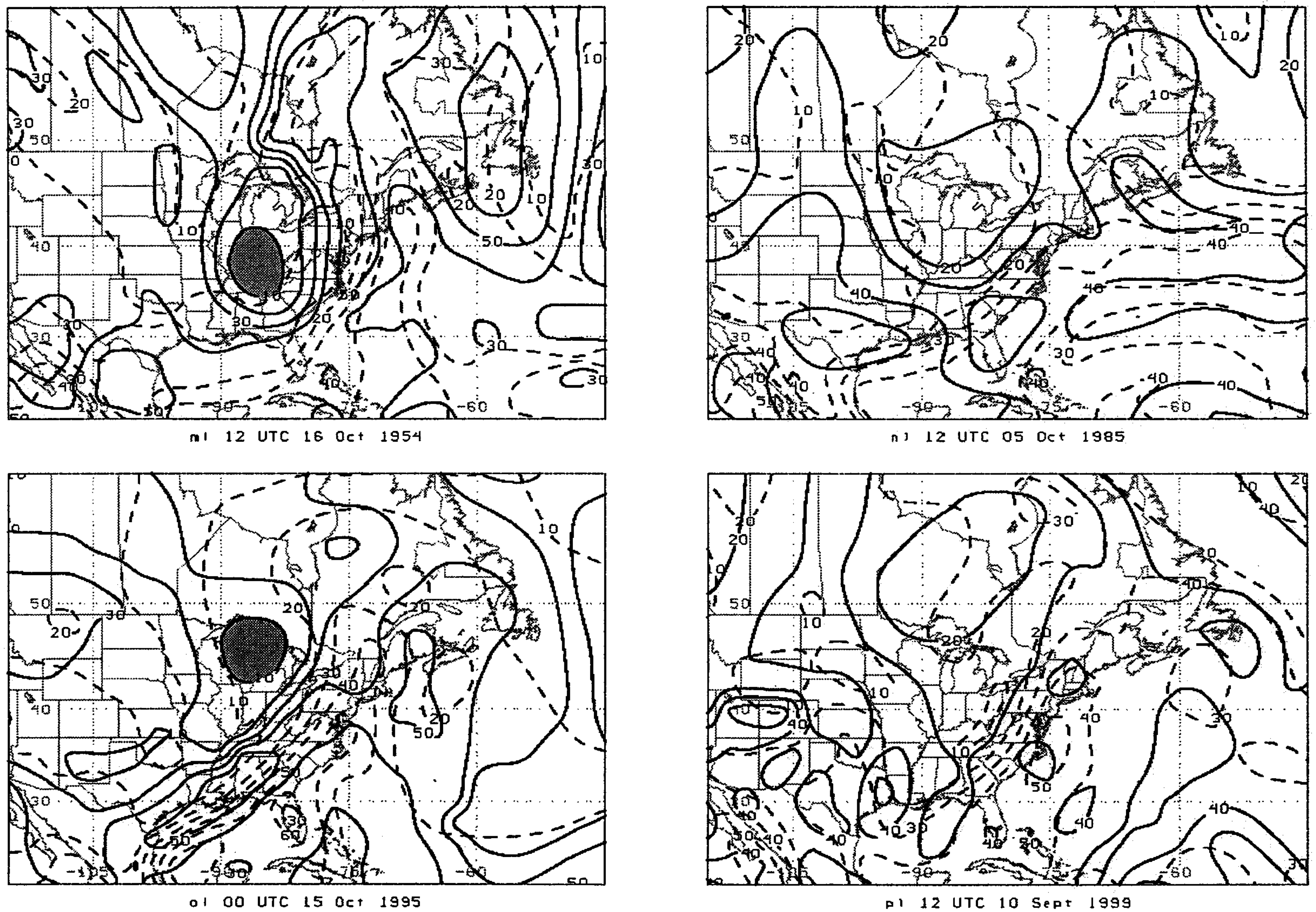

Fig. 4.5.1. (Continued) For: (m) Hazel; (n) 1985 analogue; (o) 1995 analogue; (p) 1999 analogue.

4.6 Precipitation comparison

Contrasting the objectively analyzed storm total precipitation values for all of the events confirms the outlier status of Hazel (Fig. 4.6.1). The track of heavy precipitation in 1954 stretches from South Carolina to northern Ontario, while each analogue records sporadic rainfall maximums. A band of rainfall over the New England states and eastern Quebec in 1985 peaks at 45 mm near the extreme northeast portion of the search domain. This amount of rain is insignificant when compared to 1954. 1999 precipitation is concentrated in northern Ontario and eastern Quebec, with limited spatial coverage. Quantities exceeding 45 mm are linked to the extratropical low in 1999. Rainfall from the 1995 event stretches along a moisture channel identified in section 4.5 from the Gulf of Mexico into New York state, and a large trough extending from the extratropical low to Hurricane Roxanne. Precipitation in 1985 is situated along the warm, eastern side of the midlatitude low (see section 4.3), and a strong oceanic flow of air. Slow evolution by the 1995 and 1985 analogues restricts the time over which each event occurs thereby reducing the period of time for potential precipitation, but rainfall amounts are dwarfed by the 1954 test case. The immense quantity and extensive coverage of the precipitation generated by Hazel is not readily comparable to any of the precipitation distributions coupled to the analogues.

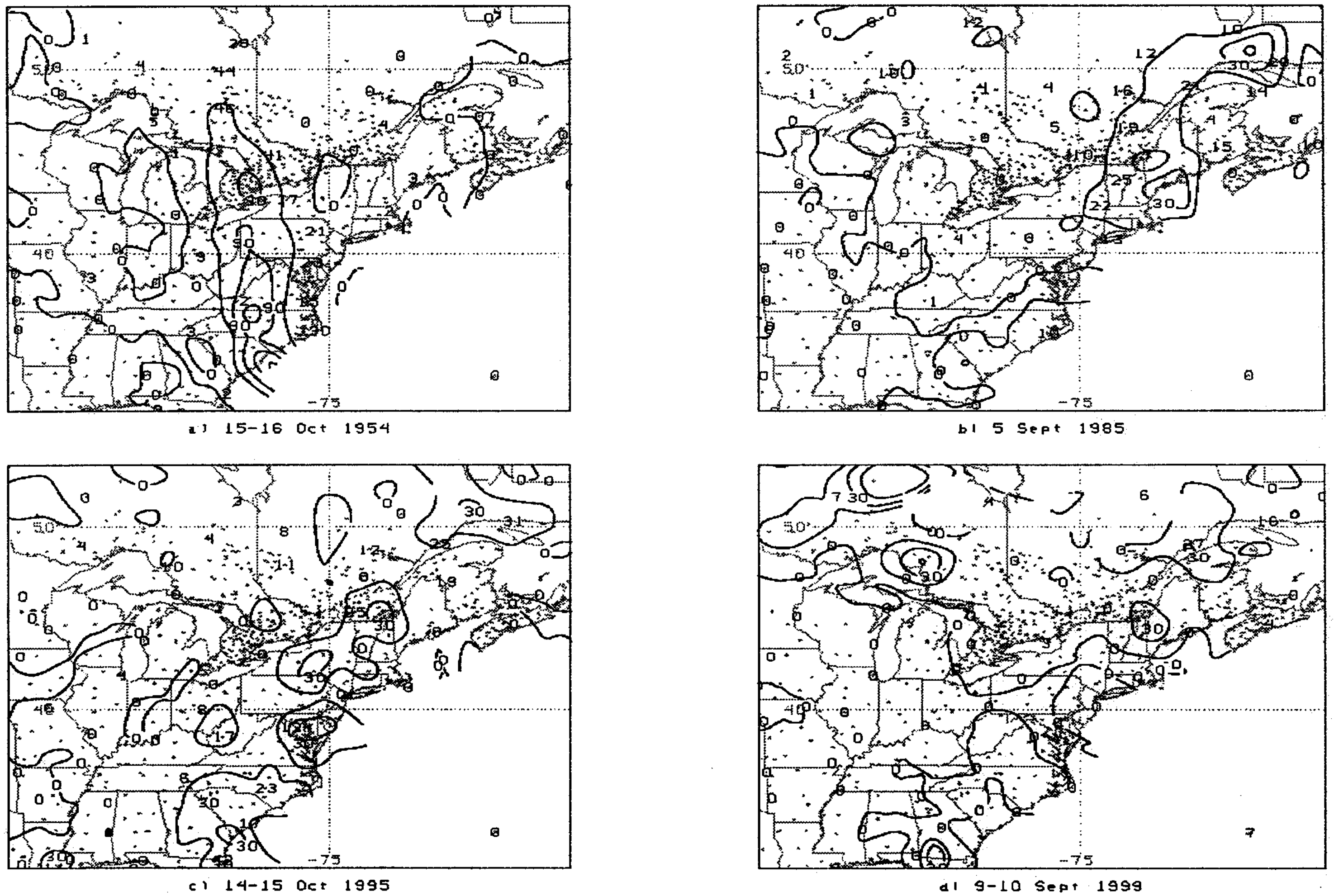

4.6.1. Storm total precipitation (contour interval of 45 mm in (a), and 15 mm in (b)-(d)). For: (a) Hazel; (b) 1985 analogue; (c) 1995 analogue; (d) 1999 analogue.

4.7 Summary of analogue search

Key differences between Hazel and the analogues exist, preventing the comparative cases from intensifying to the same degree as Hazel. The presence of an anomalously deep extratropical low pressure system over the Great Lakes, and anomalously low 1000-500 hPa thickness values over the U.S. Midwest and high values situated near Quebec create a strong correlation in all the events with Hazel. Absence of a hurricane circulation and the associated large quantity of moisture in any of the analogues reduces the likelihood of the analogues generating severe weather. Hurricane Roxanne in 1995 is located much too far from the midlatitude low to condition the atmosphere in a manner similar to that of Hazel. Atlantic Ocean air flows into the storm of 1954, providing an important source of atmospheric moisture lacking in the analogues. A steeply sloped, negatively tilted dynamic tropopause in 1954 implies that the principal baroclinic zone is significantly more intense than in the comparative events. Diabatic outflow from Hurricane Hazel results in a non-advective redistribution of isentropic surfaces that is not replicated by the other events. The atmosphere is more susceptible to convection in 1954, as evidenced by the low coupling index values. None of the analogues exhibit this broad region of potential instability. Storm total precipitation is incomparable, as Hazel yields an enormous quantity of rainfall that eclipses all of the analogues.

5. Mesoscale Modeling Study

5.1 Motivation

A conclusion to be drawn from the analogue study is that Hazel is an outlier, an unique storm without comparison in recent history. To better understand this event, a numerical modeling simulation is appropriate to discern the features crucial to the development of this deadly storm. A sensitivity study is the method of choice in this research project, to identify the elements important to the extratropical transition and intensification of Hazel. Significant forecast error was reported by Knox (1955), and an interest in this investigation is to determine if a mesoscale limited area model can accurately predict the occurrence of a case like Hazel. Sensitivities to be tested are hurricane circulatory structure and horizontal resolution. Verification of the influence of these parameters is conducted by subjective comparison of the simulation results to track positions and central pressure values by Knox (1955) and Anthes (1990), isobaric analysis from Palmén (1958) and objectively analyzed precipitation data gathered from various sources (see section 3.6).

5.2 Model description

Utilization of the Mesoscale Compressible Community (MC2) model (Benoit et al. 1997) allows for the creation of limited area simulations in this sensitivity study. This model is based on a limited area primitive equation model developed by Benoit et al. (1989). Provided by the RPN (Recherche en Prévision Numérique) branch of the MSC (Meteorological Service of Canada), the MC2 employs a three dimensional semi-Lagrangian advection scheme with semi-implicit time stepping to solve the system of equations. A viable solution over a wide range of scales in the MC2 is ensured by relaxation of the hydrostatic approximation in the Navier-Stokes equations (Tanguay et al. 1990). Benoit et al. (1997) describe the model physics and dynamics in elaborate detail. The subsequent discussion of these packages in this section, and descriptions of the MC2 runtime configuration in section 5.3 follow this reference closely. Dynamics version 4.9.5 and physics version 3.72 are operated on a NEC-SX6 supercomputer at RPN to produce the simulations.

The semi-Lagrangian method used by the MC2 has numerous advantages. The approach allows for larger time steps, produces less noise and obtains the same level of accuracy when run against a higher resolution Eulerian method. This technique interpolates the position of air parcels backwards in time to the previous step at an upstream location. The semi-implicit portion of the model deals with the time derivatives, by implicitly handling the quickly propagating waves and explicitly treating the slowly propagating waves. Use of the semi-implicit semi-Lagrangian (SISL) scheme yields stable solutions, even when making use of long time steps that cause the Courant number to exceed one. Using a Courant number greater than one is not desirable, especially over topography (Yau 2003). Partitioning of the physical and numerical wave solutions permits this configuration.

A three dimensional, staggered grid arranged in the form of an Arakawa C-grid in the horizontal and a Tokioka B-grid in the vertical allows for the calculation the space derivatives through finite differencing. The vertical coordinate system in the MC2 is the terrain following Gal-Chen coordinate. Surfaces along a Gal-Chen level are not orthogonal to the ground. Modification of the distance between each Gal-Chen level is possible to provide the desired degree of vertical resolution. Another advantage afforded by this coordinate system is the requirement that no vertical motions occur at the surface. This constraint must also be matched at the rigid top of the model domain.

A "successive corrections" technique works to generate a viable solution to the prognostic equations (McTaggart-Cowan et al. 2001). All dynamical terms are solved initially such that all variables are then known at the given time step. Following this computation, the nesting of the open boundaries is added to the variable, model physics are evaluated and incorporated, implicit horizontal diffusion is applied, and Robert's time filter is applied to control the time decoupling inherent to a three-time-level model.

The RPN physics package used to produce the aforementioned corrections contains many variables that allow the user to choose from several different physics parameterizations. Mailhot et al. (1998) provide a thorough description of this package that supplements the subsequent discussion. The force restore method predicts the surface temperature over land from a heat budget, and moisture over land is derived from a moisture balance. Sea surface temperature is specified from a monthly climatology or weekly analysis, remaining fixed for the duration of the simulation. Evaporation over ground is a function of a soil moisture availability factor, determined by using the Budyko bucket method. Infrared radiation and its interaction with water vapour, carbon dioxide, ozone and clouds is included. Solar radiation is modified by Rayleigh diffusion and multiple scattering, in addition to the previously mentioned factors. Vertically propagating gravity waves excited by statically stable flow over mesoscale topographic undulations are handled in a gravity wave drag parameterization that utilizes sub-grid scale orography.

Cloud processes are handled by many separate routines depending on the physical mechanisms at work. Shallow convection is modeled as a case in which the planetary boundary layer is saturated but not precipitating. This accounts for small cumulus cloud formation at the top of this layer, and the accompanying transport of moisture vertically. Definition of the planetary boundary layer is set by a prognostic equation for turbulent kinetic equation. Other vertical transfers are captured by a turbulent vertical diffusion scheme (Benoit et al. 1989). A coefficient controls the strength of this diffusion throughout the atmosphere, which is strongest in the planetary boundary layer. Grid scale convection generates stratiform precipitation, and if resolution is fine enough, convective precipitation. The Kong and Yau (1997) system explicitly determines the stratiform condensation in the simulations for this study. Using the SISL approach the prognostic variables of water vapour, cloud water, rainwater, graupel and ice particles are ascertained. This is accomplished by incorporating microphysical processes such as condensation, evaporation, accretion, riming, homogeneous nucleation, contact freezing and sedimentation. The low number of predicted variables and circumvention of calculations for number concentration of the particles makes this technique particularly efficient.

The presence of sub-grid scale convection requires another set of parameterizations to ensure realistic precipitation production. For the purposes of all the model runs in this research project, a widely accepted scheme known as the Kain-Fritsch parameterization is employed. The Kain-Fritsch method is based on the assumption that convective effects remove convective available potential energy (CAPE) from a grid box in an advective time period. Representative updrafts and downdrafts are imposed in the grid space with environmental air occupying the remaining room. Entrainment and detrainment lead to the exchange and dilution of moist air between the convective unit and the surroundings, facilitating the removal of CAPE. Convection begins after a positive temperature perturbation lifts a parcel to the lifting condensation level. Precipitation efficiency is dependent on the vertical wind shear and cloud base height (Kain and Fritsch 1993). Midlatitude summertime and wintertime systems, as well as tropical systems are all well simulated with Kain-Fritsch.

Additional information is required by the MC2 to prescribe the surface features. Fields include deep soil temperature, snow fraction on the ground, soil wetness, sea ice coverage, albedo, surface temperature, land-sea mask, roughness length and orography. All these fields are obtained from climatological or analytical datasets.

5.3 MC2 runtime configuration

The MC2 user has two mode options for operating the model, simulation and forecast. Forecast mode requires analysis fields at model initialization only, with no information supplied about the future atmospheric state on the lateral and upper boundaries. This independence from all future atmospheric information reduces the ability of the MC2 to forecast for long time periods, as is the case for all regional models. A prognosis of the meteorological conditions for two days is possible if the region of interest is away from the equator. An initial coarse resolution run in forecast mode sets the constant lateral boundary conditions, creating output to be ingested by the MC2 for a nested simulation. Nesting at higher resolution is conducted over a smaller sub domain farther from the equator. Normally persistent synoptic conditions in the tropics over a 24 to 48-hour period suggest that imposing constant lateral boundary conditions in this region is not an unreasonable assumption.

Simulation mode is chosen for this study, as updated boundary conditions are available from the NCEP/NCAR reanalysis dataset. This dataset is global in extent, but hemispheric model output or objectively analyzed data may also be utilized. Required input fields for the initial and boundary conditions are temperature, geopotential height, specific humidity and the meridional and zonal winds. Data on these fields is fed into the MC2 on 17 standard isobaric levels from 1000 hPa to 10 hPa, in six-hourly time increments. A sponge zone at the edge of the domain blends the nested data with the model dynamics output (with the exception of cloud water content) at each time step in the horizontal and vertical. An attenuation function weights the nesting values between zero and one. Resultant fields are composed of only nested values at the lateral boundary, and solely dynamics output at the interface between the sponge zone and the free internal domain. This procedure ensures a smooth transition between nested and non-nested values. Input data for the boundary conditions can be supplied at longer, regularly spaced time intervals than the timesteps taken by the MC2. Linear interpolation between two consecutive timesteps is performed on these input statistics to generate the necessary nesting values. The self-nesting capability of the MC2 allows for the use of MC2 output from a lower resolution run to become the boundary conditions for a higher resolution MC2 simulation. This technique accommodates the use of poorly resolved initial analyses. Delay of the initialization start time in the reduced domain cascade run is used between consecutive grids to cover the spin-up time of adjustment of the fields to the changed terrain.

Removal of any doubts regarding the balance state of the initial conditions is lessened by a type of dynamic initialization. The procedure first runs forward in time for a small number of timesteps without physics, and then reverses in time back to the simulation start point. A more balanced atmosphere is now ready for integration by the MC2. Random pressure fluctuations and the condensation spin-up problem are also reduced as a result of this initialization. This initialization is also used when initial vertical motion fields are not available for the integration. Often even when vertical motions are provided from other models the interpolation of this variable to the Gal-Chen levels results in an imbalance in the initial conditions. Imbalances are decreased and model convergence is improved with the implementation of this routine.

5.4 Control simulation

The control simulation (CONT) was initialized at 00 UTC 15 October 1954 and run for 36 hours to 12 UTC 16 October 1954 in 360 second timesteps. Choosing 00 UTC 15 as the initial time was necessary to accommodate the use of the six-hourly NCEP/NCAR reanalysis data at a time as close as possible to the synoptic observation time in 1954 prior to storm landfall (i.e. 03 UTC and 15 UTC). A horizontal resolution of 36 km was selected on a rotated Mercator projection grid true at 22.5°N. An arrangement of 200 by 200 grid points on 35 vertical levels, up to a model lid height of 35 km was selected to construct the MC2 domain. The domain covers an area stretching from the Rocky Mountains in the west to the mid-Atlantic Ocean in the east, and from the Arctic in the north to a southerly limit near Cuba.

Initially at 00 UTC 15 Hurricane Hazel in CONT is located by the Florida coast with a central pressure of 998 hPa (Fig. 5.4.1a). An extratropical low of 1000 hPa is centered near Georgian Bay in the Great Lakes system, with a weak secondary low to the north. These conditions are the result of the input atmospheric conditions from the NCEP/NCAR reanalysis plus the dynamic initialization by the MC2.

Examining the output at 03 UTC 15, the sea level pressure structure of CONT shows a strengthening trough extending south of the extratropical low over the Great Lakes and northwest of Hurricane Hazel (Fig. 5.4.1b). Hazel exhibits no signs of deepening as the central pressure is steady at 998 hPa. Actual observations place the central pressure closer to 975 hPa at this stage, much lower than the coarsely resolved estimate by the reanalysis dataset (Table 5.8.1). Large highs over the Atlantic Ocean and Rocky Mountains bound Hazel and the extratropical low. Anthes (1990) simulation is initialized at this time, qualitative comparison of the initial sea level pressure from that integration and the CONT field yields a few differences (Fig. 5.4.1c). A major disparity is between the central sea level pressure values in Hurricane Hazel, as Anthes (1990) uses 975 hPa as a starting central pressure based on the geopotential height and temperature distribution surrounding Hazel in Palmén's (1958) analyses. Location of the low pressure centers is also dissimilar, as CONT places the storm farther to the east. Aside from these differences associated with Hurricane Hazel, the major trough, ridges and high pressure systems match well between the two studies. A col is featured in both simulations near the western border of the Carolinas.

Viewing the 1000 hPa height analysis by Palmén (1958) at this time also confirms the validity of CONT (Fig. 5.4.2a). This analysis is available only in imperial units, unlike the metric-based output from the MC2. A subjective evaluation is only permitted

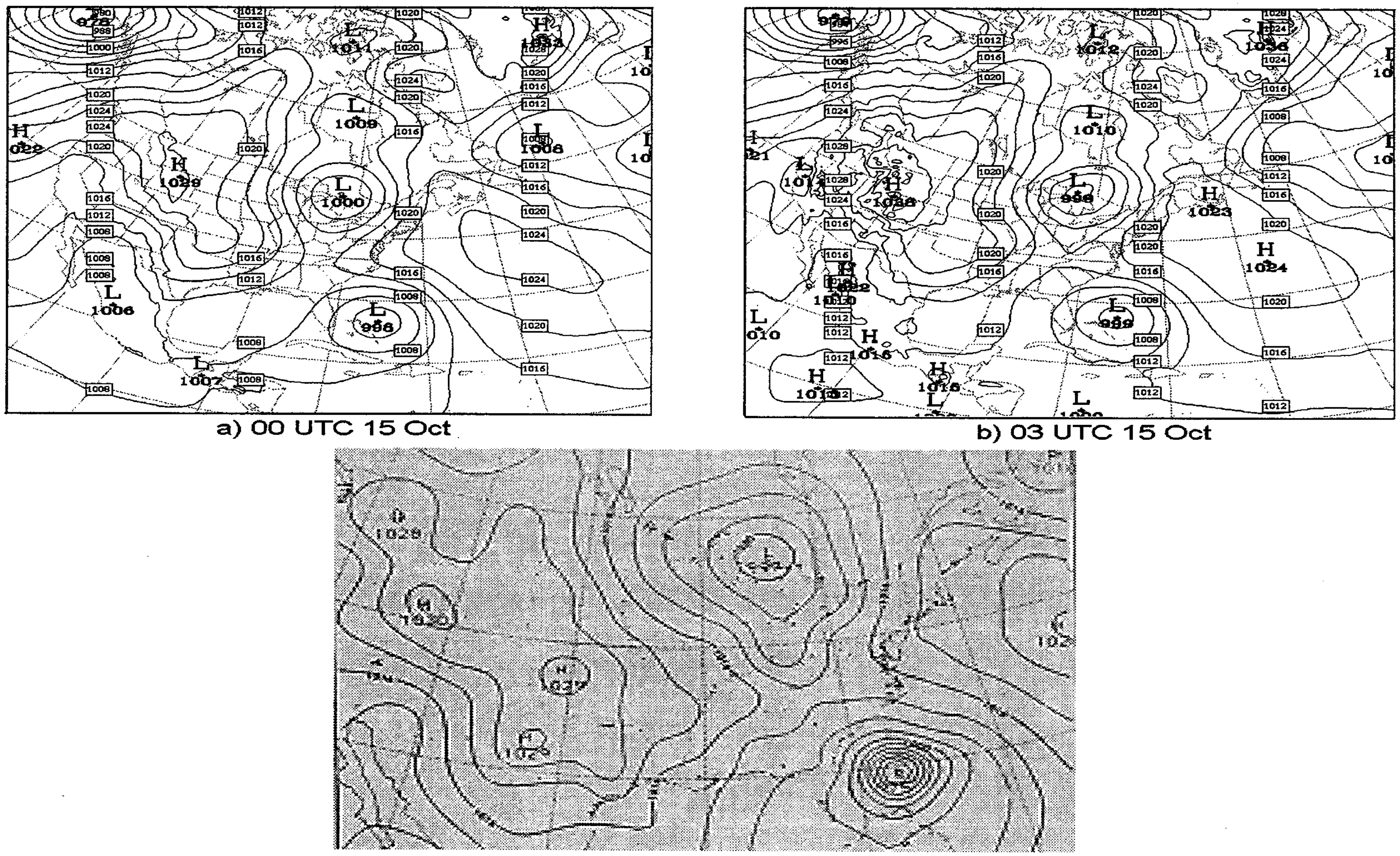

c) 03 UTC 15 Oct

Fig. 5.4.1. Sea level pressure (contour interval of 4 hPa). For: (a) and (b) CONT; (c) from Anthes (1990).

as a result of this inconsistency and the poor quality of the original figures. Again a significant problem exists with Hurricane Hazel at 1000 hPa in Fig. 5.4.2b as the vortex is too weak and not far enough north to compare well with the 1000 hPa height observations. Both simulation and analysis have a negatively sloped trough extending from Hurricane Hazel to the extratropical low, and ridging over Virginia and Tennessee that confirms the agreement in synoptic scale circulation features.

The 500 hPa heights in CONT have a qualitatively similar appearance to the analysis (Fig. 5.4.3a). A deeper midlatitude trough is present in Palmén's (1958) analysis over western Lake Superior, by roughly 3.5 dam from a subjective comparison (Fig. 5.4.3b). Orientation of the trough is meridional and well modeled by CONT, but the extension southward into Arkansas is again potentially underestimated by approximately 2.5 dam.

A northward movement of Hurricane Hazel occurs over the next nine hours up to 12 UTC on the 15th (Fig. 5.8.1a). Weak intensification is present as the center of Hazel drops to 997 hPa by 12 UTC, but is over 20 hPa too high at this point compared to observations. The approach of the hurricane is three hours delayed relative to observations by Knox (1955) in Fig. 5.8.1b starting at 09 UTC, as actual landfall should be occurring in CONT at 12 UTC 15. The storm in CONT fails to intersect the continent at this time. A lengthening of the northeast-southwest positioned trough axis of the extratropical low develops during this period.

At 15 UTC 15 the CONT run shows a 1000 hPa center in Hazel near the coast of North Carolina (Fig. 5.4.4a). Central pressure is still approximately 20 hPa above observations by Knox (1955) while falling to 993 hPa. Hazel's track is shifted eastward

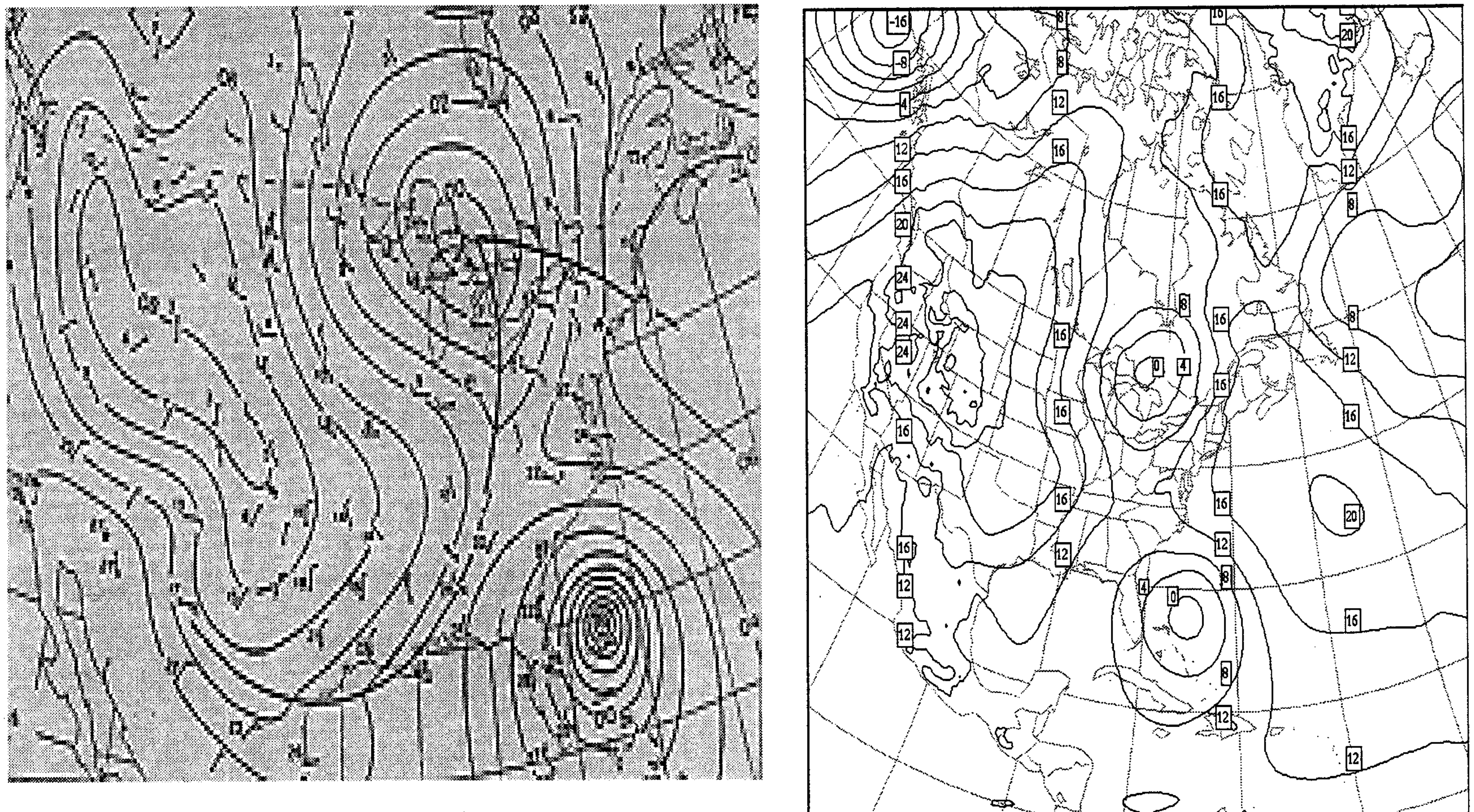

a) 03 UTC 15 Oct

b) 03 UTC 15 Oct

Fig. 5.4.2. 1000 hPa heights (contour interval of 10 feet in (a) from Palmén (1958) and 4 dam in (b)). For: (a) from Palmén (1958); (b) CONT.

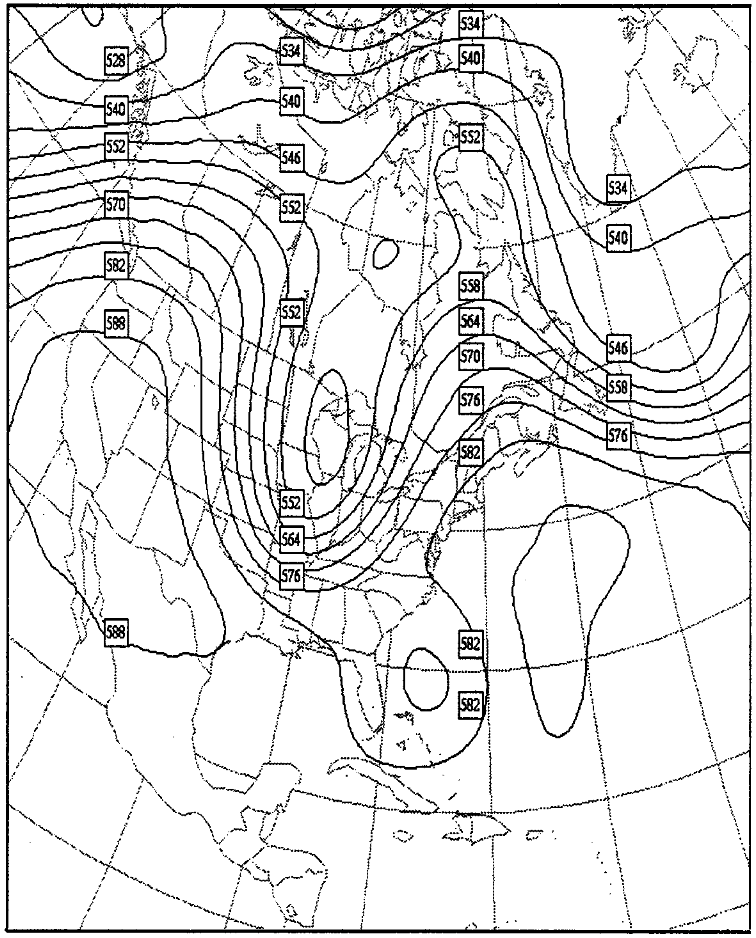

a) 03 UTC 15 Oct

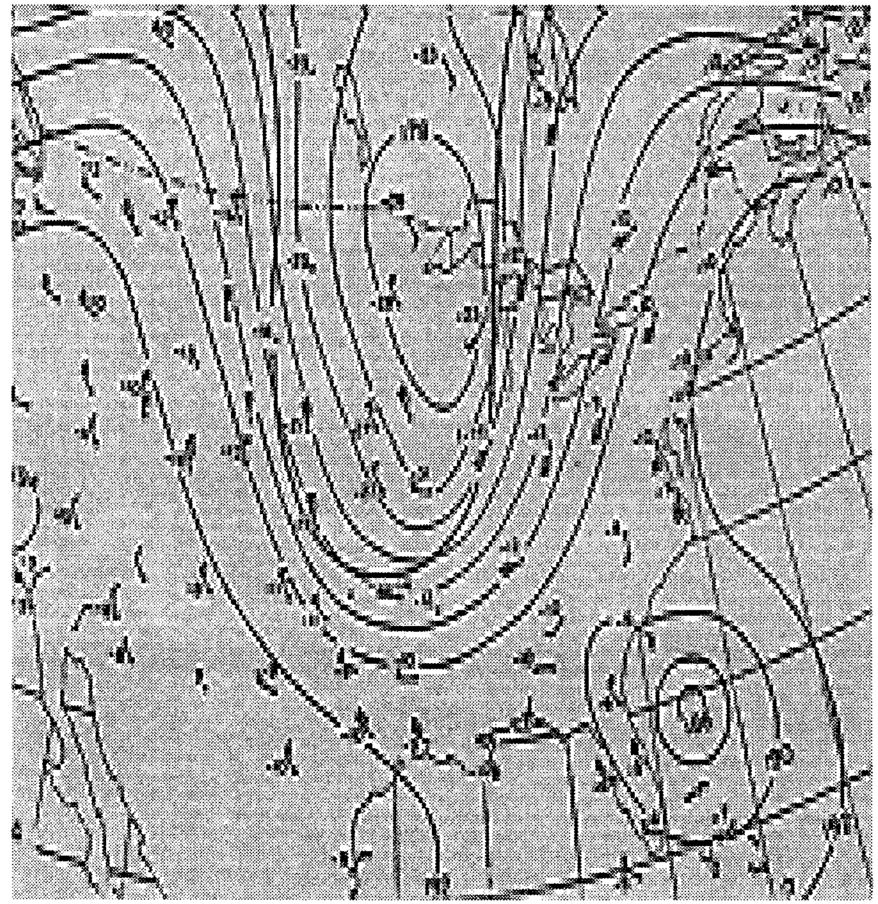

b) 03 UTC 15 Oct

Fig. 5.4.3. 500 hPa heights (contour interval of 6 dam in (a) and 20 feet in (b)). For: (a) CONT; (b) from Palmén (1958).

relative to the actual path, and the three hour lag is still evident as Hazel has yet to make landfall. Trough tilt of the extratropical low is captured by CONT as the analysis (Fig. 5.4.4b) and model integrations show a negatively tilted feature over the Great Lakes. This trough extends deep into Hurricane Hazel. An encouraging detail is the performance of CONT versus the simulation of Anthes (1990). CONT and Anthes (1990) share a virtually common storm track to this stage, with the eastward bias and three hour time delay (Fig. 5.8.1a).

Subjectively examining the CONT heights at 500 hPa (Fig. 5.4.5a) against the analysis (Fig. 5.4.5b) shows a possible overemphasis of a cutoff low region over the Great Lakes. Analysis places a height of roughly 549 dam near the Lake Michigan and Lake Huron connection, while the CONT shows a 546 dam contour. This pattern of underestimation prevails throughout the CONT 500 hPa field.

Hazel tracks from North Carolina to Maryland in CONT along the coastline over the hours from 15 UTC 15 to 00 UTC 16. Continued weak deepening takes place as Hazel supplants the extratropical low as the dominant weather feature in Ontario. Storm track in CONT is east of the observations still, and central pressures are still elevated even with the steady decline. Hazel from CONT continues to emulate the timing and path of the Anthes (1990) generated storm.

Tracking the maturing storm in CONT at 03 UTC 16 leads to a location in eastern Pennsylvania. The CONT simulation has more in common with the work produced by Anthes (1990) than it does with the actual available observations. Both events lag behind the actual Hazel, and drift much too far off to the east of the observed path.

CONT generates a negatively tilted Hazel at 1000 hPa by 03 UTC 16 (Fig. 5.4.6a)

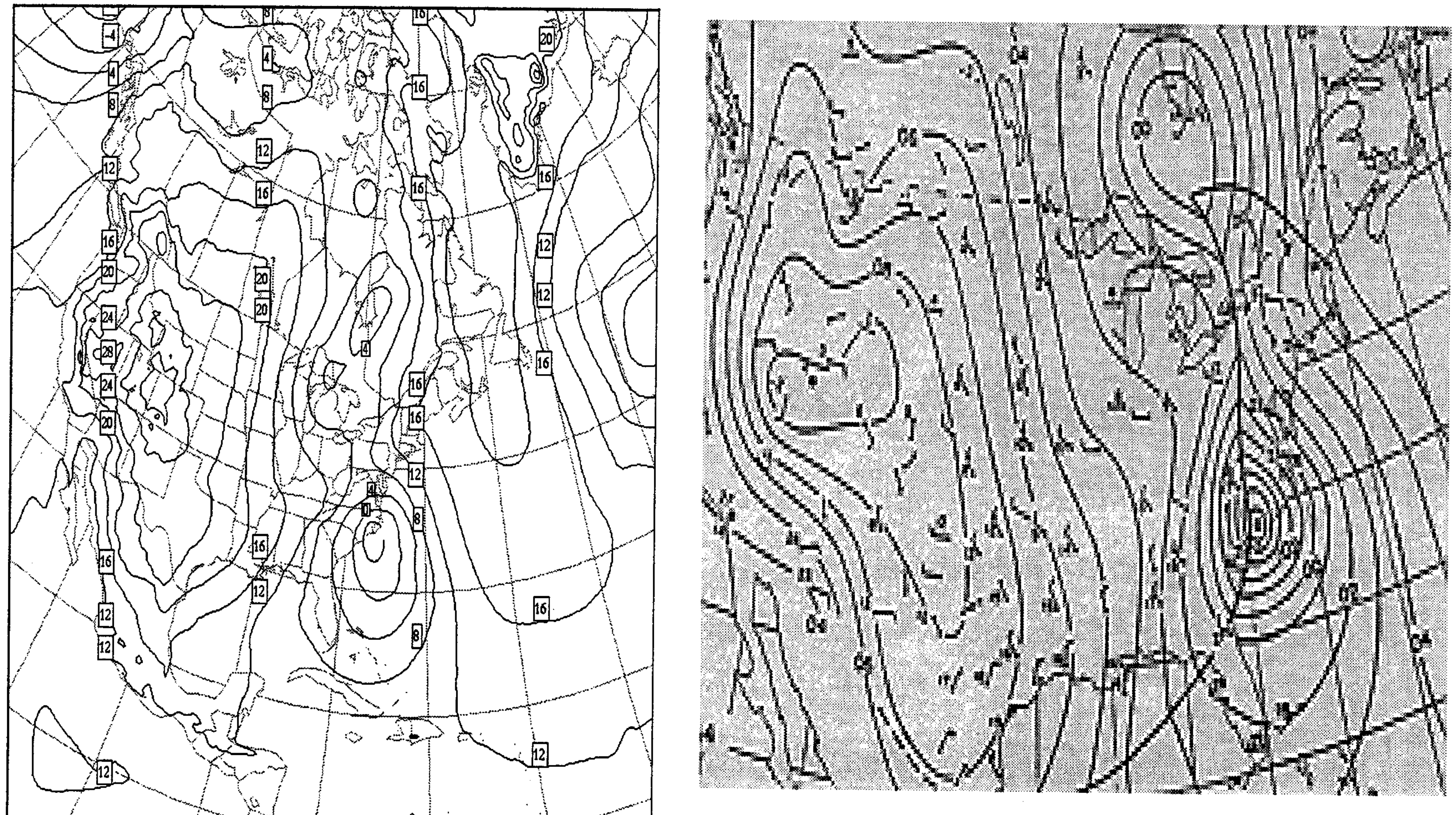

a) 15 UTC 15 Oct　　　　b) 15 UTC 15 Oct

Fig. 5.4.4. 1000 hPa heights (contour interval of 4 dam in (a) and 10 feet in (b)). For: (a) CONT; (b) from Palmén (1958).

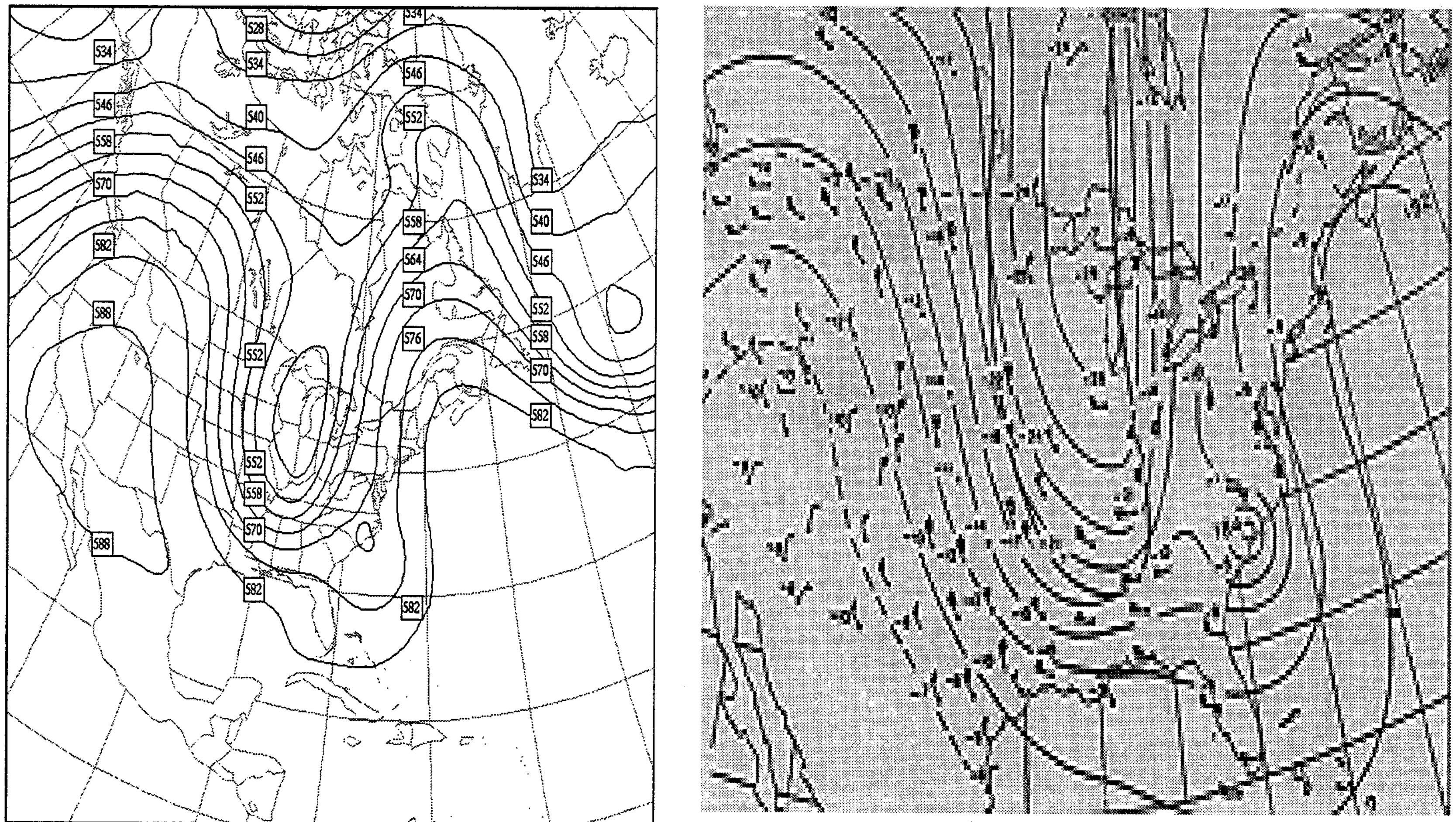

Fig. 5.4.5. 500 hPa heights (contour interval of 6 dam in (a) and 20 feet in (b)). For: (a) CONT; (b) from Palmén (1958).

that emulates the observed conditions in the analysis (Fig. 5.4.6b). A sweeping trough in both of the figures penetrates deep into the southern portion of the domain, from near Ontario to Florida. Correlation of the major features at this time is strong, and reinforces the validity of CONT.

The final storm phase shows a westward turn in the track of Hazel, an event that is embedded in the observations by Knox (1955). A final sea level pressure minimum of 981 hPa closes the gap between the CONT storm and the actual value to 6 hPa.

Fallen precipitation is shifted to the east in CONT relative to the objectively analyzed data (see section 3.6), reflecting the eastward bias in the storm track. Amounts are much lower from CONT as well, with a local maximum of 88 mm over the continent occurring in Virginia (Fig. 5.4.7). Observed values near this region approach 140 mm, indicating that CONT is underestimating the quantity of rainfall associated with Hazel. Precipitation is also diminished at the northern end of Hazel's track into Ontario, owing to the time lag in the CONT simulation. Even with the precipitation and tracking deficiencies of the CONT run, the correspondence to the analyzed sea level pressure distribution and structure, and a previous modeling study of Hazel by Anthes (1990) is sufficiently high enough to validate the use of this CONT run for the ensuing sensitivity tests.

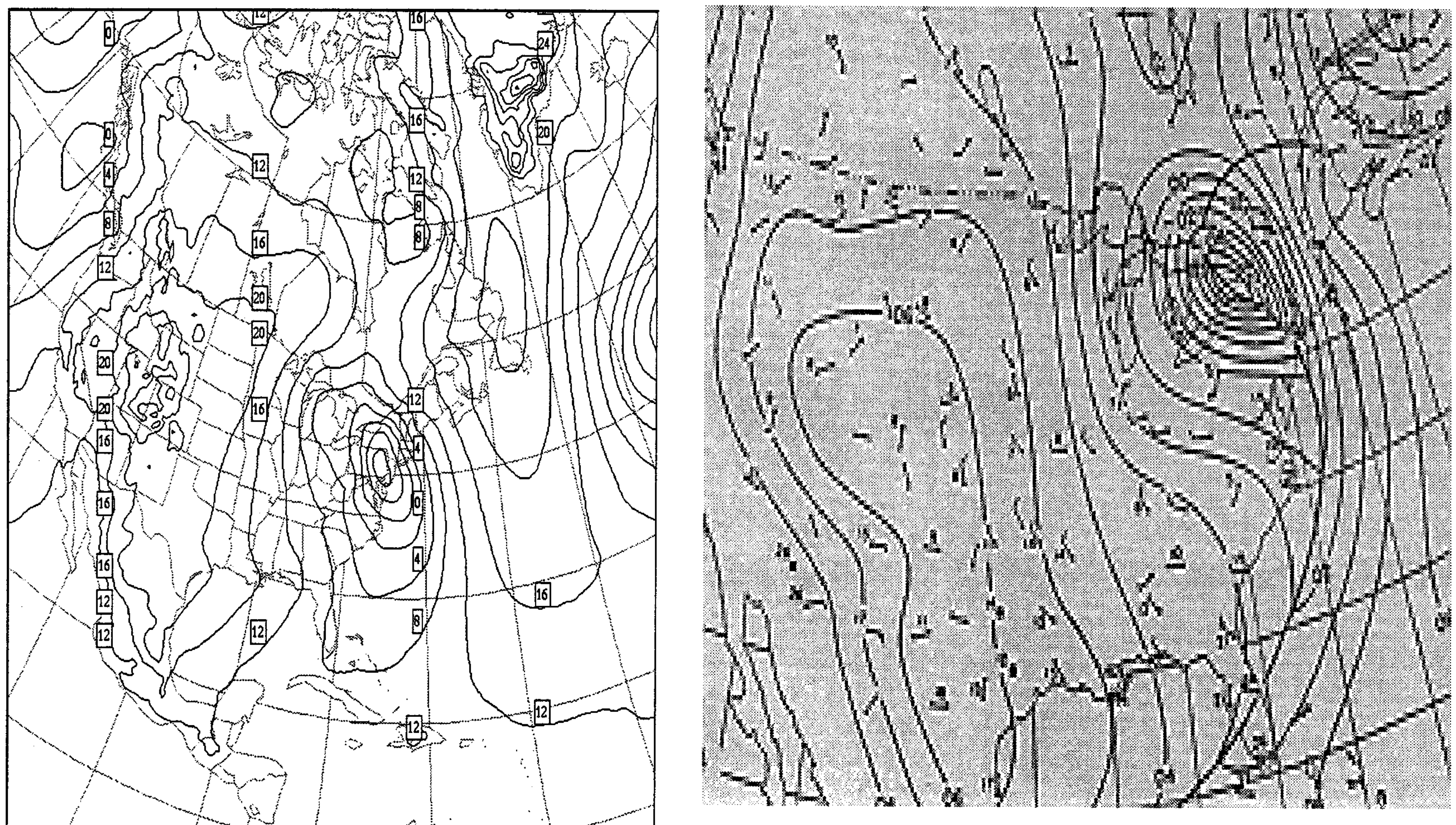

a) 03 UTC 16 Oct

b) 03 UTC 16

Fig. 5.4.6. 1000 hPa heights (contour interval of 4 dam in (a) and 10 feet in (b)). For: (a) CONT; (b) from Palmén (1958).

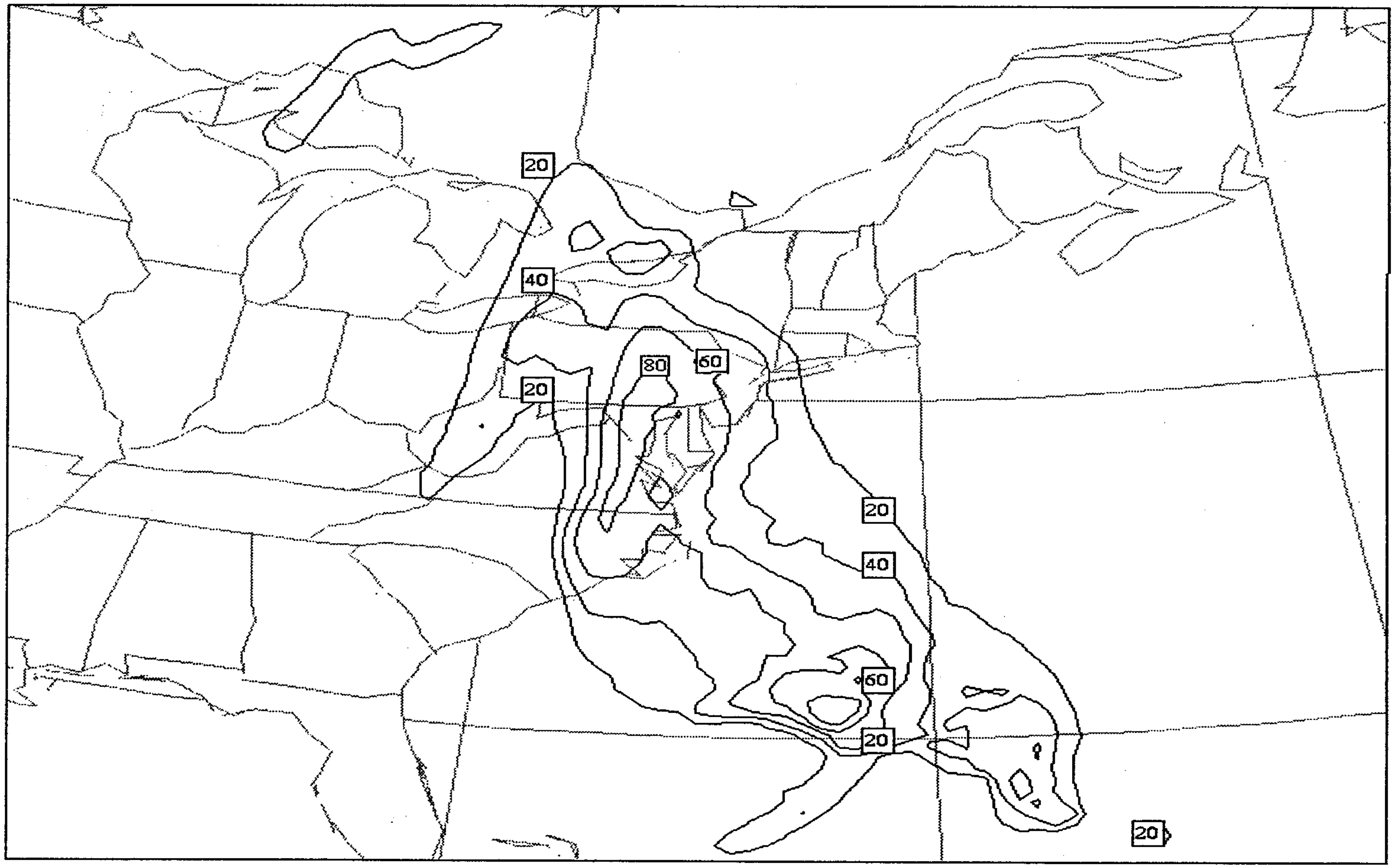

15-16 October

Fig. 5.4.7. Storm total precipitation from CONT for 36 hour period starting at 00 UTC 15 October (contour interval of 20 mm).

5.5 Vortex bogusing

Testing the sensitivity of the development of Hazel to the hurricane vortex structure was undertaken with the implementation of a bogusing routine. Vortex bogusing consists of the replacement of a poorly resolved tropical cyclone with a properly specified vortex. The technique employed in this study and discussed below follows work by Kurihara et al. (1993). The reader is directed to this reference for a more detailed explanation.

The need for vortex bogusing is evident when viewing the structure of Hurricane Hazel in the NCEP/NCAR reanalysis data, and the preceding CONT simulation. Central pressure is initialized at a value significantly higher than that reported by Knox (1955), and the circulation associated with the storm is much too weak. Large and weak vortices lead to a delayed spin-up, producing poorly forecasted storm intensity and erratic tracking in the early stages of model integration. Removing the influence of this false spin-up is necessary to improve the prediction of tropical cyclones.

Construction of a more realistic vortex is not an easy task. Kurihara et al. (1993) placed three restrictions on the vortex specification process, the first such constraint being that dynamic and thermodynamic consistency must be achieved in the new vortex. A major issue to address is the specification of an initial moisture field, which controls the vortex intensity changes. These intensity changes are manifested in the amount of diabatic heating taking place in the cyclone. Coherence between the moisture field and other variables ensures an appropriate representation of the temperature tendency. Wind and mass fields are subject to the same consistency criterion, and must be balanced prior to model integration. A second tenet is that the real storm should be approximated as well as possible in the specified vortex. Features such as the radius of the vortex and the central sea level pressure can be introduced to create a bogused vortex that best resembles the actual storm. A final precept focuses on the compatibility of the generated vortex with the resolution and physics of the MC2. False spin-up is avoided by adhering to this condition.

Preparation of the environmental field is necessary to successfully implant the new vortex. The scheme can be expressed as (equation 5.6.1):

(initial field) = (domain analysis) - (analyzed vortex) + (specified vortex) (5.6.1)

The weak analyzed vortex in the NCEP/NCAR data is viewed as a deviation from the environmental field. Far from the hurricane the initial field is composed of environmental values only, with a smooth transition to the region containing the tropical cyclone. Filtering of the fields leaves a smooth environmental field ready for the introduction of the bogused vortex. Defining the initial fields in this manner permits the removal and displacement of the analyzed vortex, as storm position in large-scale analyses can be in error by hundreds of kilometers.

An axisymmetric vortex is generated by the bogus routine that partitions the vortex into a symmetric and asymmetric component. The symmetric portion uses a tangential wind profile that is forced to approach a target wind distribution. The target profile consists of the best estimate of the tangential wind of the real hurricane. During the symmetric vortex creation, no constraint is placed on the evolution of surface pressure, temperature, moisture or radial winds. Planetary vorticity advection in the symmetric flow is accounted for by the inclusion of an asymmetric wind component.

Combination of the asymmetric and symmetric flows results in the full vortex wind field. Implantation of the new wind field into the initial fields precedes a diagnoses of the mass field from the divergence profile. A fully balanced bogused vortex is now present in the initialization and ready for model integration.

5.6 Low resolution vortex sensitivity

Beginning at 00 UTC 15 October 1954, Hurricane Hazel is situated near the Florida coast with a central pressure of 970 hPa. The bogusing only alters the features in the vicinity of Hazel. The location of this vortex for Hurricane Hazel is moved northwest with respect to CONT to agree with the position stated by the NHC (2003). In the bogused vortex runs, the 2.5° latitude-longitude gridded NCEP/NCAR reanalysis data is fed into the bogus routine after the dataset is cubically interpolated onto a 36 km rotated Mercator grid true at 22.5°N. This resolution enhancement avoids problems with the calculation of finite differences and produces a more symmetric vortex (McTaggart-Cowan 2003).

The central sea level pressure is set to 970 hPa in this simulation (BOG36), based on an estimate derived from Knox (1955) and from the NHC (2003).
An examination at 03 UTC 15 of BOG36 shows a hurricane that has filled to 975 hPa, a value consistent with the measurements by Knox (1955) (Table 5.8.1). The extratropical low structure in BOG36 is visibly different as well from CONT. A more pronounced trough forms to the south of the low pressure system over Ontario in BOG36 (Fig. 5.6.1a). Strong high pressure systems bound the extratropical low and Hurricane Hazel. Storm track is immediately showing signs of improvement, as BOG36 has Hazel farther

north and west than in CONT (Fig. 5.8.1a). The 500 hPa height field in BOG36 is much lower around Hurricane Hazel than in CONT, nearly 13 dam lower at the center (Fig. 5.6.1b). This drop in height is perhaps overdone, as the analysis by Palmén (1958) suggests that the heights are nearly 5 dam higher (Fig. 5.4.3b). A decrease in the height of the midlatitude trough is barely perceptible, and overall the pattern is virtually identical save the presence of Hazel.

A progressive deepening continues from 06 UTC 15 to 12 UTC 15 from 970 hPa to 965 hPa. These central pressures are falling much lower than observations, as much as 10 hPa lower. Structures surrounding Hurricane Hazel vary little in terms of magnitude, intensity or location relative to CONT. The most dramatic improvement is in the track, as BOG36 pulls away from CONT and exhibits little time lag or positional bias relative to the data from Knox (1955). Timing does eventually fall out of phase in BOG36 with the observations though as Hazel approaches the coast. The storm slows and is still located over ocean waters at 12 UTC 15.

Landfall occurs around 15 UTC 15 for BOG36, a three hour time lag. Viewing the sea level pressure field, intersection with the coast is near the North Carolina and South Carolina border, an improvement over CONT (Fig. 5.6.2). Hurricane central pressure in BOG36 is nearly 30 hPa lower than in CONT, but too deep to match observations well. A more meridional flow is west of Hurricane Hazel from the Great Lakes into the southern U.S., while stronger flow due to the bogused vortex drives moisture from the Atlantic into New England. Correspondence between Hazel in BOG36 and CONT is diminished substantially by the presence of the specified vortex.

From 18 UTC 15 to 00 UTC 16, BOG36 steadily outperforms CONT. BOG36

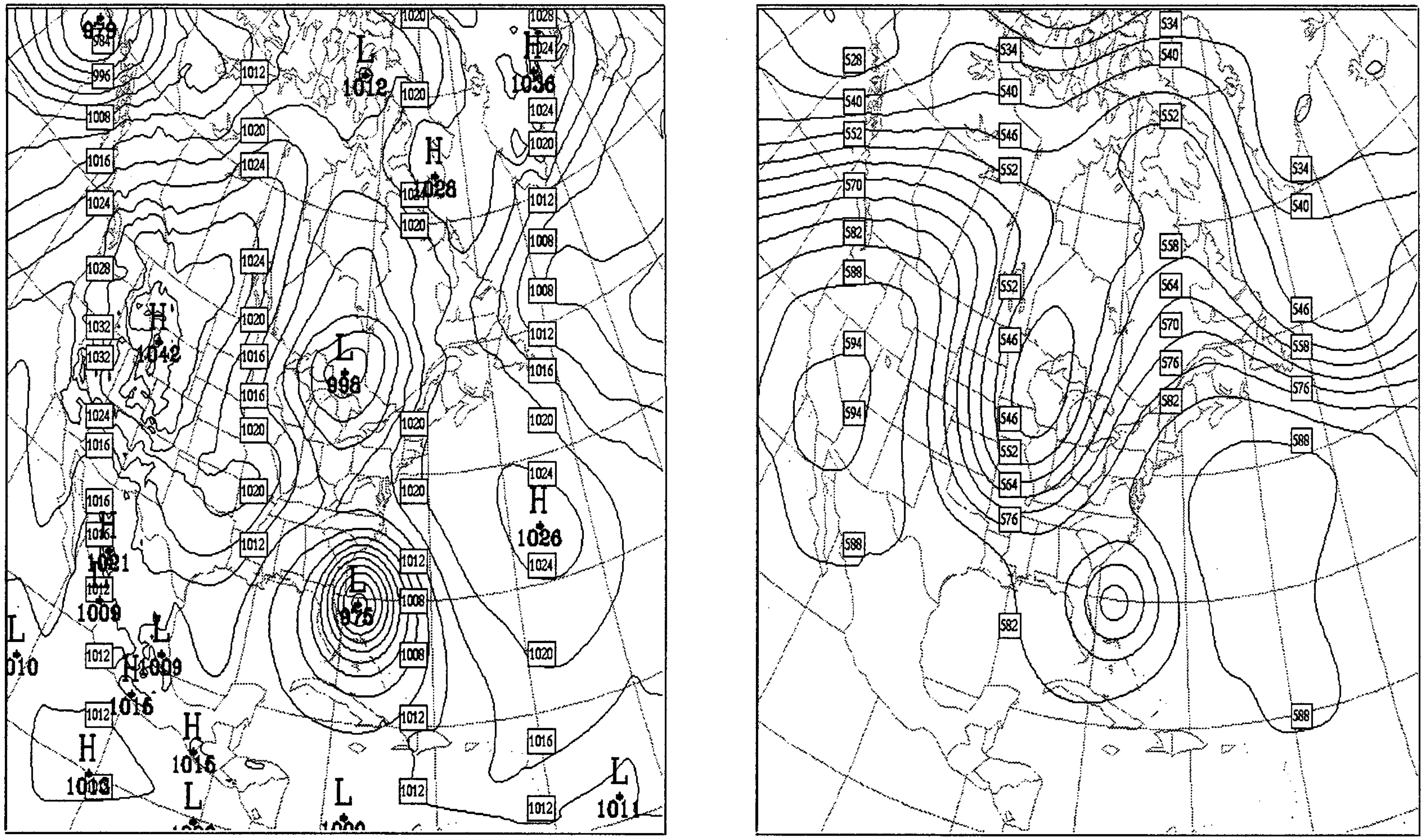

a) 03 UTC 15 Oct b) 03 UTC 15 Oct

Fig. 5.6.1. (a) BOG36 Sea level pressure (contour interval of 4 hPa); (b) BOG36 500 hPa heights (contour interval of 6 dam)

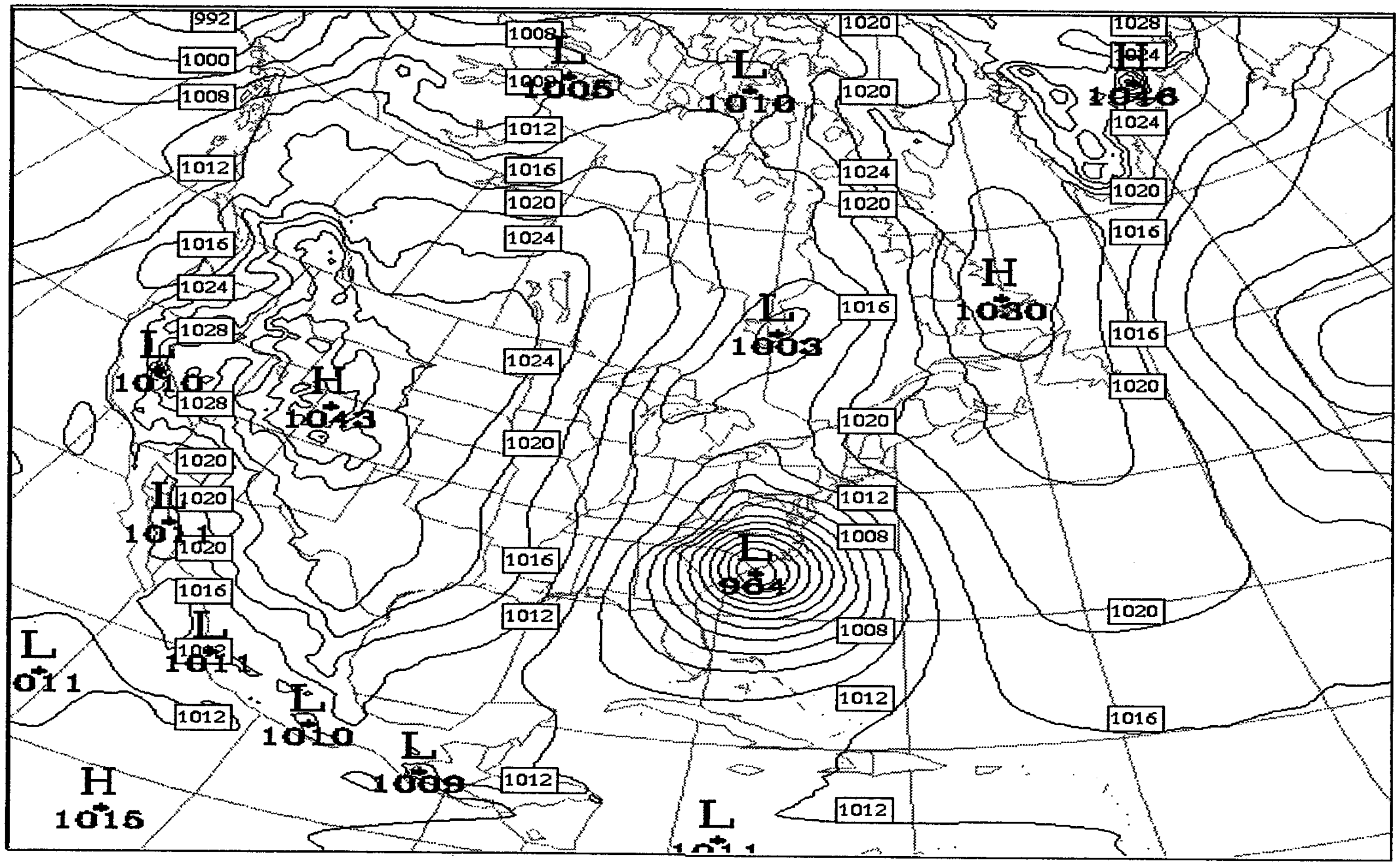

a) 15 UTC 15 Oct

Fig. 5.6.2. BOG36 Sea level pressure (contour interval of 4 hPa).

simulates a storm that matches well to the observed track, but with central pressures well below observed values. Stronger geostrophic winds in BOG36 than in CONT are channeling moisture into southern Ontario, leading to enhanced moisture conditioning at 21 UTC 15 (Fig. 5.6.3a). At 00 UTC 16 Knox (1955) analyzes a transition of sorts, by denoting two separate locations as the storm center at this time (5.8.1b). A northwest to southeast axis passes through the two points, one near Buffalo, New York and the other in central Pennsylvania. Analysis by Knox at 0030 UTC 16 confirms this configuration (Fig. 5.6.3b). At 21 UTC 15 in BOG36 the storm center extends to the northwest, and elongates over a broad area along the aforementioned axis. Three hours later the BOG36 pressure center spans the Appalachian Mountains, precisely at the time Knox defines the two distinct centers (Fig. 5.6.3c). CONT does not capture this development.

Sea level pressure at 03 UTC16 in BOG36 has a Hazel with a stronger and much more defined circulation than CONT (Fig. 5.6.4a). A pronounced trough over the east coast of the U.S. is also present, along with a more negatively tilted storm in BOG36. This is an improvement as Palmén's (1958) analysis at 1000 hPa supports this orientation (Fig. 5.4.6b). Tracking is deteriorating at this point, as BOG36 experiences an abrupt westward shift that exaggerates the pattern seen in the observations. The westward displacement does improve the situation over CONT though, and the time lag in CONT is still not evident in BOG36. Heights at 500 hPa in BOG36 vary significantly from CONT, as the cutoff midlatitude low heights cover a larger region in BOG36 (Fig. 5.6.4b). The magnitude of the heights in BOG36 is well matched to Palmén (1958) over the Great Lakes, but the extent of the isolated low is evidently too far into the southern U.S.

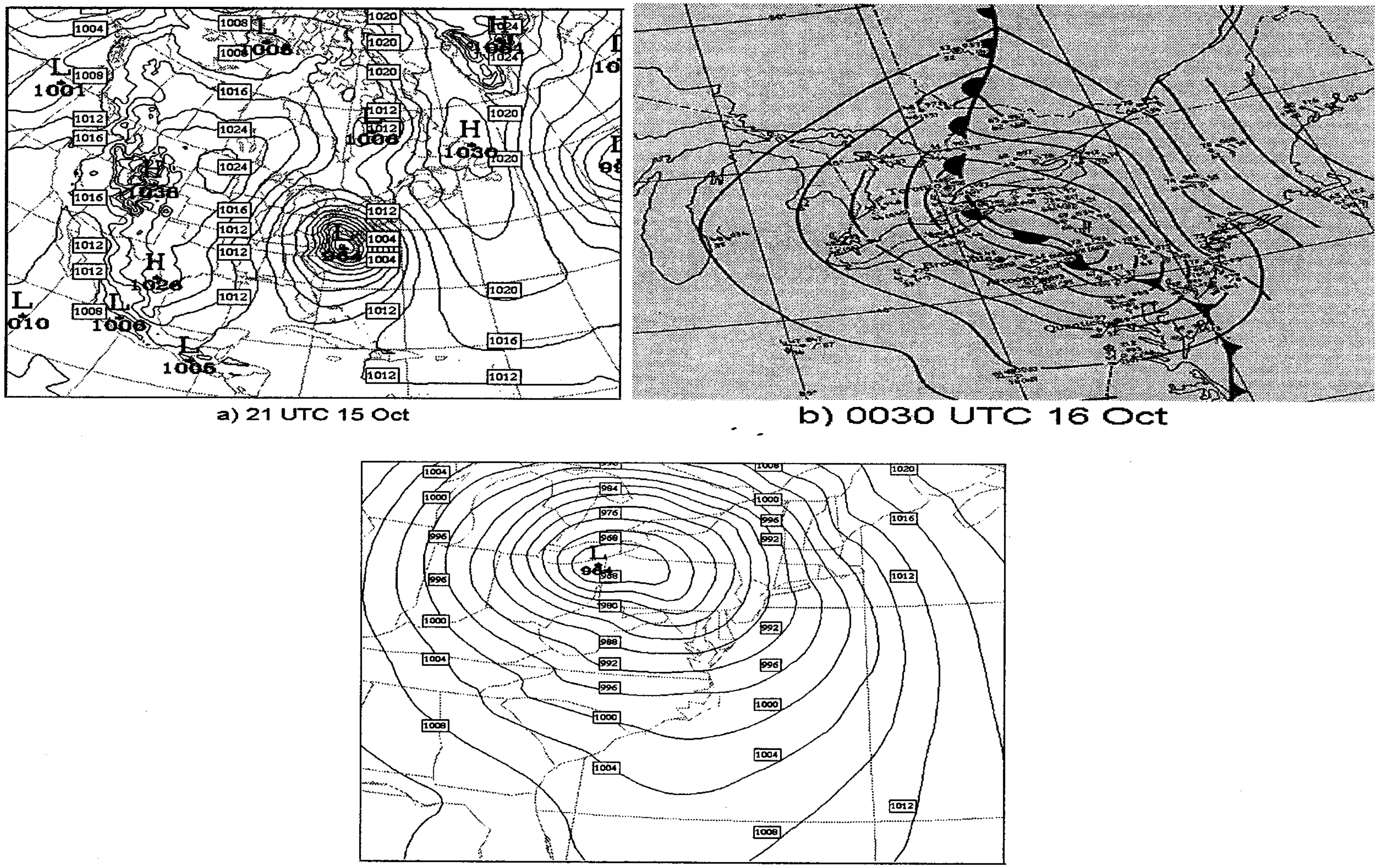

a) 21 UTC 15 Oct

b) 0030 UTC 16 Oct

c) 00 UTC 16 Oct

Fig. 5.6.3. Sea level pressure (contour interval of 4 hPa). For: (a) BOG36; (b) from Knox (1955); (c) BOG36.

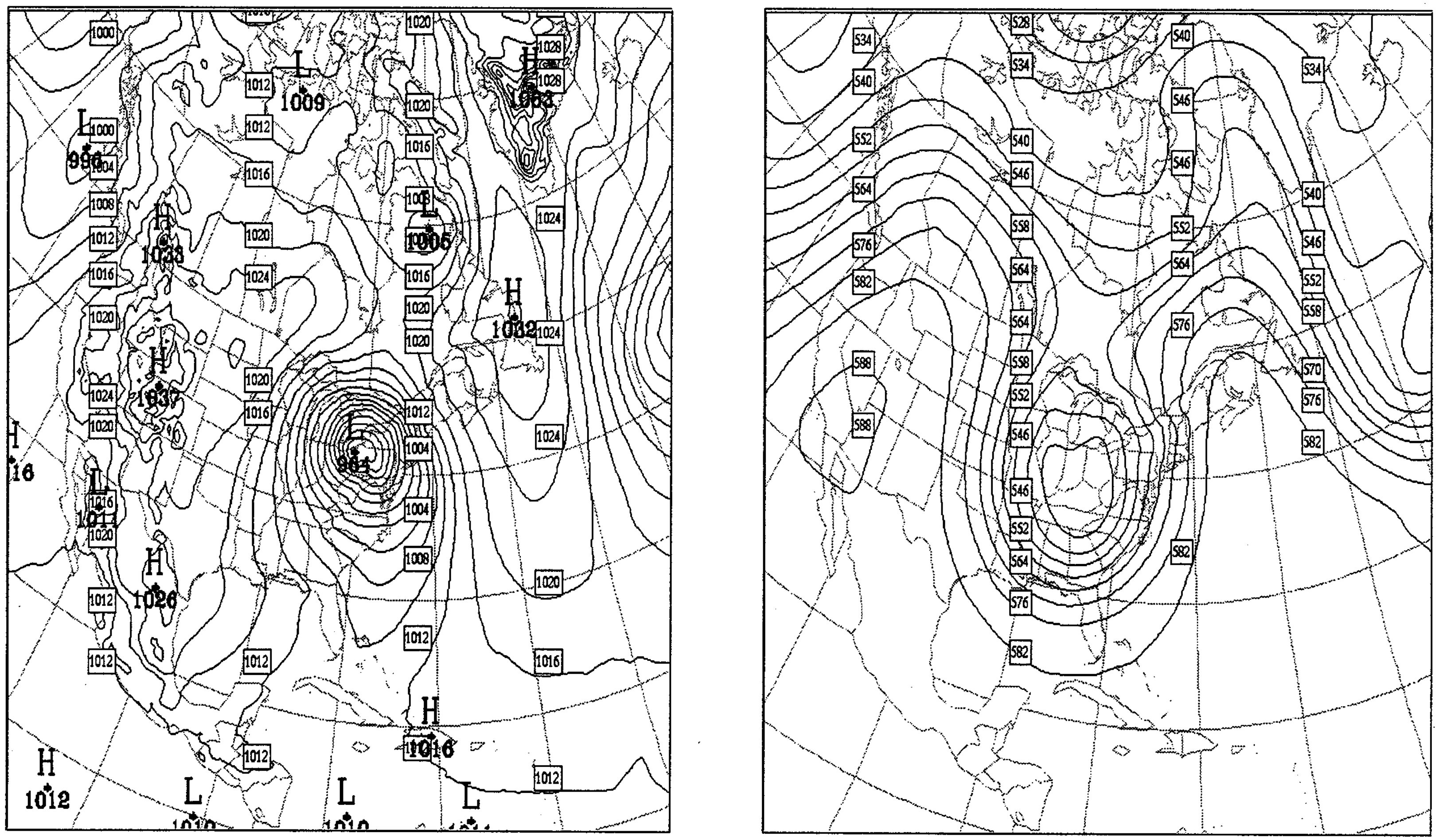

a) 03 UTC 16 Oct

b) 03 UTC 16 Oct

Fig. 5.6.4. (a) BOG36 Sea level pressure (contour interval of 4 hPa); (b) BOG36 500 hPa heights (contour interval of 6 dam).

The final nine hours to 12 UTC 16 are not comparable between CONT and BOG36. Both have storms that do exhibit an overemphasized shift westward, with BOG36 being the extreme limit. The large trough dissipates over the U.S. east coast in BOG36, while in CONT it remains with little change. A northeastward pointing extension from Hazel in BOG36 does not appear in CONT, and filling of the storm in BOG36 contradicts the deepening in CONT (Fig. 5.6.5a). BOG36 has a Hazel with a minimum pressure center still too low relative to Knox's (1955) data, and track is completely out of phase as Hazel actually exits Ontario near James Bay, not near Michigan as seen in BOG36.

Precipitation data is the most noticeable and encouraging improvement in this simulation. Comparing storm total precipitation for Hazel to the BOG36 rainfall shows a distribution with values in excess of 120 mm near Virginia, and a large region of values over 100 mm along the U.S. storm track (Fig. 5.6.5b). Amounts in southern Ontario approach 80mm in BOG36, far greater than the 40mm produced in CONT. Rainfall amounts are much larger in BOG36 than CONT. Objectively analyzed data confirms the success of BOG36 precipitation results, as the maximum of 120 mm over Virginia, the maximum of over 120 mm at the North Carolina and South Carolina border, and the precipitation track through the U.S. all fit well with the observations.

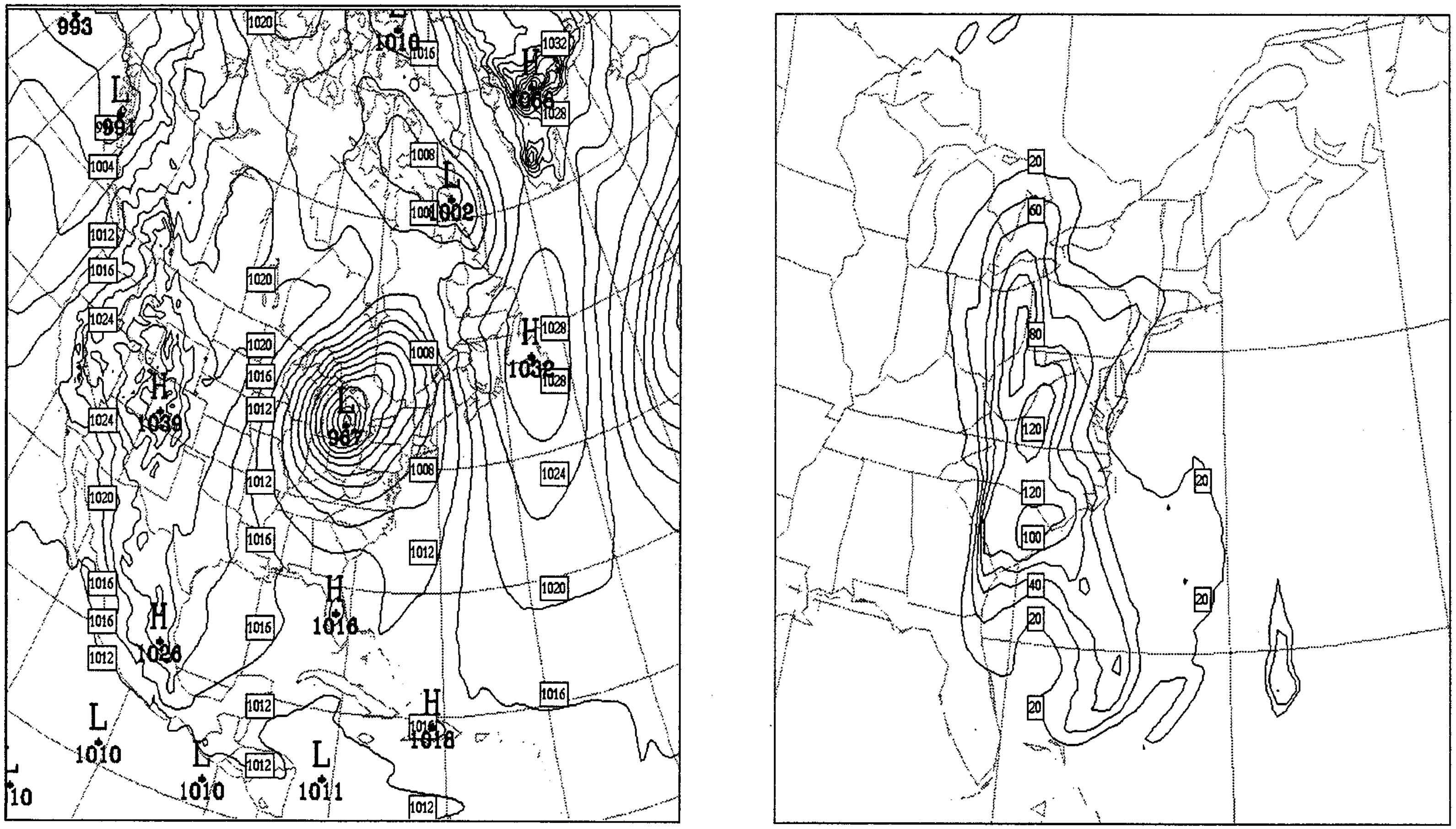

a) 12 UTC 16 Oct

b) 15-16 October

Fig. 5.6.5. (a) BOG36 Sea level pressure (contour interval of 4 hPa); (b) BOG36 Storm total precipitation for 36 hour period starting at 00 UTC 15 October (contour interval of 20 mm).

5.7 High resolution vortex sensitivity

A further extension of the bogusing sensitivity testing focuses on an increase in horizontal resolution. In this final test a specified vortex is used in combination with a spatial resolution of 12km, down from 36km in the previous runs. Direct comparison of the results from this 12km simulation (BOG12) against BOG36 allows for an assessment of the relative impact of the resolution enhancement, and contrasting with the CONT output measures the magnitude of change induced by a highly resolved, bogused vortex. Aside from the reduced grid point spacing, the few changes in the model settings are made in the number of grid points in the domain, now 250 by 280 points. This domain covers a zone from the south of Florida to northern Ontario, and the Rocky Mountains to Nova Scotia. Initialization of the model occurs at 06 UTC 15 October, six hours later than in all the other cases to avoid the condensation spin-up problem as earlier discussed. A central pressure of 973 hPa is used in this initialization, which is in close agreement with the analysis by Knox (1955).

The BOG12 simulation at 06 UTC15 contains a structure with identifiable differences from both CONT and BOG36. Central sea level pressure in Hurricane Hazel is a characteristic that exhibits this variability, as BOG12 is initialized at 973 hPa from the cascade of BOG36. This pressure is slightly higher than BOG36 and much lower than CONT. Structurally Hazel in BOG12 is less symmetric than in BOG36, especially along the western edge of the storm (Fig. 5.7.1a). Tracking Hazel in BOG12 shows a similar path to BOG36, but slightly farther northward (Fig. 5.8.1a). Looking at the extratropical low over the Great Lakes shows a system with a less circular nature, with troughs pointing to the north, south, east and west.

The pressure trend of BOG12 over the period from initialization to 12 UTC 15 shows an improvement towards the analysis. A steady 975 hPa low center in Hurricane Hazel matches the observations to within one hPa (Table 5.8.1). Storm track is highly similar to BOG36 still, bettering the results in CONT (Fig. 5.8.1a). The extratropical low and Hazel evolve to configurations in the sea level pressure field of BOG12 similar to BOG36 (Fig. 5.7.1b).

The large scale organization of BOG12 at 15 UTC 15 continues to be highly similar to BOG36. Extension of the extratropical low is farther southwest over the Great Lakes in BOG36, and the trough linking Hazel to this low pressure is shifted slightly eastward in BOG12. The orientation of this trough at 1000 hPa in BOG12 (Fig. 5.7.2a) reminiscent of the analysis provided by Palmén (1958) (Fig. 5.4.4b). BOG12 minimum central pressures in Hazel continue to perform well relative to observations, steadying at 975 hPa. The location of the extratropical low and Hazel at 1000 hPa in BOG12 correspond well to Palmén (1958), and the gap between the heights of these features diminishes greatly compared to those in CONT and BOG36. 500 hPa geopotential heights in BOG12 (Fig. 5.7.2b) do improve on the CONT (Fig. 5.4.5b) results. The cutoff low at 500 hPa in BOG12 is shifted to the northeast relative to CONT, but does not substantially affect the agreement with the analysis.

Hazel begins to deepen at 18 UTC 15, dropping three hPa to 971 hPa at 03 UTC 16. This range of sea level pressure in BOG12 is closer to observations than in CONT or BOG36. Sea level pressure fields are similar in all the cases, and the track of Hazel begins to lag in BOG12 behind the BOG36 and CONT paths by almost six hours.

The aforementioned time lag of six hours persists for Hazel in BOG12 at 03 UTC

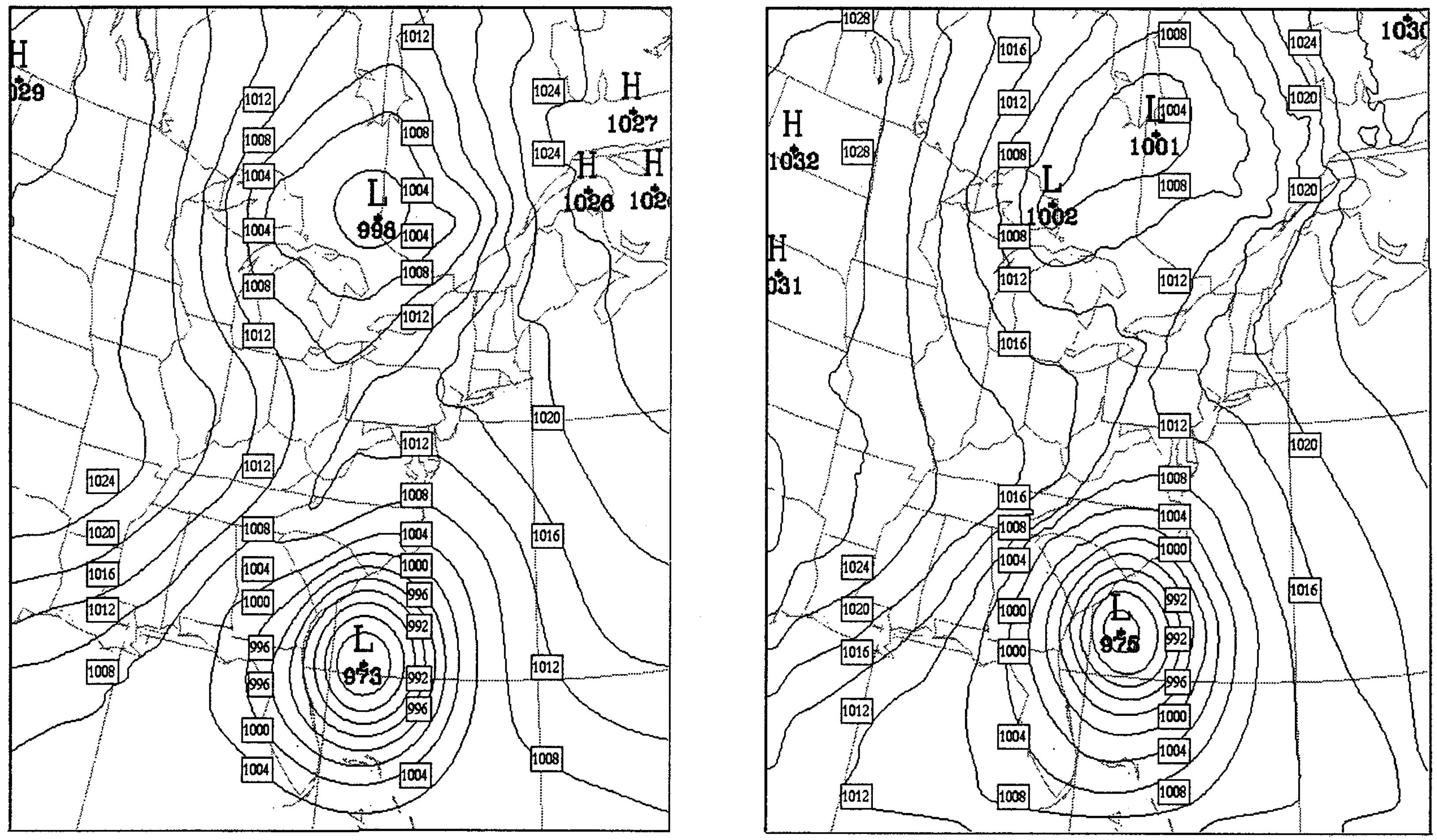

a) 06 UTC 15 Oct

b) 12 UTC 15 Oct

Fig. 5.7.1. (a) and (b): BOG12 Sea level pressure (contour interval of 4 hPa).

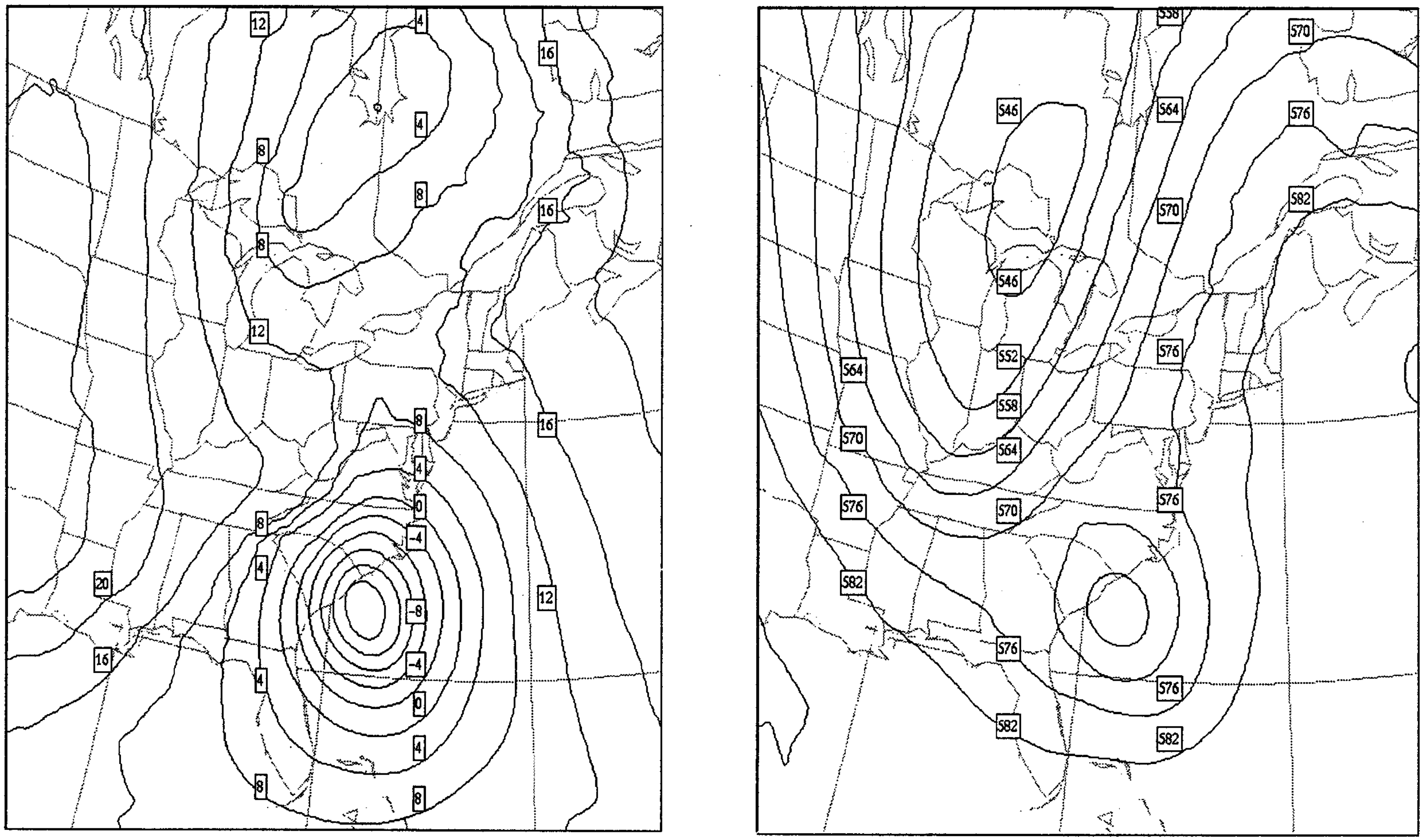

a) 15 UTC 15 Oct b) 15 UTC 15 Oct

Fig. 5.7.2. (a) BOG12 Sea level pressure (contour interval of 4 hPa); (b) BOG12 500 hPa heights (contour interval of 6 dam).

16. Viewing the path of the storm, one can see that Hazel follows the track prescribed by Knox (1955), but at a rate much too slow. A meridionally pointed storm at 1000 hPa in BOG12 contradicts the negatively sloped low pressure system in the analysis, and the center is obviously located too far south (Fig. 5.7.3a). BOG12 500 hPa heights form less of a cutoff low than in BOG36 (Fig. 5.6.4b), and the lack of isolation leads to a greater degree of weak meridional flow over Ontario in BOG12 (Fig. 5.7.3b). Geostrophic winds at this level near the northwest quadrant of Hazel do not work as efficiently at drawing the storm to the northwest as in the case of BOG36. Development of the midlatitude trough in BOG12 reduces the motion of Hazel substantially.

The final hours of BOG12 do little to improve the time lag of Hazel. Central pressures are encouraging as they fall within three hPa of actual values during the last nine hours. Storm structure fails to evolve during the slow advance of Hazel in BOG12 with respect to BOG36 and CONT, maintaining a near meridional orientation in the sea level pressure field (Fig. 5.7.4a).

Precipitation is enhanced in the BOG12 simulation, with a peak near 160 mm over Virginia (Fig. 5.7.4b). BOG12 rainfall values are noticeably lower over southern Ontario than those produced by CONT and BOG36. Both of these facts can be explained by the slow progress of Hazel northward in BOG12, due to the weak upper level circulation. Slow tracking over the U.S. leads to increased rainfall durations, and the lack of storm movement into Ontario severely limits the precipitation received. The U.S. portion of the rainfall track is similar to BOG36, but with values far in excess of the objectively analyzed observations.

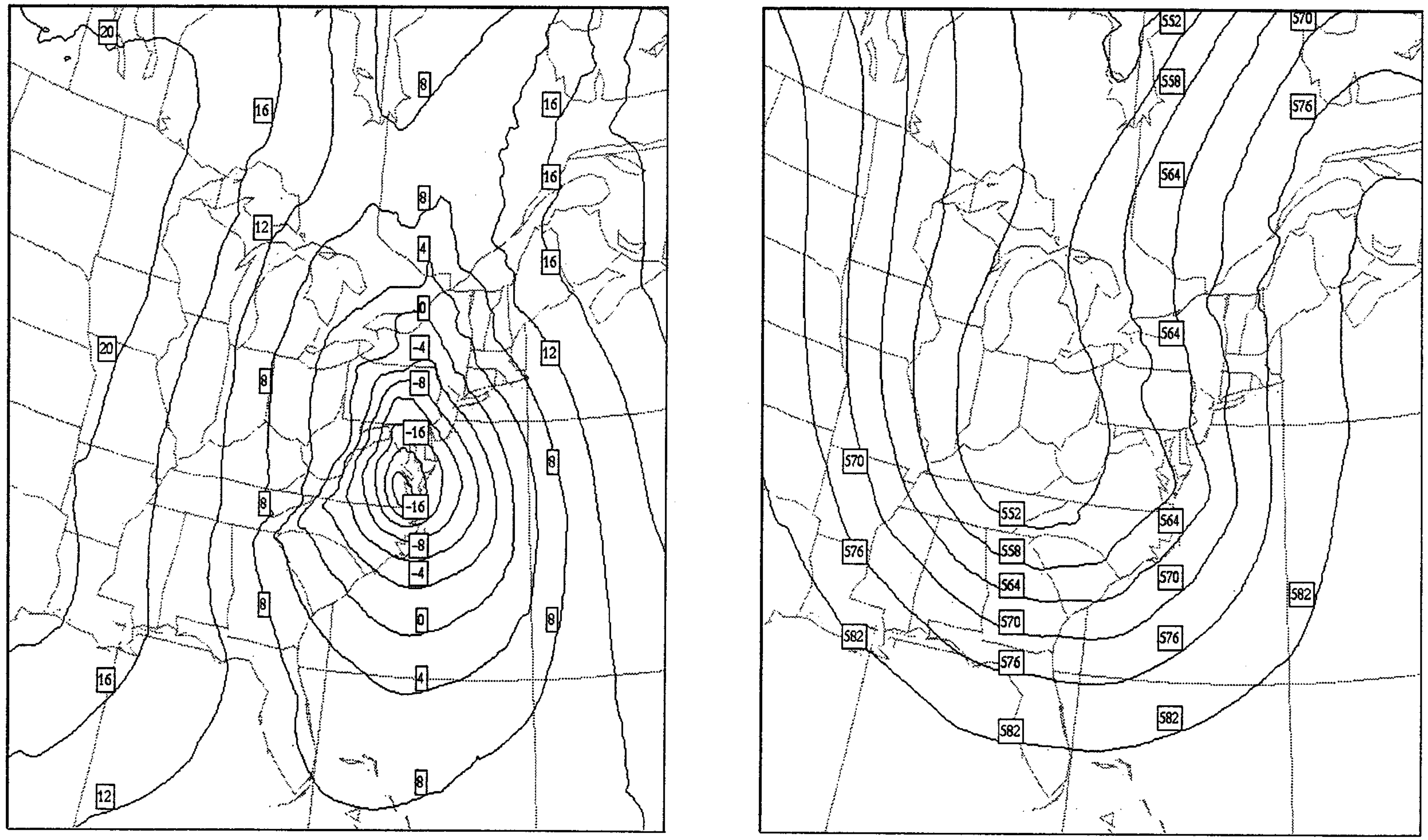

a) 03 UTC 16 Oct

b) 03 UTC 16 Oct

Fig. 5.7.3. (a) BOG12 1000 hPa heights (contour interval of 4 dam); (b) BOG12 500 hPa heights (contour interval of 6 dam).

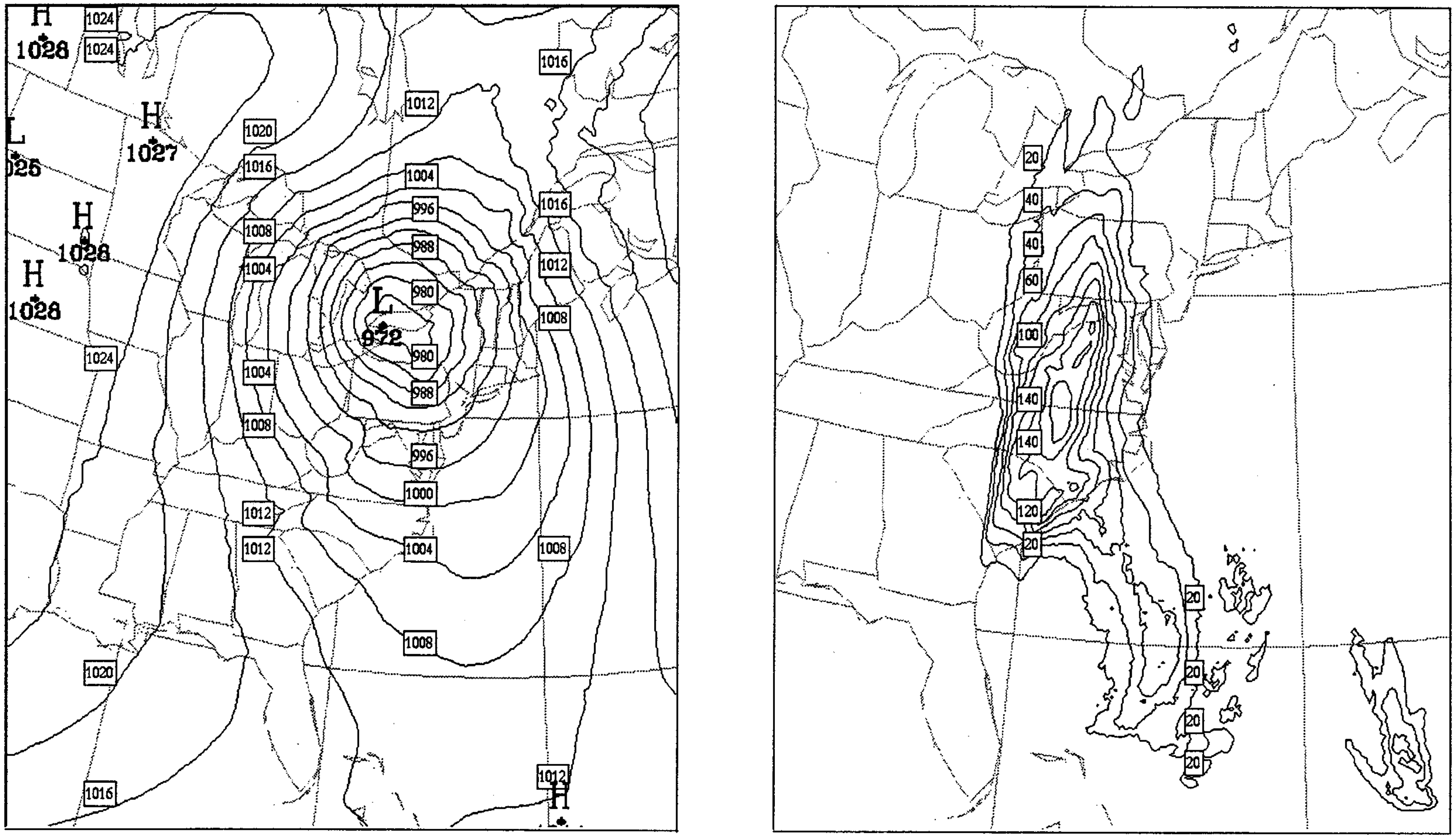

a) 12 UTC 16 Oct

b) 15-16 October

Fig. 5.7.4. (a) BOG12 Sea level pressure (contour interval of 4 hPa); (b) BOG12 Storm total precipitation for the 30 hour period starting at 06 UTC 15 October (contour interval of 20 mm).

5.8 Summary of MC2 simulations

Tracks for Hazel from observations by Knox (1955) and mesoscale modeling by Anthes (1990) are shown in Fig. 5.8.1b, while CONT, BOG36 and BOG12 are displayed in Fig. 5.8.1a. CONT is most similar to the run by Anthes (1990), in terms of both timing and location of the storm center. A strong eastward bias is present in CONT, with a three hour time delay. BOG36 is a significant improvement, with strong similarities to the observations over the first 27 hours of simulation. BOG12 does a poor job in terms of storm path, as the slow progression of Hazel in BOG12 destroys any potential phase matching with the real track specified by Knox (1955).

Central pressure values for the simulations show a mixed degree of success as well (Table 5.8.1). BOG12 returns the best results, agreeing with the observations for the duration of the simulation. BOG36 initially matches well with the actual sea level pressure minimums in Hazel, but continually intensifies until the pressures are much too low by the end of the integration. CONT shares little in common with the measurements by Knox (1955), starting at an excessively high value and exhibiting a slow deepening rate. Actual data for the central pressure of Hazel display a steady pattern, something only the BOG12 simulation could capture.

Structurally the BOG36 storm is most similar to the best available analyses. The shape and intensity of the 500 hPa midlatitude trough is best modeled in BOG36, and the development of Hazel in the lower levels of the atmosphere in this run mimics the analysis. The transition of the storm center over the Appalachian Mountains at 00 UTC 16 is particularly well resolved by BOG36. BOG12 has a poorly modeled 500 hPa trough feature that severely limits the northwesterly progression of Hazel in the latter

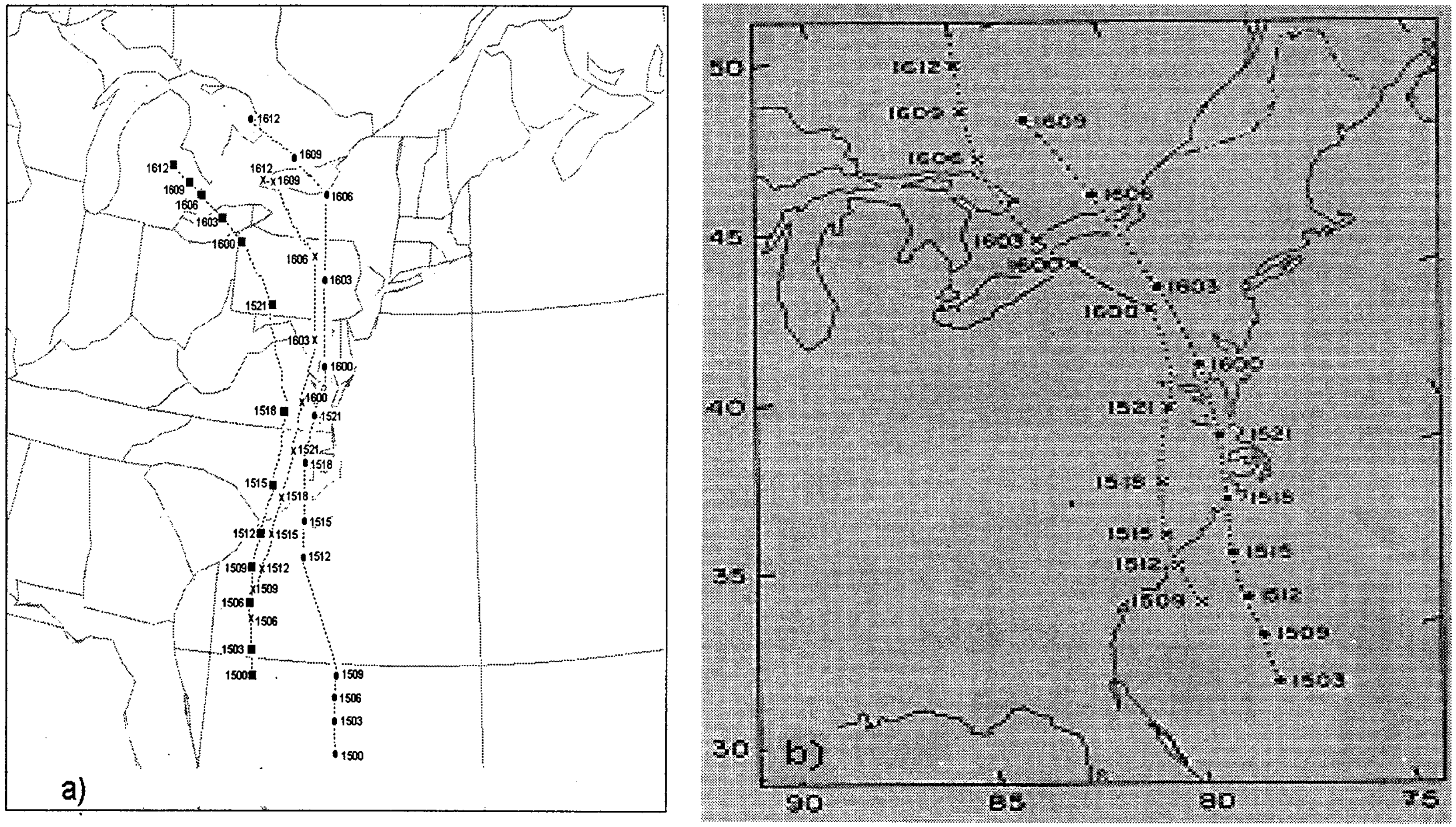

Fig. 5.8.1. (a) Tracks of Hazel in MC2 simulations (CONT in solid circles, BOG36 in solid squares, BOG12 in 'X');
(b) Tracks of Hazel in Observations (X) (Knox 1955) and control model simulation by Anthes (1990) (solid circles) from Anthes (1990).

stages of the simulation. Bogusing of the initial vortex structure in BOG36 introduces a highly realistic storm, enhancing the motion, track and intensity of Hazel. Unbogused fields in CONT leave a weak vortex in place of Hazel, constraining the ability of the MC2 to produce a viable simulation.

Table 5.8.1. Summary of central sea level pressure values (hPa).

Time	Knox (1955)	Anthes (1990)	CONT	BOG36	BOG12
00 UTC 15	-	-	998	970	-
03 UTC 15	975	975	998	975	-
06 UTC 15	975	978	997	970	973
09 UTC 15	975	976	998	967	975
12 UTC 15	975	974	997	965	975
15 UTC 15	974	973	993	964	975
18 UTC 15	974	972	990	964	974
21 UTC 15	974	970	988	964	973
00 UTC 16	975	969	985	965	972
03 UTC 16	975	970	983	964	971
06 UTC 16	-	-	981	963	972
09 UTC 16	-	-	981	965	973
12 UTC 16	-	-	981	967	973

Precipitation quantities and distribution is remarkable in BOG36, as it replicates the U.S. portion of the rainfall to a high degree of accuracy. Observed peaks in Virginia, North Carolina and Pennsylvania are depicted in BOG36. CONT produces much weaker precipitation, likely due in part to weak circulation around Hazel from the Atlantic Ocean that moistens the atmosphere. This precipitation is displaced to the east of the actual rainfall track as the storm in CONT demonstrates its eastward bias. Rainfall in BOG12 is extreme, exceeding the observed values considerably owing to the slow progression of Hazel northward.

6. Summary and Recommendations

Hurricane Hazel is scrutinized in this study, as the event occurring from 15-16 October 1954 was one of the most costly and deadly storms to strike North America. To account for the extreme amount of precipitation generated by this storm, an understanding of the dynamics and thermodynamics was sought. A picture unfolded of an atmosphere with a broad region of potentially unstable air, with a tongue of Atlantic Ocean moisture protruding over the east coast of the continent. A continuously deforming dynamic tropopause during the occurrence of Hazel led to an intensification of the principal baroclinic zone that drove the ensuing escalation of Hazel. Diabatic outflow from Hazel over Quebec forces non-advective increases in dynamic tropopause height, and augments the gradient of this element.

Following this comprehensive analysis of standard synoptic fields, moisture plots and dynamic tropopause characteristics, an analogue search to elucidate the crucial components of Hazel was conducted. Mass analogues for the 1954 event were found for three separate times, those times being 5 October 1985, 14-15 October 1995, and 9-10 September 1999. A strong correlation coefficient of over 0.7 was found in all these events, due to strong low pressure anomalies over the Great Lakes, and 1000-500 hPa thickness anomalies over Quebec and the U.S. Midwest. A lack of a dominant hurricane circulation in the search domain for any of the analogue cases was significant, as the atmospheric moisture conditioning and dynamic tropopause distortion provided by Hazel proved to be crucial to storm intensification. Precipitable water fields for the analogues showed much drier atmospheres during these events, and coupling index plots confirmed the enhanced stability of the atmospheres. The 1995 event had a weak Hurricane

Roxanne near the southern bound of the search area, and this feature accounted for 1995 being the analogue with the most similarities to the 1954 event. Both the 1999 and 1985 cases resemble the dynamic tropopause configuration of Hazel very little, while the 1995 event has a positively tilted dynamic tropopause gradient unlike the negatively tilted feature in 1954. Precipitation generated by the analogue cases is an order of magnitude smaller than the rain produced by Hazel, and in locations that do not coincide with those in the storm of 1954. The utility of such analogue searches for a case like Hazel is questionable, as this event is a rare occurrences that is unlikely to be replicated in the recent historical record.

A mesoscale modeling sensitivity study was designed to identify the important physical processes in the transformation of Hazel. A limited area model, the MC2, was employed to conduct the sensitivity tests. The major differences in each of the simulations is presented in Table 6.1. Verification of the control run was against analyses from Palmén (1958), Anthes (1990) and Knox (1955), and objectively analyzed raw precipitation data. The CONT simulation yielded a viable reproduction of Hazel, allowing for the testing of sensitivity to vortex bogusing and increased horizontal resolution. CONT had an eastward biased storm track, with a three hour time delay. Central pressures of Hazel are not deep enough in CONT, from start to finish of the integration. A pattern of falling minimum central pressure is observed in CONT, in opposition with observations. Precipitation produced by CONT is not as extreme as the observed values, as weak flow from the moist Atlantic waters leads to reduced precipitable water values. Specification of a vortex in the BOG36 simulation aimed to increase the strength of the circulation around Hazel and create a more realistic central

Table 6.1. Summary of major simulation differences

Simulation	Horizontal Resolution (km)	Bogused Vortex?	Initialization Time
CONT	36	No	00 UTC 15 October
BOG36	36	Yes	00 UTC 15 October
BOG12	12	Yes	06 UTC 15 October

pressure. The center was moved northwest to a position suggested by the National Hurricane Centre, helping improve the tracking of the storm. A noticeable improvement was found in the track as the MC2 was integrated, with a disappearance of the time lag and eastward bias in CONT. Central pressures in Hazel are closer in BOG36 to observations throughout the simulation, due to the specification of the lower sea level pressure in the bogus routine. Precipitation from BOG36 is in near agreement with the objectively analyzed data for the U.S. portion of the storm track. Maximum quantities over Pennsylvania, North Carolina and Virginia are collocated in BOG36 and the observations, with the overall rainfall pattern shifted well westward of the distribution in CONT. Using a specified vortex is a worthwhile venture, as it improves the storm track and precipitation results significantly over an unbogused simulation.

The final simulation is less encouraging, as the BOG12 results are worse than the BOG36 output with respect to precipitation, storm track and configuration. The track is initially similar to BOG36, but stalling near the end of the model run diminishes the path accuracy. Central pressure values in the storm are steady in BOG12, and virtually identical to the observed magnitudes. Precipitation values are much too high as a result of the slow movement of Hazel over the continent. A six hour time lag in BOG12 is induced by a poorly modeled 500 hPa cutoff low over the Great Lakes. The lack of development of this isolated low height region generates a weak southerly flow over Ontario, and does not sweep Hazel up effectively. Modeling by the MC2 of cutoff circulations is not currently well done, as the maintenance of this feature is due to poorly understood diabatic forcing (McTaggart-Cowan 2003). Outflow from Hurricane Hazel induces substantial latent heating near the dynamic tropopause, eroding the northern extent of the trough and developing the isolated low height zone over the Great Lakes. Misrepresentation of this latent heating inevitably leads to an unsuccessful depiction of the midlatitude trough. Davis and Bosart (2002) noted that cutoff low formation owing to anticyclonic outflow aloft enhances easterly steering flow and leads to a more westward storm track. The degree of anticyclonic outflow is influenced by the choice of cumulus convection parameterization scheme. Large sensitivities in the track and intensity changes can be directly attributed to the model physics and scale. The Kain-Fritsch cumulus parameterization is optimized for a 25 km grid, and use of higher resolution grids can result in excessive latent heating (Colle et al. 2003). Davis and Bosart (2002) found in simulations of the genesis of Hurricane Diana (1984) that the storm development was dependent on the choice of cumulus parameterization and grid spacing. Simulations using the Kain-Fritsch scheme led to a Hurricane Diana that intensified too rapidly when compared to observations. Accurate portrayal of the diabatic effects on the synoptic scale mass field is necessary to correctly simulate the explosive evolution of extratropically transforming storms such as Hazel as well (Atallah and Bosart 2003).

Bibliography

Anthes, R.A., 1990: Advances in the understanding and prediction of cyclone development. *Extratropical Cyclones, the Erik Palmén memorial volume,* C.W. Newton and E.O. Holopainen Eds., Amer. Meteor. Soc., 221-253.

Atallah, E. H., and L.F. Bosart, 2003: The extratropical transition and precipitation distribution of Hurricane Floyd (1999). *Mon. Wea. Rev.*, **131**, 1063–1081.

Benoit, R., J. Cote, and J. Mailhot, 1989: Inclusion of a TKE boundary layer parameterization in the Canadian regional finite-element model. *Mon. Wea. Rev.*, **117**, 1726-1750.

______, M. Desgagné, P. Pellerin, S. Pellerin, Y. Chartier, and S. Desjardins, 1997: The Canadian MC2: A semi-Lagrangian, semi-implicit wideband atmospheric model suited for finescale process studies and simulation. *Mon. Wea. Rev.*, **125**, 2382-2415.

Bluestein, H.B., 1992: *Synoptic-Dynamic Meteorology in Midlatitudes, Volume I: Principles of Kinematics and Dynamics.* Oxford University Press, 421 pp.

______, 1993: *Synoptic-Dynamic Meteorology in Midlatitudes, Volume II: Observations and Theory of Weather Systems.* Oxford University Press, 584 pp.

Bolton, D., 1980: The computation of equivalent potential temperature. *Mon. Wea. Rev.*, **108**, 1046-1053.

Bosart L.F. and G.M. Lackmann, 1995: Postlandfall tropical cyclone reintensification in a weakly baroclinic environment: A case study of hurricane David (September 1979). *Mon. Wea. Rev.*, **123**, 3268-3291.

Colle, B.A., J.B. Olson, and J.S. Tongue, 2003: Multiseason verification of the MM5. Part II: Evaluation of high-resolution precipitation forecasts over the Northeastern United States. *Wea. Forecasting,* **18**, 458-480.

Davis, C. and L.F. Bosart, 2002: Numerical simulations of the genesis of Hurricane Diana (1984). Part II: sensitivity of track and intensity prediction. *Mon. Wea. Rev.*, **130**, 1100–1124.

Davis, W.R., 1954: Hurricanes of 1954. *Mon. Wea. Rev.,* **82**, 370-373.

Durnford, D.A., 2001: *An analysis of Montreal's record-breaking heavy rainfall event of 8-9 November 1996, and a Comparison with its best analogue,* Master's thesis. McGill University, Dept. Atm. and Oceanic Sciences.

Eady, E., 1949: Long waves and cyclone waves. *Tellus,* **1,** 33–42.

EC, 2003: National Climate Data Archive of Canada provides limited precipitation observations at: http://www.msc-smc.ec.gc.ca/climate/data_archives/climate/index_e.cfm

Ertel, H., 1942: Ein Neuer hydrodynamischer Wirbelsatz. *Meteor. Z.,* **59**, 271–281.

FSL-NCDC, 2003: information regarding the radiosonde data for North America in 1954 from Forecast Systems Laboratory is found at: http://nndc.noaa.gov/?http://ols.nndc.noaa.gov/plolstore/plsql/olstore.prodspecific?prodnum=C00339-CDR-S0001

Glickmann, T.S., N.J. MacDonald and F. Sanders, 1977: New findings on the apparent relationship between convective activity and the shape of 500 mb troughs. *Mon. Wea. Rev.,* **105**, 1060-1061.

Gutzler, D.S. and J. Shukla, 1984: Analogs in the wintertime 500 mb height field. *J. Atmos. Sci.,* **41**, 177-189.

Gyakum, J.R., 2002a: The extratropical transformation: A scientific challenge. *Atmosphere-Ocean Interactions*, W. Perrie Ed., WIT Press, 47-81.

______, 2002b: Class notes from course on Synoptic Meteorology. McGill University, Dept. Atm. and Oceanic Sciences.

______ and P.J. Roebber, 2001: The 1998 Ice Storm - An analysis of a planetary scale event. *Mon. Wea. Rev.*, **129**, 2983-2997.

Hart, R.E., and J.L. Evans, 2001: A climatology of the extratropical transition of Atlantic tropical cyclones. *Journal of Climate,* **14**, 546-564.

Henderson, J.M., G.M. Lackmann and J.R. Gyakum, 1999: An analysis of Hurricane Opal's forecast track errors using quasigeostrophic potential vorticity inversion. *Mon. Wea. Rev.,* **127**, 292-307.

Hollingsworth, A., K. Arpe, M. Tiedtke, M. Capaldo and H. Savijarvi, 1980: The performance of a medium-range forecast model in winter - impact of physical parameterizations. *Mon. Wea. Rev.*, **108**, 1736-1773.

Huo, Z., Zhang, D.-L., Gyakum, J.R. and A. Staniforth, 1995: A diagnostic analysis of the Superstorm of March 1993. *Mon. Wea. Rev.*, **123**, 1740–1761.

Kain, J.S., and J.M. Fritsch, 1993: Convective parameterization for mesoscale models: The Kain-Fritsch scheme. *The Representation of Cumulus in Numerical Models, Meteor. Monogr.*, No. 46, Amer. Meteor. Soc., 165-177.

Kalnay, E., and co-authors, 1996: The NCEP/NCAR 40-year reanalysis project. *Bull. Amer. Meteor. Soc.*, **77**, 437-471.

Kistler, R., and co-authors, 2001: The NCEP–NCAR 50–Year reanalysis: monthly means CD–ROM and documentation. *Bull. Amer. Meteor. Soc.*, **82**, 247-268.

Klein, P.M., P.A. Harr and R.L. Elsberry, 2002: Extratropical transformation of western North Pacific tropical cyclones: midlatitude and tropical cyclone contributions to reintensification. *Mon. Wea. Rev.,* **130**, 2240-2259.

Knox, J.L., 1955: The storm "Hazel". *Bull. Amer. Meteor. Soc.*, **36**, 239-246.

Koch, S.E., M. DesJardins and P.J. Kocin, 1983: An interactive Barnes objective map analysis scheme for use with satellite and conventional data. *J. Climate and App. Met.*, **22**, 1487-1503.

Kong, F. and M.K. Yau, 1997: An explicit approach to microphysics in MC2. *Atmos. Ocean.* **33**, 257-291.

Kurihara, Y., M.A. Bender, and R.J. Ross, 1993: An initialization scheme of hurricane models by vortex specification. *Mon. Wea. Rev.,* **121**, 2030–2045.

Lorenz, E.N., 1969: Atmospheric predictability as revealed by naturally occurring analogues. *J. Atmos. Sci.*, **26**, 636-646.

Lund, I.A., 1963: Map-pattern classification by statistical methods. *J. Appl. Met.*, **2**, 56-65.

Mailhot, J., and co-authors, 1998: Scientific description of RPN physics library—Version 3.6. Atmospheric Environment Service Tech. Rep. v. 3.6, 188 pp.

Malmquist, D., 1999: Meteorologists and insurers explore extratropical transition of tropical cyclones. *EOS Trans. Amer. Geophys. Union,* **80**, 79-80.

Mason, A.H., M.K. Thomas and D.W. Boyd, 1955: The October 15-16, 1954 storm, "Hurricane Hazel" in Ontario. Technical circular no.: CIR-2606 TEC-210 (unpublished internal report); 49 pp.

McTaggart-Cowan, R., 2003: personal communication. McGill University, Dept. Atm. and Oceanic Sciences.

McTaggart-Cowan, R., J.R. Gyakum and M.K. Yau, 2001: Sensitivity testing of extratropical transitions using potential vorticity inversions to modify initial conditions: hurricane Earl case study. *Mon. Wea. Rev*:, **129**, 1617–1636.

Morgan, M. C. and J.W. Nielsen-Gammon, 1998: Using tropopause maps to diagnose midlatitude weather systems. *Mon. Wea. Rev.,* **126**, 2555–2579.

NCDC, 2003: Available data is described under the Global Climate Observing System link at: http://www.ncdc.noaa.gov/ol/climate/climatedata.html#DAILY

Newton, C.W., 1990: Erik Palmén's contributions to the development of cyclone concepts. *Extratropical Cyclones, the Erik Palmén memorial volume*, C.W. Newton and E.O. Holopainen Eds., Amer. Meteor. Soc., 1-18.

NHC, 2003: Statistics from the National Hurricane Center on hurricane Hazel are located at: http://www.nhc.noaa.gov/track1851to2001_atl.txt

Nielsen-Gammon, J. W., 2001: A visualization of the global dynamic tropopause. *Bull. Amer. Meteor. Soc.,* **82**, 1151–1168.

Palmén, E., 1958: Vertical circulation and release of kinetic energy during the development of Hurricane Hazel into an extratropical storm. *Tellus,* **10**,1-23.

Radinovic, D., 1975: An analogue method for weather forecasting using the 500/1000 mb Relative Topography. *Mon. Wea. Rev.*, **103**, 639–649.

Roebber, P.J. and L.F. Bosart, 1998: The sensitivity of precipitation to circulation details. Part I: An analysis of regional analogs. *Mon. Wea. Rev.,* **126**, 437-455.

Rogers, R.R. and M.K. Yau, 1994: *A Short Course in Cloud Physics.* Pergamom, 3rd ed., 284 pp.

Ruosteenoja, K., 1988: Factors affecting the occurrence and lifetime of 500 mb height analogues: a study based on a large amount of data. *Mon. Wea. Rev.*, **116**, 368–376.

Simpson, R. H., 1976: The hurricane disaster potential scale. *Weatherwise,* **27,** 169–186.

Tanguay, M., A. Robert and R. Laprise, 1990: A semi-implicit semi-Lagrangian fully compressible regional forecast model. *Mon. Wea. Rev.*, **118**, 1970-1980.

UCAR, 2003a: Formulation of the equation to calculate sea level pressures is found on the world wide web at: http://dss.ucar.edu/pub/reanalysis/FAQ.html

UCAR, 2003b: Descriptions of the U.S. First Order Summary of the Day, U.S. Control Cooperative Hourly Precipitation, Air Weather Service (AWS) Global Surface Observations, and the Canada Summary of the Day data can be located at: http://dss.ucar.edu/datasets

van den Dool, H.M., 1989: A new look at weather forecasting through analogues. *Mon. Wea. Rev.,* **117**, 2230–2247.

Yau, M.K., 2003: personal communication. McGill University, Dept. Atm. and Oceanic Sciences.